Material Recovery Potential from Solar Photovoltaics: Predictive Modeling and Characterization to Advance the Circular Economy

by

Nicole Bakker

Master in Design Engineering, Harvard University (2018)
Bachelor in Structural Engineering (with honors), Noordelijke Hogeschool Leeuwarden, The Netherlands (2015)

Submitted to the Program in Media Arts and Sciences,
School of Architecture and Planning,
in partial fulfillment of the requirements for the degree of

Master of Science

at the

MASSACHUSETTS INSTITUTE OF TECHNOLOGY

May 2024

Author_____

Nicole Bakker
Program in Media Arts and Sciences
May 17, 2024

Certified by_____

Kevin Esvelt
Associate Professor of Media Arts and Sciences
Program in Media Arts and Sciences
Thesis Supervisor

Accepted by_____

Joseph Paradiso
Academic Head
Program in Media Arts and Sciences

Material Recovery Potential from Solar Photovoltaics: Predictive Modeling and Characterization to Advance the Circular Economy

by

Nicole Bakker

Submitted to the Program in Media Arts and Sciences,
School of Architecture and Planning,
on May 17, 2024, in partial fulfillment of the
requirements for the degree of
Master of Science

Abstract

In the next two decades, an exponentially growing quantity of waste will be generated as solar panels reach their end-of-life. Meanwhile, demand for new solar capacity will increase the value of key raw materials, underscoring the importance of recycling and movement toward a "circular economy". However, uncertainties over the quantity and the exact material composition of solar panel waste hamper investments by recyclers, manufacturers, and governments. In this study, I construct a Material Flow Analysis model to forecast the global quantity of recoverable materials through 2100, informed by an experimental characterization of representative solar panels from the 1930s to 2020s. To account for potential changes in future demand, I develop two distinct scenarios: one explores the growing electricity demand from artificial intelligence use ('Artificial Intelligence Boom'), while the other features renewable hydrogen production for steelmaking, shipping and the chemical industry ('Green Hydrogen Takes Off'). The combined model predicts a lower material demand for silicon than previously anticipated in the base case, with a cumulative installed solar PV capacity of 50 TW and a waste volume of 3,600 metric megatonnes by 2100. This will require 45 megatonnes of solar-grade silicon by 2100, while 18 megatonnes could theoretically be obtained from recovered material. Achieving a circular economy for silicon is possible by the mid-2040s, but will require recovery rates above 70% and continued improvements in material efficiency as observed in the retrospective analysis. Recovery would suffice for all silicon demand through the mid-2060s, but not through 2100, because the demand for new solar panels and replacements outpace secondary supply. Of specific concern for material recovery is the material composition: results from characterization indicate the presence of toxic materials, including lead, and scarce elements in solar cells.

Thesis Supervisor: Kevin Esvelt
Title: Associate Professor of Media Arts and Sciences, Program in Media Arts and Sciences

Material Recovery Potential from Solar Photovoltaics: Predictive Modeling and Characterization to Advance the Circular Economy

by

Nicole Bakker

This thesis has been reviewed and approved by the following committee members:

Thesis Reader_____

Kevin Esvelt
Associate Professor of Media Arts and Sciences
Media Lab, Massachusetts Institute of Technology

Thesis Reader_____

Christine Ortiz
Morris Cohen Professor of Materials Science and Engineering
DMSE, Massachusetts Institute of Technology

Thesis Reader_____

Ellan Spero
Instructor
DMSE, Massachusetts Institute of Technology

Thesis Reader_____

Elsa A. Olivetti
Professor of Materials Science and Engineering
DMSE, Massachusetts Institute of Technology

Acknowledgment

First and foremost, I'd like to express deep gratitude to *Kevin Esvelt*. Without your unwavering support this thesis would certainly be less interesting—even though this topic has nothing to do with synthetic biology, you have been the best mentor I could possibly wish for. Our thought-provoking conversations pushed me to think creatively and bring open science principles into practice. *Christine Ortiz* and *Ellan Spero*, your wisdom and guidance brought a deeper layer of synthesis into this thesis, which was highly informative for the retrospective analysis and materials characterization. Your unique approach to education is truly innovative, enabling a deep understanding about environmental and sociotechnical impacts of technology for generations to come. Huge thanks also to *Elsa Olivetti*, *Jeremy Gregory*, and the teaching team of the class Industrial Ecology of Materials. This formed a core foundation for the model in this work, based on principles for Material Flow Analysis and Life Cycle Assessment. To *James Weaver* I'd like to express gratitude for your help with materials characterization. Whether it is for analyzing the material composition of solar cells or lyophilization of algae samples during my previous studies, you're always here to help and one of the kindest people I know. This work was performed in part in the MIT.nano Characterization Facilities, and I express gratitude for their support. Especially to *Anna Osherov* for her guidance, and *Charlie Settens* who taught me the ropes of X-Ray Fluorescence. Thanks also to *Tom* for connecting me to the right people, and *Jordan* and *Timothy* for providing machine training. In the Department of Materials Science and Engineering, I'd like to appreciate *Don Baskin* for opening my eyes to the field of materials science, in particular structural materials and fracture mechanics. Lastly, I'm thankful to *Mike* and *Christopher* for providing access to measurement instruments.

External collaborators include *Karl Wagner* and *Danielle Rhodes*, founders of the Museum of Solar Energy. It is incredibly exciting to study almost a century of solar cell artifacts and I am beyond grateful you provided over forty samples for analysis and characterization at MIT. Karl, as a solar energy expert, your feedback has been invaluable. In addition, thanks to *Brian* and *Tim* from Greentech Renewables in Woburn for donating a pile of decommis-

sioned solar panels, and *Alex Bonnema* and *Klaas Jetze Hoekstra* for demonstrating your solar panel recycling pilot plant in the Northern Netherlands.

It should also be acknowledged that the building blocks that made this work possible have roots in prior years. The MDE program at Harvard allowed me to expand my horizons and special thanks to *Joanna Aizenberg* for offering the opportunity to learn about chemistry for materials science. *Neri Oxman*, my former advisor, has been a major catalyst for learning to design across scales, co-advised by *David Kong* with whom it was an exciting time to build the Global Community Bio Summit from the ground up. Unfortunately, I had to take a medical leave during my first semester at MIT and I'm incredibly grateful for Neri's support as she went above and beyond. *Neil Gershenfeld* opened the door to come back to the lab, and the classes How to Make (Almost) Anything and The Nature of Mathematical Modeling cultivated a strong maker-mindset. Finally, thanks to the staff at the MIT Distinctive Collections, MIT Libraries, the Writing and Communication Center, MAS, and OGE. Mahy, Linda, Sarra, Liz, Chris, Pamela, and Megan, I am so thankful for your support and encouragement.

Two years ago, I never thought it would be possible to stand here today. This journey certainly has not been easy, and I want to give thanks to the team at MIT Health and my physical therapists Abbe and Matt for identifying and treating post-concussive symptoms. It has been an intense revalidation process alongside my studies, but it gave my life back. To anyone experiencing a similar healing journey I would like to say: keep following your dreams, even if you move forward at glacial speed and have to crawl to the finish line. Thanks to my family and friends, and everyone who supported me in this.

To my fiance, Age: returning to MIT with you by my side has made this a deeply meaningful experience. The world has so much more color with you, and no words can explain how grateful I am that we decided to take on this adventure together.

To all who remained overseas, a Frisian expression applies to both this thesis topic and our transatlantic connection: *Wer't wy op 'e wrâld ek binne, oer ús skynt deselde sinne.*

Contents

List of Figures

List of Tables

Chapter 1

Introduction: Why is material recovery from solar cells important?

How can predictive modeling and characterization improve the material recovery potential of decommissioned solar panels? Experimental research and theoretical modeling are traditionally two distinct scientific disciplines. Unique challenges in the transition to a *circular economy*, which can simply be defined as the reduction of primary material use and the elimination of waste, demand systemic interventions that impact complex, multi-layered systems of production; from materials selection to product design, collaboration within supply chains, economic shifts, and regulatory reform.

Difficult trade-offs need to be made for material selection, specifically for renewable energy infrastructure, including solar photovoltaics. Sustainability is improved by efficiency gains and long-term product stability (e.g., through the use of strong adhesives), which can in turn compromise recoverability of valuable materials at end-of-life, thereby opposing circular economy goals. To make the right decisions, a holistic and interdisciplinary framework is needed along with accurate data. In this light, an approach that combines experimental research and predictive modeling is a logical choice. Characterization yields information

about material composition relevant to recycling at end-of-life, and future technology predictions give an indication of the scale of the waste problem in the future so that we can take appropriate action today.

In this thesis, I explore the scale and implications of the growing number of end-of-life solar panels entering the global waste treatment system. This is partially motivated through a personal connection to this theme, with prior work on the integration of solar photovoltaics in historic built environments just over ten years ago [1]. In the current work, the downstream effects of solar PV are evaluated from a materials perspective to examine the potential for secondary materials recovery from discarded solar panels, aiming to contribute to the circular economy. A leading axis of this work is temporal: by looking back in time (almost a century) and projecting just over 75 years into the future (up to the year 2100), insights are generated to evaluate the feasibility of material recovery from end-of-life solar photovoltaic (PV) panels.

1.1 Our relationship with technical materials

Materials are deeply entangled with technological progress. It is no coincidence that many eras in human history are named after the materials that transformed the course of society; the Stone, Bronze, and Iron Age all appeal to our imagination. One could argue we're currently in the Silicon Age, with this material at the heart of our chips and electronics that power everything from refrigerators, medical devices, computers, and items in our everyday life. Our survival depends on it, similar to the salient materials in preceding times. In fact, Ashby proposed we already dwell in the Age of Molecular Engineering [2], yet as you can see in figure 1-1 we still rely deeply on engineered metals, polymers, and composites. Although these materials are highlighted for their critical roles in distinct eras, there is continuity and longevity that needs to be recognized, especially when it comes to persistence of materials and technologies. Consequences across the life cycle involve wide-ranging social and environmental impacts. With technological advancement and digitization, electronic waste is now a growing global problem. What happens when these products are discarded?

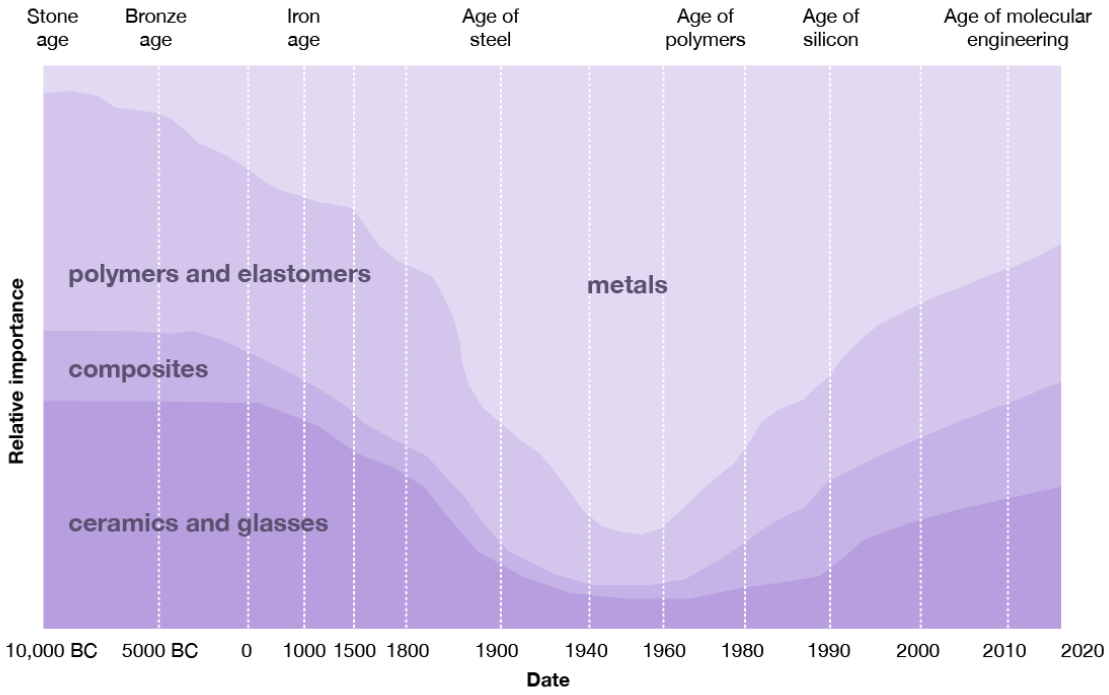

Figure 1-1: Evolution of Engineering Materials (Adapted from Ashby [2])

Where valuable bronze and iron tools were remelted and reused in prehistoric times, current high-value and rare earth minerals are carelessly discarded in landfills. The most notable example is our smartphone—it contains almost the entire periodic table, and is often replaced within 1-3 years [3]. From a product design perspective, a contributing factor is termed 'planned obsolescence' [4]. During the Great Depression, industrial production had to be ramped up for economic recovery, and as a solution, products were intentionally designed to wear faster. Disposable products were introduced, so manufacturers could sell more [5]. This leads to exceeding the earth's planetary boundaries [6], and more sustainable visions are needed to mitigate the laundry list of negative externalities, ranging from climate change to waste, pollution, toxicity, and social injustice. In speculative fiction, technologies are envisioned that support *solarpunk* futures [7]. In all of the above, generating power from the sun is seen as the symbolic icon of sustainability. This thesis brings in the materials perspective, to make solar photovoltaics a truly regenerative technology.

1.2 A brief introduction to solar photovoltaics

This section introduces definitions, materials-related issues in renewable energy infrastructure, seminal studies on the projected solar PV waste streams, recycling policies, an overview of the main solar cell technologies, and environmental and social impacts.

Definitions. To clarify solar PV terminology, an exploded-view diagram of solar panel architecture is given in figure 1-2. The circular economy is a relatively new concept, and the exact definition is still debated among scholars [8]. The following definition is selected to guide this research:

"The Circular Economy is a regenerative system in which resource input and waste, emission, and energy leakage are minimised by slowing, closing, and narrowing material and energy loops. This can be achieved through long-lasting design, maintenance, repair, reuse, remanufacturing, refurbishing, and recycling." [9].

Materials and renewable energy infrastructure. Materials play an essential role in enabling the renewable energy transition. Studies have pointed out that while materials are crucial for shifting toward a low-carbon society, their heightened utilization might intensify environmental and social issues [10]. Current environmental and supply chain challenges of PV panels include high embodied carbon, limited systems for recycling, the use of rare minor minerals, and hazardous waste after disposal. Policies such as the IEA Net-Zero emission by 2050 scenario further drive material demand for scarce elements [11]. Simultaneously, geopolitical tensions in areas with mineral ores can aggravate global supply chain issues and hinder clean energy development [12]. Combined with global pledges to become a circular economy in 2050, as proposed in the EU Green Deal and Circular Economy Action Plan (2015), it is important to accurately predict material quantities and composition of the products we are currently placing on the market, as they will become waste in the future.

Growing PV waste streams. With an average lifespan of 25-30 years, PV panels are increasingly reaching their end-of-life (EOL). Figure 1-3 shows how the cumulative installed solar PV capacity has grown significantly. Due to large scale deployment of solar photovoltaics in recent decades, waste generated from decommissioned solar panels is considered

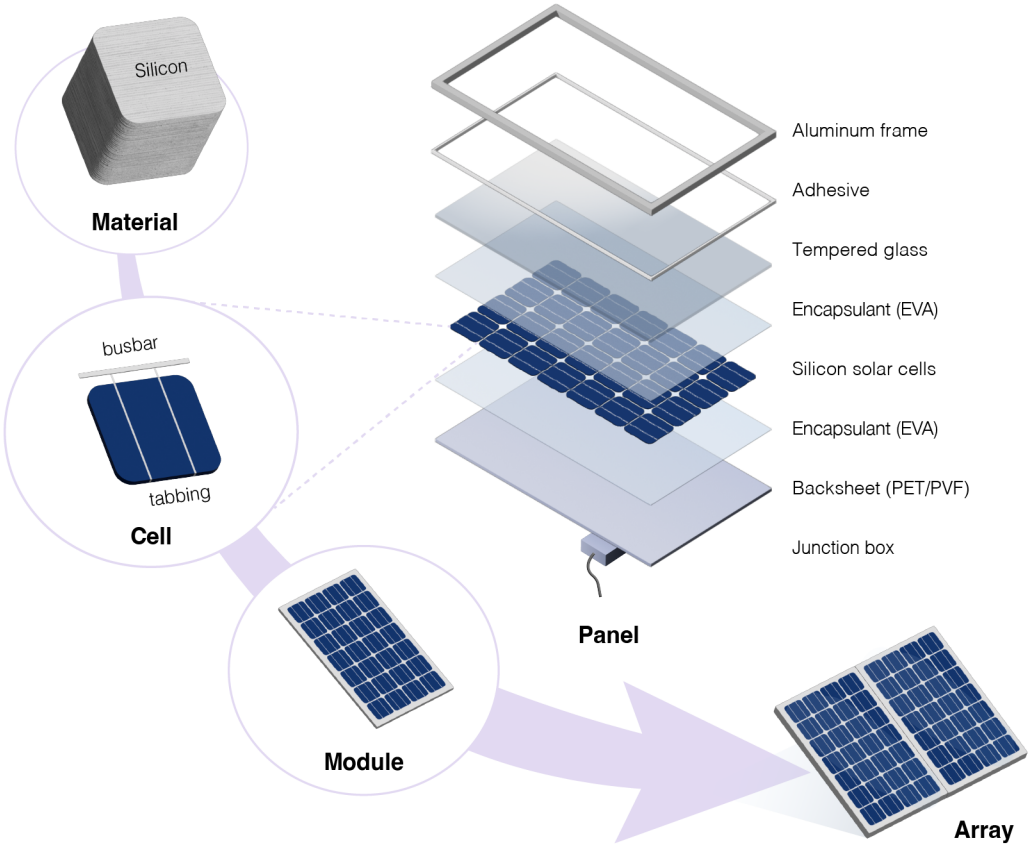

Figure 1-2: Illustration of a solar cell, module, panel and array.

to be one of the future challenging waste streams. At present, only 10% of the discarded PV modules are estimated to be recycled by mass in the United States [14], and collection and recycling rates are scarcely reported.

Solar PV recycling policies. In the United States, no federal policy yet exists. Some states, including Washington [16] and California [17], have PV waste disposal policies, while others recognize the issue and have plans under development, including New York State [18] and Massachusetts [19]. In the U.S. Department of Energy's report 'Photovoltaics End-of-Life Action Plan' the following statements are given:

"To date, the volume and rate of PV EOL generation has been low and sporadic, and information related to PV EOL is scarce. The community has indicated that data on bill

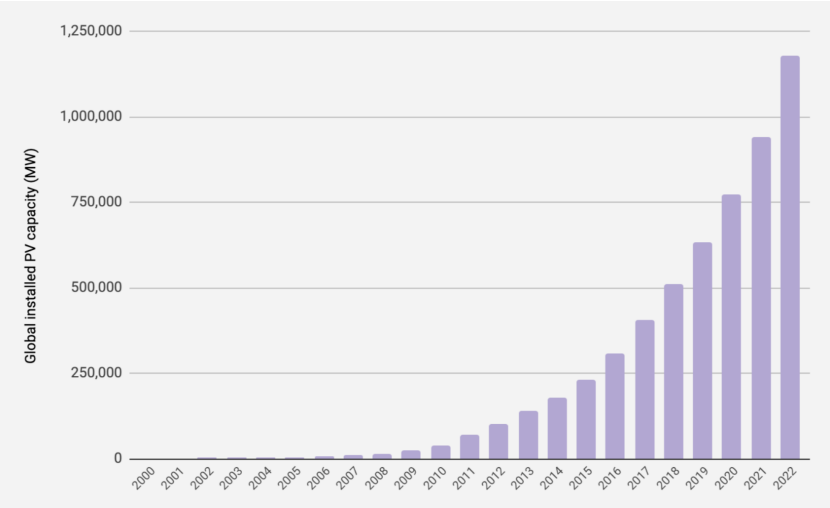

Figure 1-3: Cumulative installed solar PV capacity (MW) from 2000 to 2022. Adapted from [13]

of materials, quantity, age, location, cause of EOL, and EOL handling for modules would be most useful. Establishing quality data on PV EOL would help communities, the solar industry, and EOL industries better understand the current state of EOL and make decisions based on informed analysis" [20].

In Europe, solar PV systems have already been subject to recycling policies for over ten years. The Waste of Electrical and Electronic Equipment (WEEE) Directive mandates a material recovery fraction of 70% by mass for PV panels [21], yet figure 1-4 shows this requirement is mostly satisfied by the recycling of the panels' glass layers and aluminum frames. Valuable materials, including silver, copper and high-purity silicon, are currently lost in landfills or mechanical recycling [22].

This is a missed opportunity because recycled silicon PV panels are reported to require 40% less energy during production than cells made from raw materials [23] [24]. Yet, as Libby et al. point out, "Only a few life cycle inventories (LCI) of energy and material flows are available for the industrial recycling processes that are used today to recycle crystalline silicon based (c-Si) PV modules." [22]. Furthermore, the inventories that are available are often outdated. To mitigate the growing waste and supply chain problems—and ultimately achieve a circular economy—we need to investigate options for secondary materials recovery

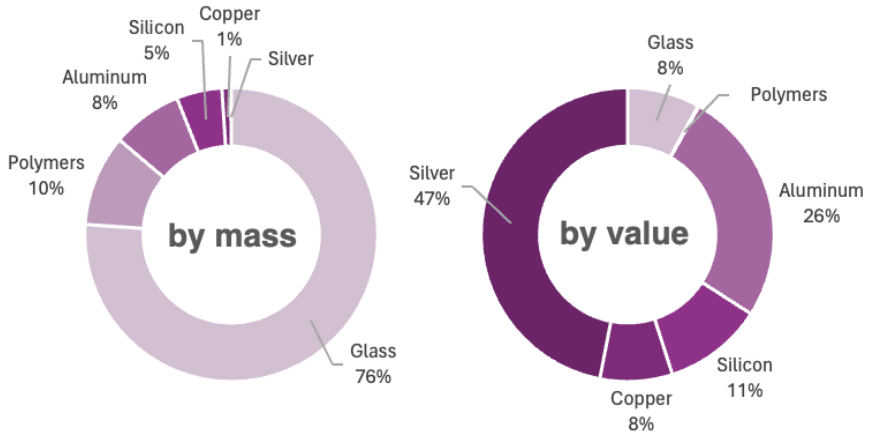

Figure 1-4: Material composition of a typical c-Si PV module. Adapted from [15]

from discarded PV panels. Solutions are needed to recover not only materials that constitute the largest share by mass, but also high-value materials that appear in smaller quantities. This starts with quantifying how much EOL material will become available, and its timing. In this thesis, a predictive model is presented to answer that question.

Landmark study. An important foundational and often-cited report is End-Of-Life Management: Solar Photovoltaic Panels by the International Renewable Energy Agency (IRENA) and International Energy Agency (IEA) in 2016 [15]. This is the first global prediction of cumulative PV capacity and waste volume until 2050. This report indicates a PV waste volume surge in 2030-2050. Specifically, global cumulative end-of-life panels could total 8 million metric tonnes by 2030 and up to 60-78 million tonnes by 2050. Limitations of the IRENA study include the use of outdated input data and simplified model assumptions. In this thesis, references will be made to this report, and the model is updated with new insights and scenarios.

Three generations of solar cell technologies. A conventional way to classify solar photovoltaic cell development is by first-, second-, and third-generation technology [27]. Cross-sections of the most common solar cells are presented in Figure 1-5. First-generation technology is marked by silicon wafers with p-n junctions, which emerged at useful efficiencies in the 1950s. Both monocrystalline (mono c-Si) and polycrystalline silicon (poly c-Si) cells belong to this category, with best research cell efficiencies ranging from 21.2-27.6%

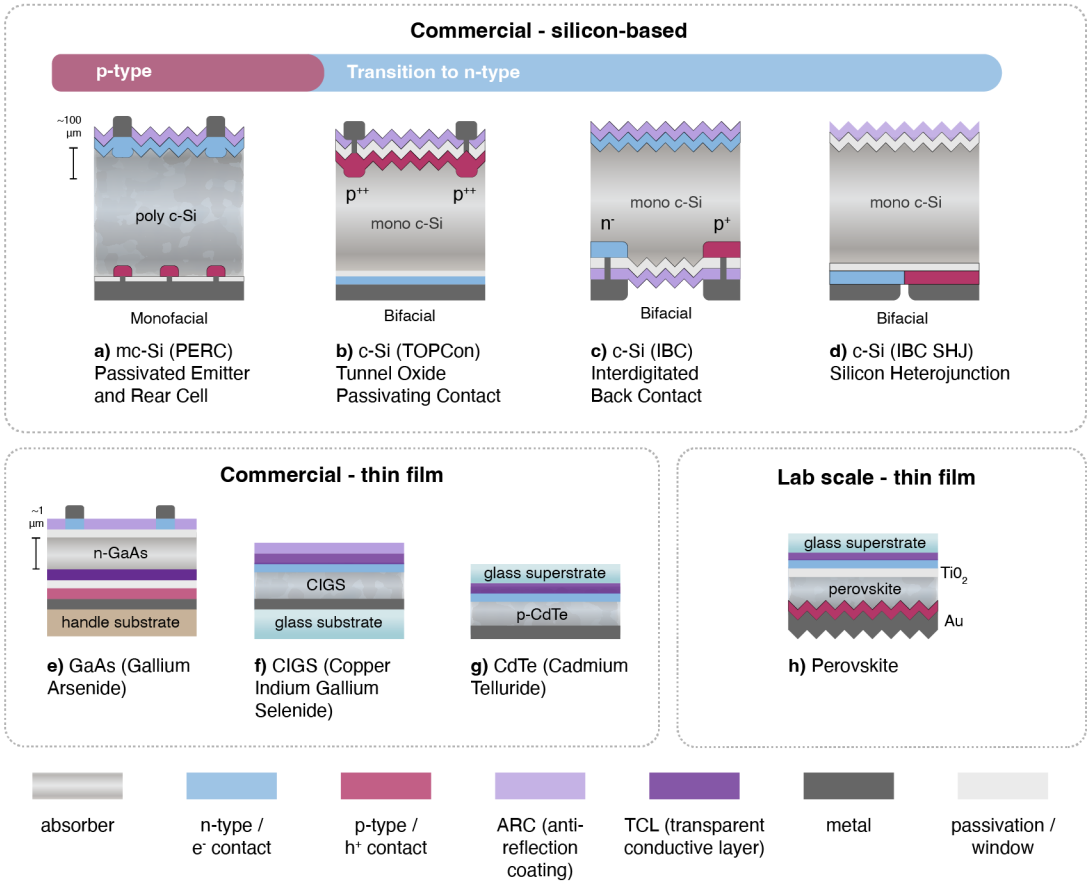

Figure 1-5: Cross-sections of the most common PV panels, adapted from [25][26]

[28]. First-generation solar cells currently make up the largest market share. A note on terminology: polycrystalline is the name of the raw material before it is made into the final ingot. Multicrystalline silicon is the technical name for the final product, but is referred to by both names, and will be called poly c-Si in this thesis because this is most often used.

Second-generation solar cells emerged in the 1970s with thin film technologies. Thin films have photoactive layers of just a few microns (µm) and efficiencies ranging from 14-23.6% [28]. Typically, technologies in this category are named after their active materials: amorphous thin-film silicon (a-Si), gallium arsenide (GaAs), copper indium gallium selenide (CIGS), cadmium telluride (CdTe), copper sulfide (Cu2S) and cadmium sulfide (CdS).

Third-generation solar cells include high-efficiency technologies that exceed the Shockley-

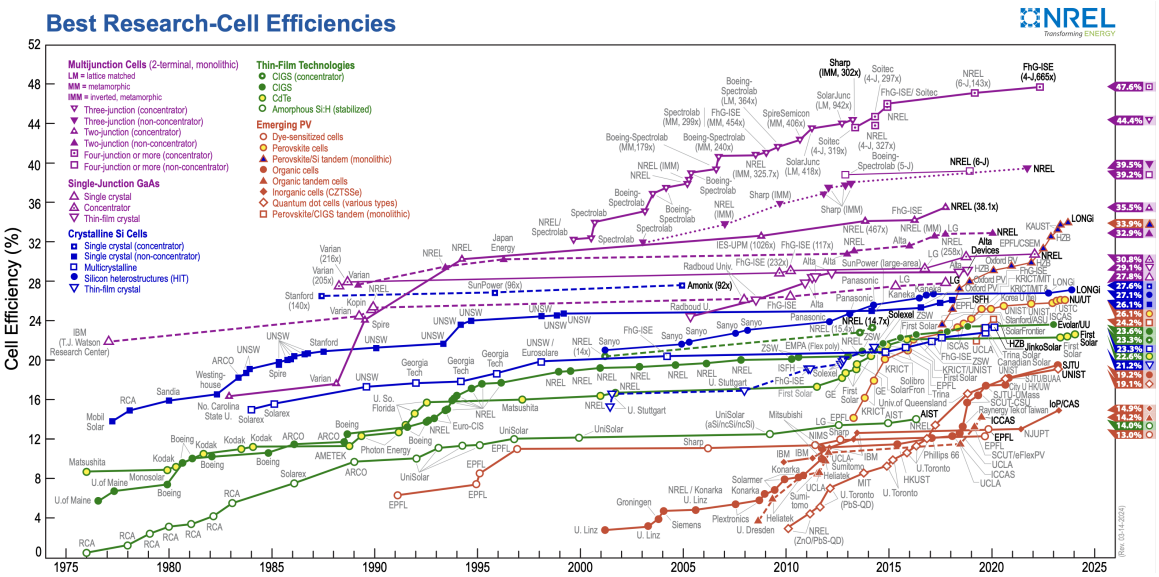

Figure 1-6: Record research cell efficiencies of solar PV technologies. This plot is courtesy of the National Renewable Energy Laboratory, Golden, CO. [28]

Queisser limit (SQ) for single-junction solar cells. With research cell efficiencies up to 47.6% [28], these solar cells perform above the maximum efficiency of about 33% at silicon's band gap of 1.1 eV and closer to the thermodynamic limit of 93% [29]. Multi-junction, concentrator, quantum dot, or intermediate band gap solar cells are all considered third-generation technologies [30]. A recent trend is a shift from monofacial to bifacial PV modules, where energy is captured on both sides of the panel to increase efficiency [26].

The photovoltaics industry is a fast-paced sector, and record PV cell efficiencies are updated periodically by NREL (see figure 1-6). To insiders, this graph is well-known and a primary focus of their research efforts. Chapter 2 provides a more in-depth historic perspective on materials used in solar PV technologies.

Environmental and social impacts: silicon in solar cells. As shown in figure 1-3, silicon is the fourth largest material in a c-Si PV panel by mass, and third-most valuable material after silver and copper. Because most panels on the market are silicon-based, there is a relatively large volume of this material in the waste fraction, offering significant opportunities for recovery. Therefore, specific focus is given to silicon in this thesis. Although this is one of the most abundant elements on the planet, the high-purity required for solar

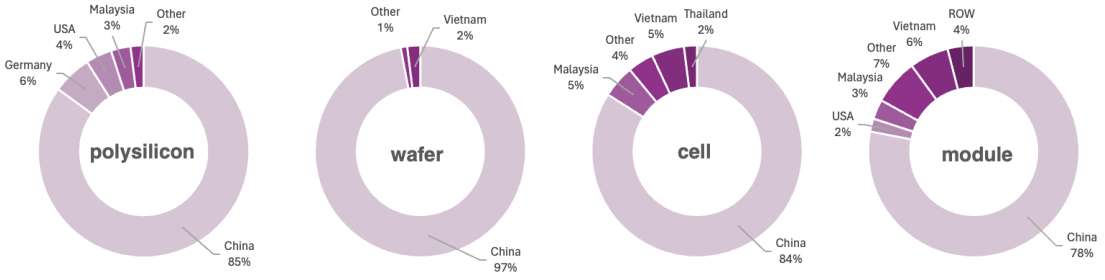

Figure 1-7: Production locations of high-purity solar-grade silicon (9R purity) into wafers, solar cells and PV modules. Adapted from [31]

cells demands significant processing. Prior research indicates that the highest embodied carbon in c-Si panels can be attributed to silicon production, especially the purification processes [32]. This is confirmed by an LCA study that evaluates the energy payback time and greenhouse gas (GHG) emissions of five technologies: mono c-Si, poly c-Si, a-Si, CdTe and CIS (copper indium selenide). Energy requirements were found to be highest for mono c-Si, and lowest for CdTe [33]. However, thin films pose a toxicity issue, and are known to use scarce minerals [34]. If toxicity is included as a metric, poly-Si performs better than CdTe on social impacts for health and safety, based on a study on domestic production in the US [35]. Figure 1-7 shows that the majority of polysilicon mining and processing of wafers, cells and modules occurs in China. An Environmental and Social Life Cycle Assessment of silicon PV modules indicate social hotspots during production, with forced labor of indigenous people from the Xinjiang region [36]. Compared to raw material extraction of silicon, solar PV recycling can offer social and environmental benefits. An integral LCA study to the environmental, social and economic effects of PV recycling in the Yucatan region in Mexico shows that recycling can reduce human toxicity and freshwater ecotoxicity by 78% [37]. Global supply chain security can also be improved through silicon recovery from end-of-life solar panels [12]. Despite these benefits, material recovery from end-of-life PV panels has not yet taken off due to economic and technical barriers [24]. In 2018, waste volumes were not high enough to justify recycling capacity, and companies went out of business [22]. Predictive modeling is needed to better time the material recovery potential.

1.3 Objectives

This study aims to provide insight into the expected quantities of materials in solar panels to reach end-of-life up to the year 2100. Most studies to date reach to 2050, and although this seems far away, it is already in about 26 years. All solar panels we place on the market today, will become waste in 2050. Given the large quantities of PV panels that will be decommissioned in the coming decades, the lifespan of a PV panel, and the consequences for recycling infrastructure investments, it is worthwhile exploring the stocks and flows at a larger timescale. The objective of this study is to quantify solar PV material demand, waste flows and secondary materials. Three questions are answered:

- What is the material composition of solar cells, and how does this impact the material recovery potential at end-of-life?
- How much waste from solar PV modules can we expect worldwide, from now to the year 2100?
- Is recovered silicon from recycling PV modules sufficient to meet demand for future panel production, and if so, when?

1.4 Scope

This study is a stock-based dynamic Material Flow Analysis (MFA) on solar photovoltaics. Three representative solar panel technologies are considered: mono c-Si, poly c-Si, and thin film including CdTe. These technologies are included because they form an heterogeneous waste profile at end-of-life.

Based on data availability, the geographic scope is global. For growth predictions, specific focus is given to countries with large installed capacity and emerging developing countries. The model is set up in a way to accommodate for regional analyses in the future. Historical data from the 1930s until 2023 is used for an analysis of current PV waste streams and its

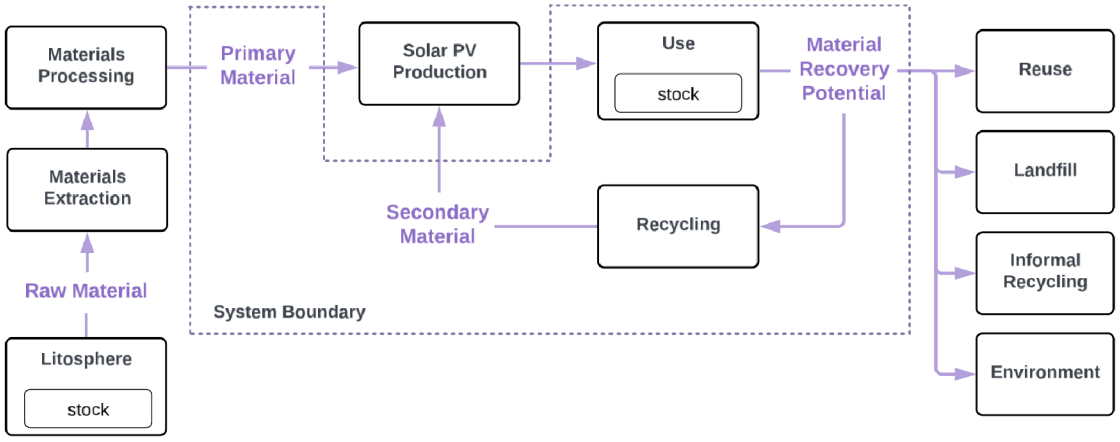

Figure 1-8: System boundary and key processes, stocks and flows.

composition in 2024. Future flows are predicted for 2024-2100. Main applications of solar PV include rooftop-mounted systems on residential and commercial buildings. In addition, dedicated solar fields are emerging end-uses with large installed capacity. Figure 1-8 shows the system boundary.

What this thesis isn't covering. This thesis solely focuses on solar photovoltaic (PV) technologies. Thermal heat and power generation, including solar thermal collectors and concentrated solar power (CSP), are out of scope. Only PV modules are considered, excluding mounting and inverters. Economic analysis is also out of scope for this study. While acknowledging the importance of costs as a driver for solar PV recycling behavior [38] and material recovery [39][40], it is not a main objective of this study to analyze financial aspects of solar PV material flows as this is sufficiently studied by others. Although the model calculates quantities of all materials in solar cells, valuable elements including silver and copper are not specifically highlighted in this thesis, because there already is an economic incentive for material recovery [41] [40].

1.5 Research design

The research design of this study is shown in figure 1-9. In the next chapter, the material composition of solar panels is evaluated based on characterization of historical artifacts. Chapter 3 introduces a mathematical model for predicting material flows and evaluating material recovery potentials from end-of-life solar panels. This chapter also provides an in-depth sensitivity analysis for the element silicon, and two future scenarios for solar energy demand. Conclusions and recommendations are given in chapter 4.

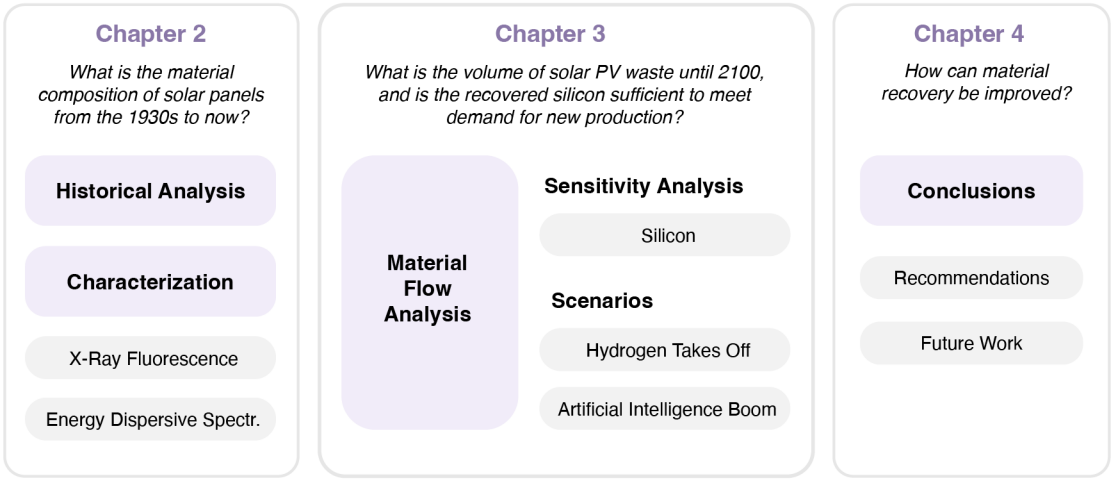

Figure 1-9: Research design of the study

1.6 Contributions

This research builds on prior methods and validates the reproducibility of the IRENA study. In addition, new insights are generated through the use of timely data and updated methods. The following contributions are made:

- Most analyses stop in 2050. This study continues to beyond 2100. Because a longer timescale is considered, replacement of existing installed capacity is included, and dynamic behavior is observed. This allows stakeholders to plan recycling capacity in a timely manner between now and the year 2100.

- This study considers all solar photovoltaic technologies and provides a retrospective analysis on cells from the 1930s to 2020s. Input assumptions in landmark papers are evaluated and new primary data (e.g. on material composition) is created through archival research and material characterization, in collaboration with the Museum of Solar Energy.

- The technology breakdown per material in this study adds more granularity to the potential waste streams, which allows for detailed predictions of secondary supply of materials of interest. Sensitivity analysis is made for silicon, for six parameters: installed solar PV capacity, thin film share, power per panel, weight-to-power ratio, average lifetime, and recovery rate.

- Two new scenarios are developed for projected installed solar PV capacity: demand from hydrogen production and artificial intelligence.

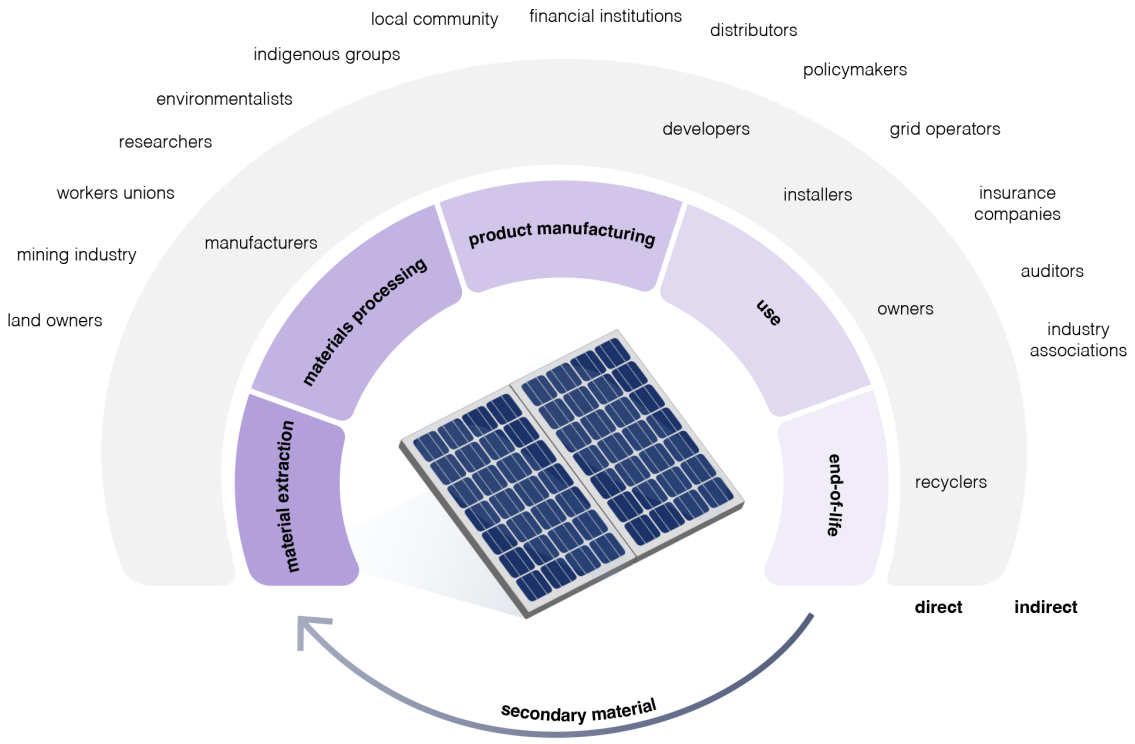

Figure 1-10: Direct and indirect stakeholders in the solar PV life cycle

To accelerate implementation of solar panel recycling on global and regional scales, this model helps five primary stakeholders gain more insight. Waste from end-of-life solar panels is recognized as a growing concern of *policymakers*, and this work can help regional governments define future policy and program development. For *recyclers*, it helps identify and plan future investments in recycling capacity. To *manufacturers*, this work is relevant in three ways; it helps predict the amount of secondary material available for circular production, proactively develop a take-back program to comply to the Extended Producer Responsibility (EPR), already in effect in Europe [21] and the state of Washington [16], and inspires to consider redesigning PV panels with EOL in mind. *Installers* can identify opportunities for expanding their business model to the decommissioning of PV modules. And lastly, it is useful to (prospective) *owners* or *developers* of photovoltaic systems to know more about what happens with the panels at the end of their service life. Secondary stakeholders include insurance companies, environmental groups and financial institutions.

1.7 Data availability

This research is preregistered with the Open Science Foundation (OSF). The project has a unique identifier (DOI 10.17605/OSF.IO/9DBJE) and the data repository can be accessed here: `https://osf.io/9dbje/`.

Chapter 2

Historical Analysis: What is the composition of solar cells?

> *"It doesn't matter how beautiful your theory is. If it disagrees with experiment, it's wrong. In that simple statement is the key to science."*–Richard Feynman

In a circular economy, traceability of materials is important. Material passports are proposed to gain information on composition. Yet the material composition of solar cells lacks granularity, as suppliers prefer to keep this information proprietary. Meaningful predictions on future waste (or resource) flows from discarded solar panels are based in a historic analysis of solar panels in prior decades. What can we learn from the past, to inform future design for recyclablity and reuse? The research objective of this chapter is:

What is the material composition of solar panels from 1990s until now?

To answer this question, a historical analysis is made based on primary sources in literature, artifacts from the Museum of Solar Energy will be studied, and two types of characterization experiments are prepared: X-Ray Fluorescence (XRF) and elemental analysis with Energy Dispersive Spectroscopy (EDS). Results are used as a benchmark to validate assumptions in the model in the next chapter.

2.1 State-of-the-art solar PV data

In policy recommendations for recycling of solar photovoltaics, the 2016 IRENA report is often cited for material composition. Figure 2-1 shows what materials are in c-Si, CIGS, and CdTe panels. Note that the 'other' category—accounting for 0.5% to 1% by mass—contains the active elements, such as cadmium (Cd) and Indium (In). In addition, as we will see in this chapter, the material composition and content changes over time. This figure does not take that into account, and offers insufficient granularity for policy decisions.

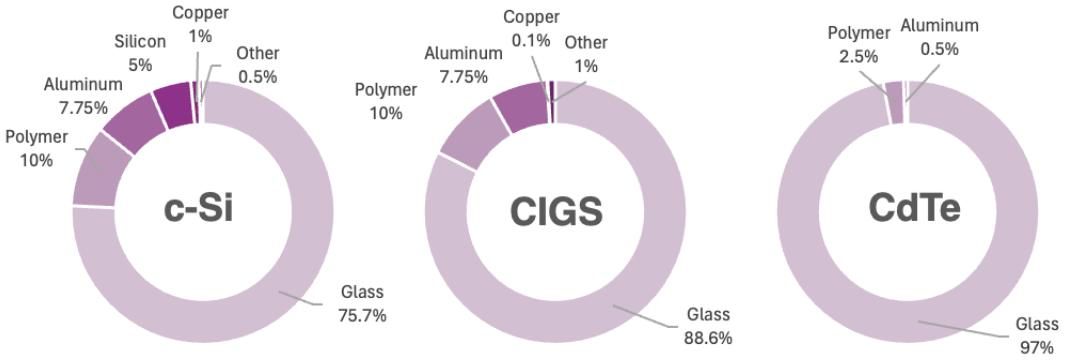

Figure 2-1: Materials required for PV panel production, sorted by technology (percent of weight) Adapted from [15].

Two datasets are needed to make future predictions on material flows: the annual share of PV technology (%) and material composition of the modules (%). State-of-the-art estimations of historical data and future predictions as known in literature are provided below, along with a brief evaluation of the uncertainties in these datasets. Figure 2-2 shows an estimation of the historical breakdown by PV technology deployment from 1980 to 2022, distinguishing between thin films and mono- and poly-crystalline silicon [42]. Fraunhofer is a leading solar PV research institute in Germany, and although this is a reliable source, a drawback of this report is that is not peer-reviewed.

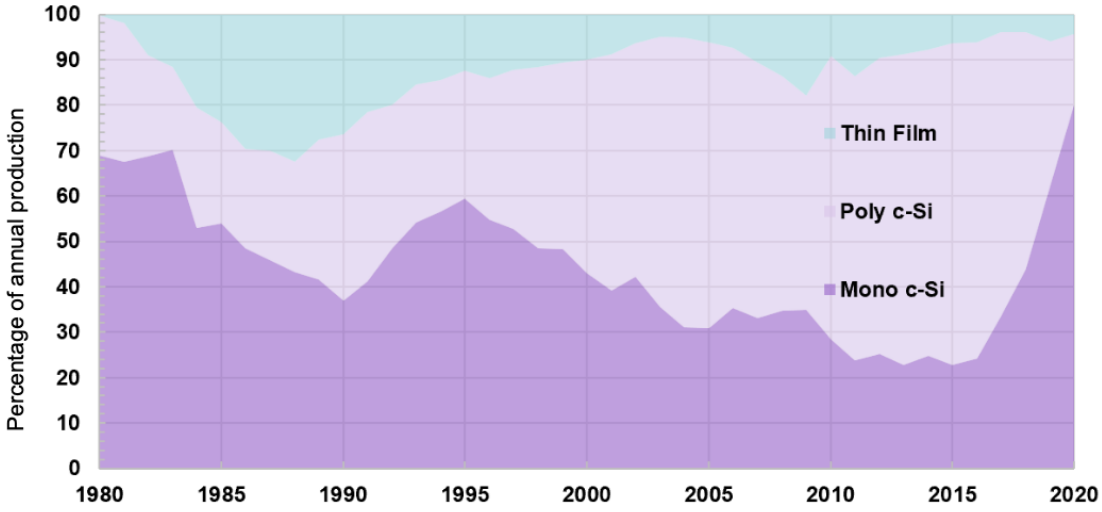

Figure 2-2: Breakdown by PV technology (Adapted from Fraunhofer [42])

Zooming in on material composition, Ovaitt et al. estimate the module composition (%) by mass over time, with historical data from 1995 to 2022 and future predictions until 2050 (see figure 2-3). In this study, the authors highlight the inconsistency between reporting sources and identify two main areas of potential error: historical data and projections [38]. This plot a best effort based on available data, and it should be noted that it contains subjective judgment. For example, module composition from 2030 to 2050 is assumed to be flat. As Jaxa-Rozen & Trutnevyte point out, "there are major sources of uncertainty in long-term global scenarios of solar photovoltaic technology" [43]. Therefore, the next section introduces sources that could reveal historical data about solar PV material composition.

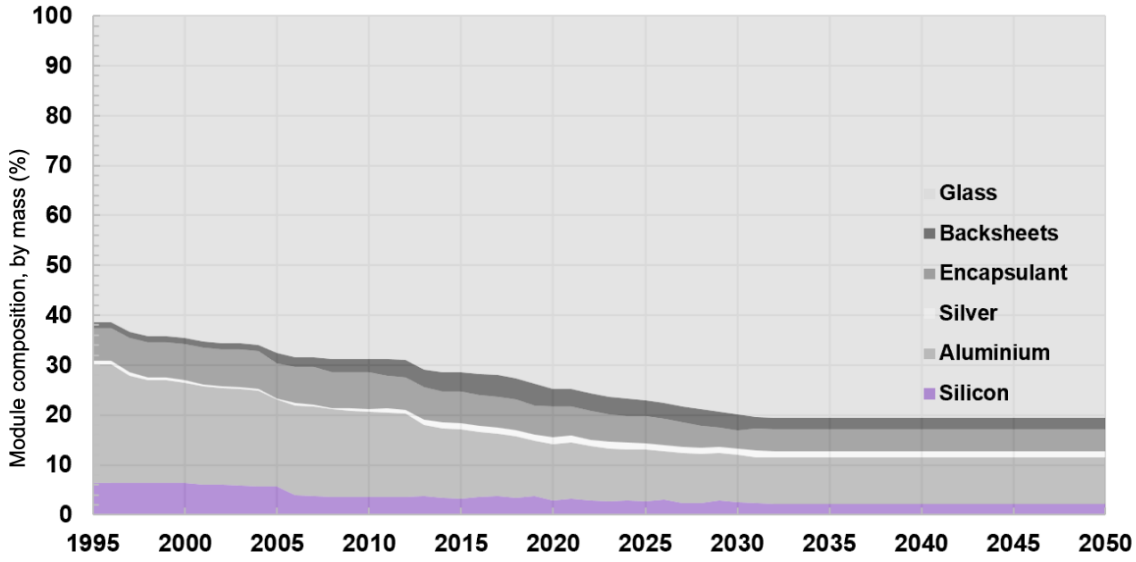

Figure 2-3: Annual module composition by mass percentage, as calculated from the material baselines presented here. 2030 values are assumed to be constant through 2050 (Adapted from Ovaitt et al.[38]) Silicon is highlighted.

2.2 Historical analysis of solar PV material composition

In search of information on the material composition of solar cells, I came across a promising source: the Museum of Solar Energy (MOSE) in Minnesota. Its curators have an extensive physical collection and maintain a digital archive [44], representing solar PV products of every decade from the 1920s up to the present day. The digital archive is primarily a repository of photos, supplemented by basic documentation including the name of the manufacturer, year of production, cell type, whether or not the solar cell is flexible and its primary use. The collection includes unique cells that once were consumer products, used in experimental research, went into space, or powered residential and commercial applications.

Material composition in datasheets. Although many older solar panels lack documentation, newer products often contain additional information on mass, efficiency, and dimensions. Some artifacts provide links to datasheets and supplemental information. Disclosure of the material composition of the cells and modules is limited to a generic description, such as 'Silicon', because manufacturers are not required to report the material composition of solar cells. The standards EU EN 50380, "Datasheet and nameplate information for photovoltaic modules" and IEC 62446-1:2016+A1:2018, "Photovoltaic (PV) systems - Requirements for testing, documentation and maintenance", prescribe to report PV module dimensions, power ratings at standard test conditions, and measures to ensure proper and safe operation. Newer datasheets contain material information at the module-level. For instance, a datasheet from First Solar reports: Cell Type (Thin film CdTe semiconductor, up to 264 cells), Frame Material (Anodized Aluminum), Front Glass (Heat strengthened), Back Glass (Heat strengthened), Encapsulation (Laminate material with edge seal), and Frame to Glass Adhesive (Silicone) [45]. On the datasheet, detailed information on solar cell materials or potentially hazardous substances are not provided.

Solar PV materials in science kit. To build popular support for technology in the 1960s, researchers at Bell Labs developed a series of four educational kits: From Sun to Sound (this included a small solar cell premade), Speech Synthesis, Experiments with Crystals and Light, and the Solar Energy Experiment (see figure 2-4). High school students were the

Figure 2-4: Bell Solar Energy Experiment, 1962. Karl Wagner / Museum of Solar Energy. Image used with permission.

intended audience and the creator of the solar energy kit, researcher Daryl Chapin, aimed to inspire and train new scientists to work in the field of solar energy, "so that you may use your own imagination to conceive future possibilities in this growing field." [46].

A photo of the inside of the box reveals information on material composition: Carborundum #280, Nickel Chloride (3 gr), Ammonium Chloride (2 gr), Sodium Hypophosphite, Boric Acid, Carborundum #600, Alundum, Ammonium Citrate (6.5 gr), and Calcium Fluoride. After inquiring additional information, the corresponding book was recommended: Energy From The Sun written by D.M. Chaplin for Bell Telephone Laboratories in 1962. What immediately stands out, is that the author seemed less concerned about material toxicity at the time of writing. The kit contained lead, three sheets of asbestos, and all kinds of chemicals including hydrofluoric acid. A firm warning is given in the introduction: this kit should only be used under supervision of a teacher, yet consequences of unsupervised use remain unclear. A strength of this book is that it provides both physics concepts and

practical how-to's with exact material quantities and protocols, described in meticulous detail rarely seen in contemporary academic papers. Anyone can understand this and make a solar panel from scratch. Therefore, this educational material can be seen as a precursor to contemporary DIY kits, for example those of the open-source synthetic biology movement. Future work offers opportunities to draw parallels and analyze why Bell Labs discontinued this experiment.

Obtained solar cells and modules for characterization. The Museum of Solar Energy generously provided a total of 43 artifacts, of which 30 solar cells and 13 modules, for material characterization at MIT. Tables 2.1 and 2.2 show that these items span almost a century of solar PV history, from the 1930s until 2020s. For each product the cell type is indicated along with a further specification, if available. For example, p-type and n-type indicate whether the silicon is either positively (P) or negatively (N) doped. When not specified, it is a conventional p-n junction. In the next section, the history of solar cell development will be told from a materials perspective, and the p-n junction is described in more detail.

Nº	**Year**	**Manufacture**	**Cell Type**	**Specification**
014	1954	Bell Labs	Mono c-Si	N-Type
070	1937	GE	Selenium	
190	2007	Suntech	Mono c-Si	
262	1931	Weston	Selenium	
265	2021	Ricoh	Thin Film	Dye-sensitized
296	2018	LG	Mono c-Si	N-type
298	2005	BP	Poly c-Si	
299	1998	Siemens	CIS	Copper Indium Diselenide
300	2004	GE	Mono c-Si	
301	1997	Siemens	Mono c-Si	
303	2003	UniSolar	Thin Film	Amorphous Si
306	2016	ACOPower	Mono c-Si	
307	1990s	Chronar	Amorphous Si	

Table 2.1: Solar modules provided by the Museum of Solar Energy, for nondestructive testing.

Nº	Year	Manufacture	Cell Type	Specification
003	2010	NanoSolar	CIGS	MWT
004	1998	UniSolar	Thin Film	Amorphous Si, triple-junction
006	1960s	IRC Astro	Mono c-Si	
009	1990s	Powerfilm	Thin Film	
011	1998	Spectrolab	Mono c-Si	Bi-Facial
015	2009	CSUN	Mono c-Si	
022	1998	Siemens	Mono c-Si	
027	2011	Canadian Solar	Mono c-Si	MWT
102	2017	DOW	CIGS	
109	1990s	Unknown	Poly c-Si	
117	1990s	Unknown	Poly c-Si	
118	1994	Evergreen	Poly c-Si	
119	2001	Sharp	Mono c-Si	
121	2018	Viko	Mono c-Si	Bi-Facial
123	1990s	Unknown	Poly c-Si	
124	1990s	Unknown	Poly c-Si	
155	1990s	Mobil?	Poly c-Si	
158	1970s	Unknown	Mono c-Si	
284	2004	SunPower	Mono c-Si	MWT
290	2020s	ALLMEJORES	Mono c-Si	Bi-Facial
291	2019	Ecosolifer	Mono c-Si	Bi-Facial, Heterojunction (HST)
292	2019	SunPower	Mono c-Si	
293	2003	SunPower	Mono c-Si	
294	2010	Unknown	Mono c-Si	
295	1990s	Unknown	Poly c-Si	
308	2008	Sanyo	Thin Film	Amorphous Si
309	1970s	Automatic Power	Mono c-Si	
310	1980s	Tandy Corp.	Poly c-Si	
311	2010s	ASCA	Organic	Dye synthesized (DSSE), transparent
312	2023	ALLMEJORES	Mono c-Si	Bi-Facial, PERC

Table 2.2: Solar cells provided by the Museum of Solar Energy, for destructive and/or nondestructive testing. MWT = Metal Wrap Through, a type of cell without busbars, Bi-Facial = cell collects light from both sides.

2.3 Historical context and development of solar cell materials

The historical context and trajectory of the development of solar cell materials can be organized in four eras: Early Discoveries, Development of Silicon Solar Cells, Emergence of Thin Films, and Nanofabrication and Tandem Solar Cells. Artifacts listed in the collection of the Museum of Solar Energy are a guiding reference for this analysis.

Early Discoveries (1839-1950s). When the French physicist Alexandre-Edmond Becquerel discovered the photovoltaic effect in 1839 [47], the possibility of harvesting electrical energy from the sun became a reality. Materials used in Becquerels' experiment include "an electrolytic cell consisting of platinum and silver plates separated by a thin membrane immersed in an acidic silver chloride solution" [48]. At the time of discovery, the fundamental principle of photoelectricity was not yet understood. That changed in 1905, when Albert Einstein described the photoelectric effect [49] —a phenomenon where particles are emitted from a material exposed to light or electromagnetic radiation—for which he received the 1921 Nobel Prize in Physics. Electrical engineer Willoughby Smith discovered the photoconductivity of another material, selenium, in 1873 [50], but it wasn't until 1883 when the first selenium-based solar cell was invented by Charles Fritts. Using "many different metals and substances as bases for selenium cells", he preferred to use "brass, zinc, iron or copper thinly coated with tin." [51]

Bell Labs was a leading institute in the early history of solar cell development. In 1940, researcher Russell Shoemaker Ohl accidentally discovered the foundational principle of a solar cell: the p-n junction. By purposefully introducing impurities into the semiconducting material silicon, a method called doping, electrical properties of a material are altered. A crack in Ohl's silicon sample caused a gap between positively charged holes (p) and the negative charge of the electrons (n), resulting in electric current flowing into one direction [52]; hence, the working principle of a solar cell (US Patent US2402662A [53]). Though promising, these early prototypes with silicon wafers were expensive and had low performance, with less than 1% efficiency.

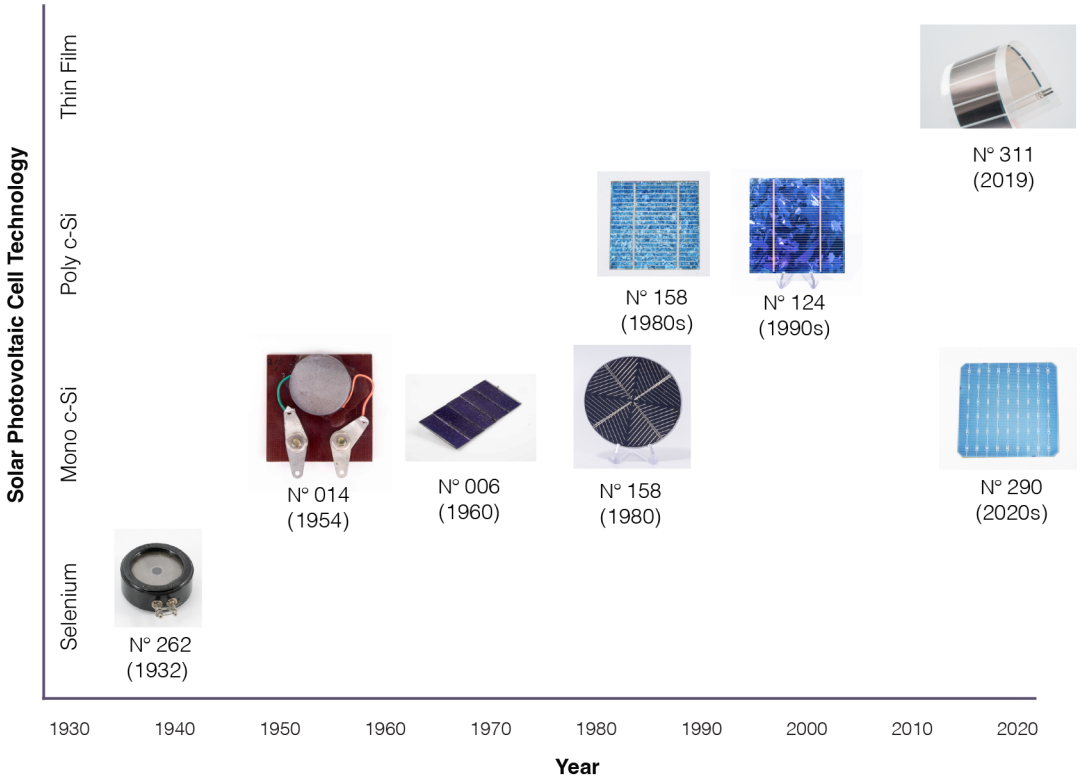

Figure 2-5: PV technology timeline based on selected solar cells and modules provided by the Museum of Solar Energy. Image credits for pictograms: Karl Wagner / Museum of Solar Energy. Images used with permission.

Development of Silicon Solar Cells (1950s-1970s). By the 1950's, most research efforts still focused on selenium solar cells (artifacts 262, 277, 1743). At the time, engineer Daryl Chapin was a solar cell researcher at Bell Labs. His colleagues, chemist Calvin Fuller and physicist Gerald Pearson, convinced Chapin to shift focus away from selenium to silicon, after they succeeded in making a p-n junction by introducing gallium impurities to silicon and dipping it in lithium. The three started a collaboration, and lithium was replaced by arsenic and boron to overcome technical performance issues. A more stable p-n junction with better electrical contacts was created, and in this material composition impurities no longer migrated away from the surface [52]. This was a successful endeavor—the Bell Labs team presented the first practical solar cell in the spring of 1954, with a record efficiency of 6% [54]. According to MOSE, these solar cells (artifact 2068) still produce power today.

This invention marked the beginning of monocrystalline silicon solar cell development. In the 1950s and 60s, most solar photovoltaic products were developed for aerospace applications, such as the IRC Astro (artifact 006) and small consumer electronics including radios, toys, and small motors (e.g. artifacts 3411, 214 and 1844). In 1962, Chapin launched the educational Solar Energy Experiment Kit (artifact 264) that includes all materials to make a solar cell and describes step-by-step processes in great detail. In the 1970s, the first commercial and residential solar cells appeared. As a result of the cylindrical shape of a silicon ingot, cell geometry of these early solar panels was circle-shaped. In consumer electronics, solar cells were now integrated in more products including watches, jewelry and calculators. In the 1980s, cell arrangement was optimized for space savings with rectangular-shaped cell geometries, which led to higher cell packing density and module power outputs.

In the 1970s, polycrystalline silicon emerged as a cheaper alternative to monocrystalline silicon. Instead of the Czochralski crystal growth process (accounting for 40% of the cost of a mono-c-Si module [55]) the directional solidification technique [56] was used to create lower-cost polysilicon with large grains [57]. Ribbon cells are another effort to reduce costs and waste of solar cell production. Instead of slicing wafers from ingots, silicon is directly grown in sheets or ribbons. Processes include edge-defined film-fed growth (EFG), dendritic web approach [56], and edge stabilized ribbon (ESR) by MIT professor Emanuel Sachs [58].

Emergence of Thin Films (1970s-2000s). In the Fraunhofer diagram of PV production by technology in figure 2-2, thin films made up 30% of the market share in the late 1980s. What technologies and materials were dominant during that time? In 1976, the first amorphous silicon (a-Si) cells were developed by Carlson and Wronski. This cell is only 1 µm thick, has a band gap of 1.55 eV, is cheaper than single-crystal silicon, and has a reported efficiency of 2.4%. The authors estimate the theoretical efficiency to be 14-15%. Materials used are boron (doping in SiH4 and B2H6 atmosphere), indium, tin oxide, glass, phosphorus (doping in SiH4 and PH3 atmosphere), and aluminum [59]. Other thin films developed in the mid 1970s and continued until the present day include copper indium gallium diselenide (CIGS) cells with a reported lab efficiency of 23% and cadmium telluride (CdTe) cells with a present-day efficiency of 22.1% by First Solar. Unfortunately, both technologies require materials that are either scarce (indium, tellurium, gallium) or toxic (cadmium). Another drawback of CIGS cells is that they deteriorate faster in outdoor conditions than the more robust silicon cells [48]. Similarly, Cu2S-CdS cells experienced stability problems due to the selection of contact materials. A paper in 1984 describes the Clevite production process and demonstrates how the use of silver for the CdS layers and electroplated gold or graphite for the Cu2S layers is instrumental in solving this issue [60].

Nanofabrication and Tandem Solar Cells (2010s-Present). Examples of emerging technologies include dye-synthesized, perovskites, organic solar cells, and quantum dots. Two technologies are highlighted here: perovskites and organic photovoltaics. Perovskite nanocrystals—first discovered in 1839 as calcium titanate (CaTiO3)—first applied in a solar cell in 2009 [61]. Novel manufacturing methods, including roll-to-roll fabrication of perovskite modules [62], allow for faster production and lower cost. In tandem, perovskites are combined with (poly)crystalline cells [63], with research cells reaching up to 33.9% efficiency [28]. Materials in perovskite solar cells include TiO2 and CH3NH3PbI3, leading to concerns about the toxicity of lead. Therefore, an emerging research area for solar cells include solutions that aim to rely less on scarce and toxic materials. Organic photovoltaics (OPV) are polymer-based thin films and offer interesting material properties including transparency [64] and flexibility, making them suitable candidates for aesthetic integrations in buildings and consumer products. Examples of materials in these devices are polyethylene

terephthalate (PET), Parylene-C, silver nanowire ink, tin oxide nanoparticles, tin-coated copper tape, Dyneema Composite Fabric, and ITO (indium tin oxide) [65]. In this context, the term 'organic' may be confusing to the broader public. Lastly, we are coming full circle with selenium. After more than 70 years, this element is back on the scientific radar, as selenium-silicon cells are now combined in tandem devices [66].

2.4 Characterization with X-Ray Fluorescence

Materials characterization makes it possible to learn more about the elemental composition of the 43 solar cells and modules. The search space is large, because we do not know exactly what materials are in the samples. Nondestructive characterization is performed with X-Ray Fluorescence (XRF) using a Bruker Tracer-iii Handheld XRF instrument. This method identifies what elements are present in the solar cells (especially metals and heavier elements), and gives a general idea of material composition. Semi-quantitative analysis can be performed under certain conditions. It should be noted, however, that this approach does not provide a quantitative analysis of the amount of materials in a sample. Another limitation of this technique is that the instrument only detects elements with atomic numbers above 12 (magnesium). Lighter elements including boron (atomic number 5), often used as doping, will not be detected. Results should therefore be treated as indicative and preliminary. Still, given these limitations, we can roughly determine what materials are in the samples and identify regions in the spectra that would benefit from more detailed examination in future research. This instrument is the appropriate tool for that purpose.

2.4.1 Experimental setup and approach

This work was performed in part in the MIT.nano Characterization Facilities, and the test setup and sample placement are shown in figure 2-6. For improved safety, the handheld XRF instrument is fixed on a mount and samples are positioned on top. A cap blocks ionizing radiation from the x-rays and the process is closely monitored with a Geiger counter. The following parameters were used: voltage: 40 kV, current 10 µA, time 60 sec, and no filters were used.

Of the 43 solar cells and modules, 33 were successfully scanned. Most of the modules were unsuitable for XRF in the current setup due to space constraints. The only attempt to scan a module was with the selenium-based Weston from 1931 (sample 262) and some thin films. Selenium was not detected in the results, because the x-ray depth was insufficient to probe through the glass. After this experiment, focus was redirected to cells. Three representative

Figure 2-6: X-Ray Fluorescence setup.

silicon cells from various decades are selected for in-depth analysis in this section. These are sample 309—a monocrystalline silicon cell from the 1970s, sample 118—a polycrystalline cell from 1994, and sample 312—a Bi-Facial PERC monocrystalline silicon cell from 2023. Raw data from the XRF scans of these samples is presented and interpreted in the section below. All other results are available in the supplementary information to keep this chapter focused.

Before samples are scanned, a blank scan was taken to determine background noise levels (table 2.3). For example, rhodium is emitted from the x-ray source and palladium from the detector. Traces of other elements naturally appear in the air, or are part of the plastic sheet (e.g. aluminum, silicon, calcium, titanium and iron). During data interpretation, the net intensity (Net) of the blank is subtracted from the sample's net intensity, resulting in a corrected net intensity (Net_corrected). This will either confirm the presence of an element, or indicate levels so low it may be in the error margin.

No.	Element	Line	Energy/keV	Cycl.	Net	Backgr.	Sigma	Chi
1	Al	K12	1.486	10	153	915	45	1
2	Si	K12	1.74	10	54	954	44	0.84
3	P	K12	2.01	10	87	1250	51	2.2
4	S	K12	2.309	10	413	2383	72	5.91
5	Ar	K12	2.958	10	17166	5226	166	4.26
6	Ca	K12	3.692	10	1169	3483	90	0.84
7	Ti	K12	4.512	10	1037	5594	111	2.98
8	Fe	K12	6.405	10	3837	9692	152	33.29
9	Ni	K12	7.48	10	2617	9557	147	13.5
10	Cu	K12	8.046	10	2838	8664	142	2.72
11	Zn	K12	8.637	10	1162	8271	133	1.67
12	Rh	K12	20.216	10	813	2320	74	1.12
13	Rh	L1	2.697	10	22880	4849	180	11.63
14	Pd	K12	21.177	10	2089	1724	74	5.29
15	Pd	L1	2.838	10	1532	5213	109	6

Table 2.3: Blank XRF scan to identify background levels.

2.4.2 Data analysis

Data analysis is performed in Bruker Artax Spectra software. The XRF User Guide [67] by a former Bruker employee is consulted for data analysis and interpretation. The basic principle of X-Ray Fluorescence is that atomic energy levels of elements are detected by firing high energy photons (gamma rays) onto a sample. Atoms consist of various electron shells (K, L, M, N), and the migration of electrons between these shells is relevant to XRF interpretation. If an element is present, the x-rays knock out electrons from the atom's inner shell. Atoms are now in an excited state and the open position in the shell (valence) is filled with an electron from an outer shell, releasing fluorescence radiation in the process. Each element has a characteristic energy level, and this is how elements can be identified on XRF spectra. In the spectra presented below, two axes are plotted: pulse count on the y-axis and x-ray emission level (keV) on the x-axis. Peaks with high pulse counts indicate energy levels emitted from a specific electron shell. When identifying elements, there has to be a match for the K and L emission lines.

Pulses per keV (red line) are analyzed with a Bayesian Deconvolution algorithm (blue line). At approximately 18.5-19.5 keV, the inelastic scatter results in a *compton peak*. This peak can be disregarded in the analysis. In addition, *sum peaks* may appear when the energy of two photons from an element with a sufficiently high count are detected as one single photon and incorrectly summed up at higher atomic energy levels in the spectrum. We will likely encounter sum peaks as a result of the major presence of silicon in solar cells. To indicate confidence in the results, a 'low', 'medium', or 'high' certainty is given for each element. The section below provides an interpretation of the spectra for three representative solar cells from the 1970s, '90s, and '20s.

Sample 309. Preliminary results of identified elements in solar cell 309 are shown in table 2.4. For this mono c-Si solar cell from the 1970s, the XRF spectra in figure 2-7 shows distinct peaks for tin (Sn) and lead (Pb). Therefore, a high certainty is given for these elements. Similarly, silicon and nickel are also clearly visible. Medium certainty is given to copper because the K-beta line is in the shoulder of lead, which makes it harder to distinguish. Elements that received low certainty are calcium and iron. Calcium is detected with a high

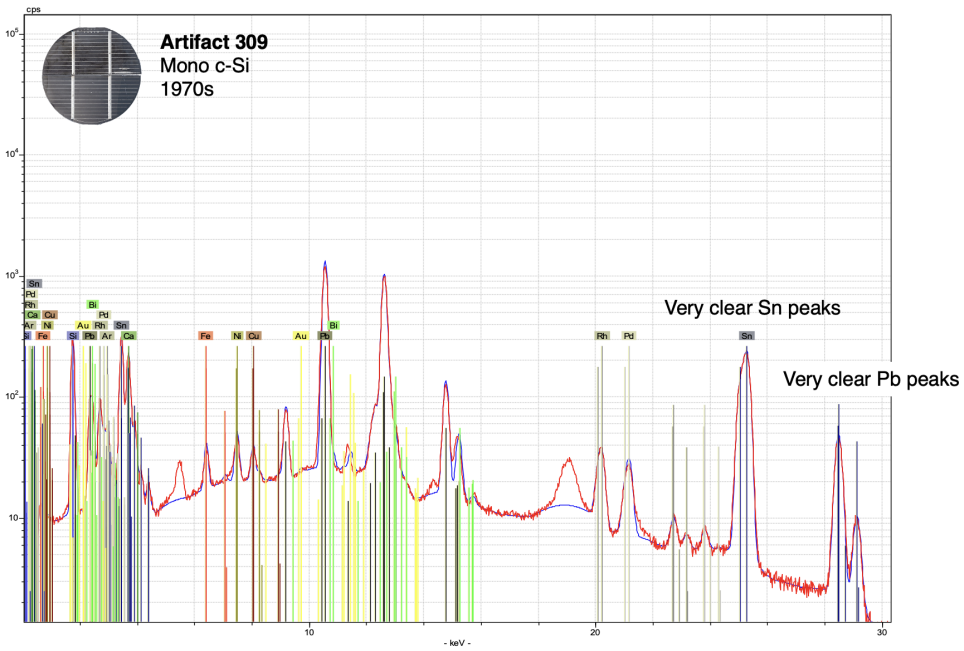

Figure 2-7: XRF results of solar cell 309. Pictogram of a monocrystalline silicon cell from the 1970s. Karl Wagner / Museum of Solar Energy. Image used with permission.

net count at approximately 3.7 energy/keV, but this also appears to be in the region of the K-beta peaks of tin. Iron may or may not be present, because there is no K-beta peak at the position where this is expected, at approximately 7 keV.

The following elements identified by the software are ignored: argon, rhodium, palladium, bismuth and gold. After subtracting the net intensity of the blank test, argon's corrected net intensity becomes negative. The elements rhodium and palladium have a negative L1 peak and are also discarded. The software identified bismuth in the L1 shell, but lacks a clear M1 line. Most energy is allocated to the background noise, and bismuth is therefore omitted from the results. Lastly, gold has an L1 line but lacks the M1 line and is excluded for this reason.

Sample 118. Preliminary results of identified elements in this polycrystalline silicon cell from 1994 are presented in table 2.5 and the raw data is displayed in figure 2-8. Identified elements with high certainty include silicon and silver. With medium certainty, aluminum, nickel, zinc, and lead are present. Two elements of higher uncertainty are germanium and

Element	Line	Energy/keV	Net	Backgr.	Net_corrected	Certainty
Si	K12	1.74	93015	6909	92862	High
Ca	K12	3.692	13656	17890	12487	Low
Fe	K12	6.405	10200	16523	6363	Low
Ni	K12	7.48	14050	20314	11433	High
Cu	K12	8.046	9007	20322	6169	Medium
Sn	K12	25.271	242156	10295	242156	High
Sn	L1	3.444	108582	16195	108582	High
Pb	L1	10.551	653981	27198	653981	High
Pb	M1	2.342	22407	11575	22407	High

Table 2.4: Preliminary XRF spectra results of solar cell 309.

palladium. After correction, germanium has a net intensity of 2847 counts, and palladium 1952 in the K12 line and 4812 in the L1 line; higher than observed in other samples. No conclusive answer can be given for these elements, however, and this preliminary observation requires re-testing and further examination. Holmium, a rare earth element, was identified in the Bayesian deconvolution, but is removed because it has a negative value in the M1 line. Copper is also removed from the analysis, because its corrected net intensity in the K12 line yields a negative value. Similarly, bismuth has an M1 line of 0 after correction. Gold is removed because its M1 line only has a count of 1.

Championed as the most sustainable solar cell on the market in the 1990s, sample 118 is advertised for the use of lead-free solder. Yet, the measured results indicate the presence of small quantities of lead. In the datasheet, Evergreen Solar claims to "outperform thin films and achieve comparable performance to bulk crystalline technologies while using half as much silicon", where the reduction in silicon is achieved through string ribbon technology. Compared to other samples, the peak is indeed smaller. In future work, this claim can be confirmed with methods capable of quantitative analysis.

Sample 312. The newest solar cell is a Bi-Facial monocrystalline silicon PERC cell from 2023. XRF results can be found in table 2.6 and figure 2-9 displays the spectra. With high confidence, silicon is present in this solar cell. Medium confidence is given for the presence of silver. Despite the clearly visible peaks at 2.9 keV and 22 keV, the L1 line only shows a count of 1 after correction. In the region between 4 and 14 keV this sample shows a

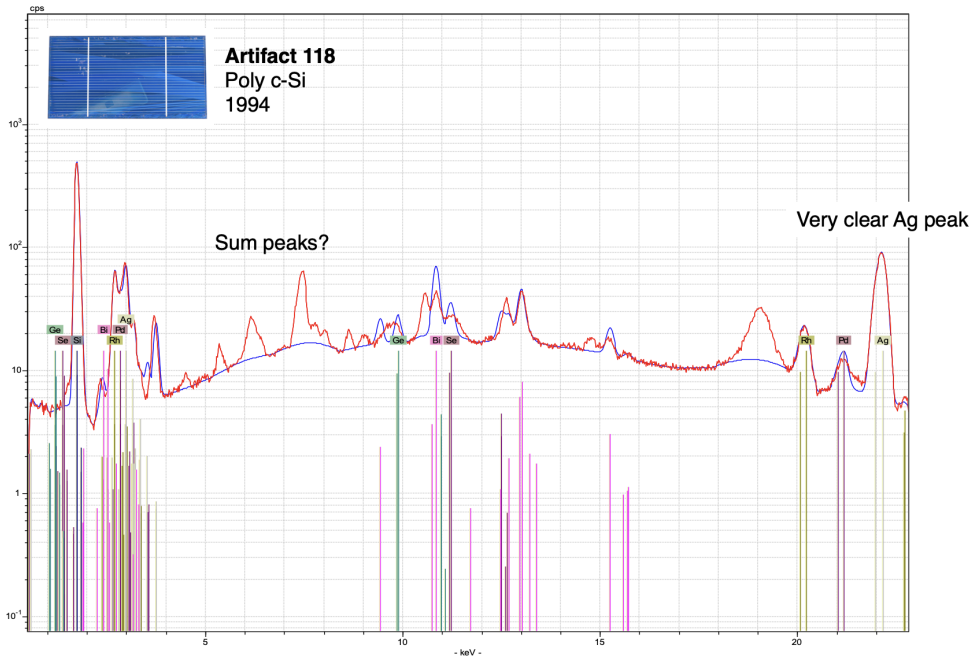

Figure 2-8: XRF results of solar cell 118. Pictogram of a polycrystalline cell from 1994. Karl Wagner / Museum of Solar Energy. Image used with permission.

different pattern compared to cells from other decades. More smaller peaks are visible, and the line is flatter. Because of the small peaks, nickel, copper and zinc are identified with medium certainty. Also with medium confidence, is the presence of cobalt in this spectrum. An order of magnitude higher activation energy is measured with gallium and bromide. Medium certainty is given to bromide because the Bayesian Deconvolution maps a peak in a region where the K-beta line is not present. This seems to be a sum peak, because of the wide base of the peak. The peak of gallium has a more narrow base, but this may also be a sum peak or back-scatter. Elements discarded from the analysis are sulfur, argon, calcium, and titanium, because their energy levels give a negative net count after correction for environmental noise. Palladium is listed with a low certainty, because the corrected net value still has a remaining energy level in both K12 and L1 levels. Low certainty is given because the presence of palladium in solar cells seems unlikely. This will be further discussed in section 2.5.1.

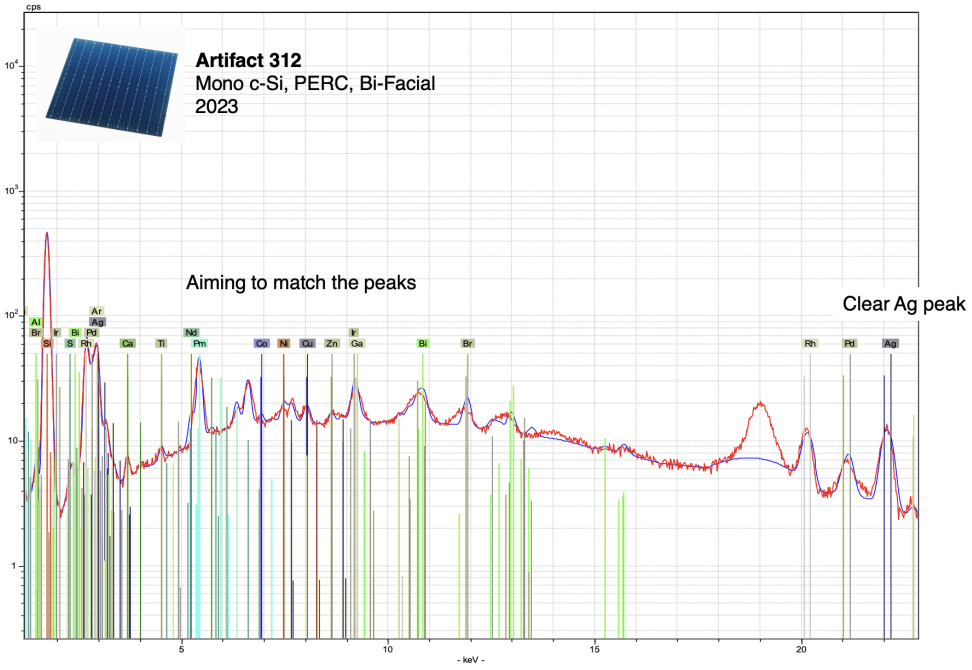

Figure 2-9: XRF results of solar cell 312. Pictogram of a Bi-Facial PERC monocrystalline silicon cell from 2023. Karl Wagner / Museum of Solar Energy. Image used with permission.

2.4.3 Validation with Energy Dispersive Spectroscopy

Next, the three solar cells are examined with a second characterization method. To evaluate the material composition from a different perspective, Energy Dispersive Spectroscopy (EDS) was performed. This characterization method enables semi-quantitative analysis, and is not only able to identify *what* elements, but also approximate *how much* of the elements are present. Of primary concern is the concentration of silicon, to benchmark assumptions made in literature and prior work.

This is semi-quantitative preliminary data, and additional samples will need to be analyzed for better statistics. All elements with concentrations down to 0.25 atomic percent in the upper few microns of material are indicated. Elements with concentrations below 0.25 atomic percent cannot be reliably detected using this approach, but could be measured using other techniques in future work. Figure 2-10 contains the compositional results from the three samples.

Element	Line	Energy/keV	Net	Backgr.	Net_corrected	Certainty
Al	K12	1.486	802	3096	649	Medium
Si	K12	1.74	145290	2831	145236	High
Ni	K12	7.48	11025	16040	8408	Medium
Zn	K12	8.637	30822	17609	29660	Medium
Ge	K12	9.886	2847	18450	2847	Low
Pd	K12	21.177	4041	7940	1952	Low
Pd	L1	2.838	6344	8972	4812	Low
Ag	K12	22.163	29225	6941	29225	High
Ag	L1	2.983	21522	9330	21522	High
Pb	L1	10.551	3305	17584	3305	Medium
Pb	M1	2.342	362	3648	362	Medium

Table 2.5: Preliminary XRF spectra results of solar cell 118.

Element	Line	Energy/keV	Net	Backgr.	Net_corrected	Certainty
Al	K12	1.486	1126	2681	973	Medium
Si	K12	1.74	164400	2789	164346	High
Co	K12	6.931	721	14438	721	Medium
Ni	K12	7.48	3121	15765	504	Medium
Cu	K12	8.046	2390	15543	504	Medium
Zn	K12	8.637	1848	16132	686	Medium
Ga	K12	9.251	3310	16389	3310	Medium
Br	K12	11.924	5633	17501	5633	Medium
Pd	K12	21.177	3957	7297	1868	Low
Pd	L1	2.838	1843	6900	311	Low
Ag	K12	22.163	9650	6101	9650	Medium
Ag	L1	2.983	1	6532	1	Medium

Table 2.6: Preliminary XRF spectra results of solar cell 312.

In addition, elemental composition can vary across a sample depending on the regions analyzed, the extent of surface damage or contamination, the depth/volume analyzed, and the features that are present, such as traces and contacts. To try to reduce some of these variabilities, a 5 mm x 5 mm area of each sample was analyzed.

The comparison of EDS and XRF results is presented in figure 2-11. For each cell, four elements overlap. Confirmed elements across the two methods include silicon, tin, lead and aluminum for the solar cell from the 1970s (sample 309). The polycrystalline silicon cell from 1994 (sample 118) contains silicon, silver, aluminum and zinc. Sample 312, the Bi-Facial PERC cell from 2023 contains silicon, silver, aluminum and zinc. It should be

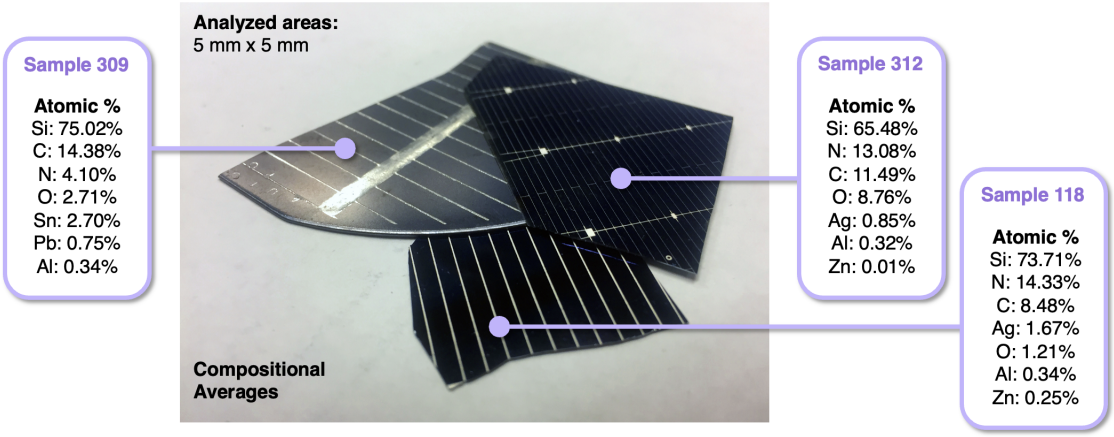

Figure 2-10: Material composition of samples 309, 118 and 312 through Energy Dispersive Spectroscopy (EDS). Photo credits: James Weaver

noted that with the current XRF setup, aluminum is more challenging to identify because it is a light element (atomic number 13) at the edge of the detection limits. In addition, its energy level (1.486 keV) is close to that of silicon (1.74 keV) in the spectrum, with photons becoming almost indiscernible in the vicinity of the high Si peaks. Because EDS considers the presence of elements based on concentrations above 0.25 atomic percent, this technique is more reliable for the detection of aluminum.

Based on three data points, the concentration of silicon seems to decline over time across technologies, from 75.02% in the 1970s, to 73.71% in 1994 and 65.48% in 2023. Aluminum is present in all three cells, with a steady 0.34% in the '70s and '90s and lowers to 0.32% in 2023. Silver is only present in the two newer cells, with almost double the concentration in the cell from the '90s (1.67%) compared to the one from the 2020s (0.85%). Tin is only used in the cell from the '70s, and zinc in 1994 and 2023, with a concentration of 0.25% and 0.01% respectively. Future work includes more measurements on all solar cells, to draw comprehensive conclusions.

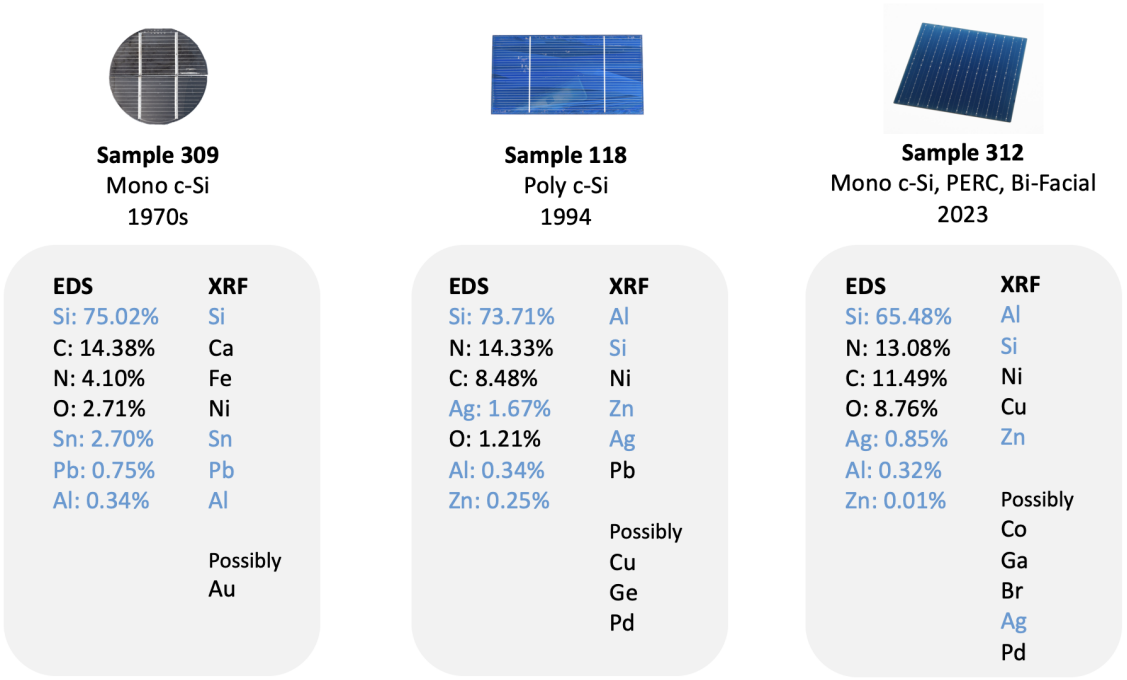

Figure 2-11: Comparison of preliminary EDS and XRF results for samples 309, 118 and 312. Corresponding elements are indicated in blue. Pictograms of solar cells. Karl Wagner / Museum of Solar Energy. Images used with permission.

2.5 Lead in solar cells

It is well-known that lead has high toxicity, leading to a range of irreversible health issues [68]. The presence of lead in samples 309 and 118 gave rise to the need for further examination and XRF positively confirmed this element in 14 out of 33 solar cells (Figure 2-12). A trend in lead-use over time is observed in mono- and poly c-Si cells, especially in cells until 2010. None of the tested thin films in this collection showed the presence of this element, although it is known that scientists working on perovskites try to move away from lead-use [69]. As mentioned above, sample 118 from 1994 still contained lead, but peaks were less strong relative to the other cells. The claim of the manufacturer seems justified, and can be quantitatively verified with destructive research and more extensive sample preparation. PV panels from the '80s and '90s are now entering the waste stream, and solar cell recycling facilities should take caution to protect their workers from exposure.

2.5.1 Preliminary data: rare-earth elements and conflict minerals

Preliminary XRF measurements indicated the possible presence of rare earth elements (REE) in solar cells. Of the three studied samples, this is mostly visible with the PERC solar cell sample (nr.312). When peaks are identified in the software, the Bayesian deconvolution poorly correlates experimental data in the region between 4.5 and 7 keV. However, when neodymium and promethium are included in the spectrum, the Bayesian fit matches the trajectory of the peaks, as was shown in figure 2-9. Some, but not all, of these results can be explained by sum peaks and should be ignored. Yet, if this observation is correct, the 'flatter' and more conjugated region (4.5-7 keV) compared to older solar cells seems to indicate an interaction between multiple elements. Given that these were only found with XRF and not with EDS, scarce and rare earth elements are likely present in small quantities below the detection limit of EDS (0.25 atomic percent). Because this phenomenon was also observed in other samples (mostly from recent years) it requires follow-up testing.

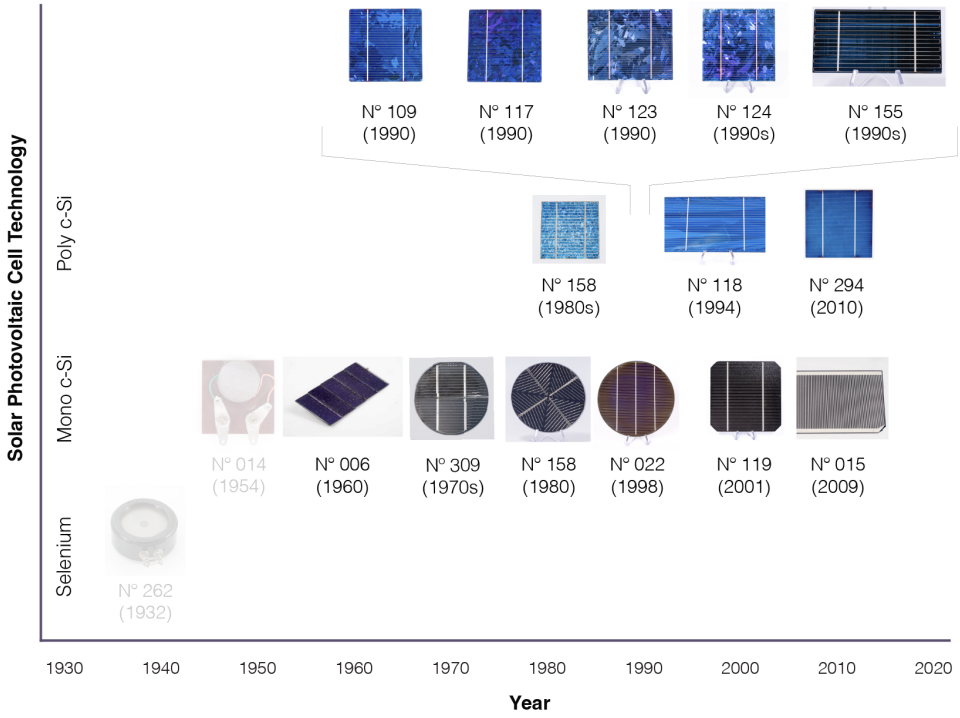

Figure 2-12: Various mono- and poly c-Si solar cells contain lead. Pictograms of solar cells. Karl Wagner / Museum of Solar Energy. Images used with permission.

In the broader search space of all 33 scanned solar cells, results may indicate the presence of traces of praseodymium (Pr), holmium (Ho), erbium (Er), ytterbium (Yb), neodymium (Nd), praseodymium (Pm), europium (Eu), scandium (Sc), indium (In), germanium (Ge) and gallium (Ga), to name a few. Cobalt (Co), bismuth (Bi) and tantalum (Ta) were found.

An observation in the XRF results is that the lack of a strong M1-line alongside a high L1 count does not necessarily mean an element is not present. For instance, with solar cell 312, silver received 'low certainty' because of the weak L1 peak. Yet, EDS revealed a silver concentration of 0.85% and confirmed its presence. In other samples, gold and rare earths have a similar net intensity profile as the silver in sample 312, and may therefore exist despite low net intensity in XRF results. Before conclusions are drawn too quickly, it should be stressed that results are indicative and testing with filters for the 4.5-7 keV region is required to confirm this. Until then, these elements are omitted from table 2.6.

Compared to the literature, it is verified that most of these materials are used solar cells. For example, a substance flow analysis from 2015 demonstrates the presence of germanium, gallium and indium [70]. In an effort to reduce lead in perovskites, 1% samarium iodide (SmI2) was added [71]. Solar PV supply chain challenges for silver, indium and bismuth are extensively covered in another study [72]. Neodymium is used as doping for TiO2 in dye sensitized solar cells [73] and to partially substitute lead (II) ion in perovskites, where the authors mention that rare earth ions "such as Nd3+, Eu3+ and Sm3+, have been widely used to reduce the impurity phases" [74].

Palladium is another element that was found with XRF. This element is in the detector of the handheld XRF instrument. Some samples show a significant net intensity for palladium after subtracting the blank scan, which may indicate the presence of this element in solar cells. In multi-junction GaAs-based thin-films, palladium nanoparticles are used for performance improvements [75]. For organic solar cells, palladium impurities are a problem due to residuals from its use as a catalyst to make the conjugated polymers [76].

Less rare, but still a critical material [77] and conflict mineral, is cobalt. For mono c-Si PERC cells, cobalt is widely reported as an impurity introduced during the sawing process of silicon ingots [78]. Dye-sensitized solar cells are known to have cobalt as an input material [79]. Given that these were not found with EDS, scarce and rare earth elements are likely present in small quantities (e.g., applied as coatings).

It is already more profitable to recover gold (and copper) from e-waste than to mine it [80], with significantly lower environmental impact [81]. Compared to a TV, cellphone, or refrigerator, solar panels are simple products. Being able to recover scarce and rare elements from discarded panels will likely be more cost-effective than mining them.

2.6 Weight-to-power ratio based on experimental results

After identifying the material composition of solar cells, we can zoom out again and turn our focus to observing trends in solar PV development over time. The weight-to-power-ratio of each cell is now calculated, and this ratio will be used as an input variable for the model in the next chapter.

Mass, density and surface area. Physical properties are measured with basic instruments to allow for comparison between the cells and modules across decades. Results of these measurements can be found in Appendix A. Mass, thickness, and calculated values for surface area and density are shown in table A.1 for the modules, table A.2 for the cells, and table A.3 for cells 309, 118 and 312 measured with higher precision. The mass of each solar cell is measured with the digital scale OHAUS Compass CX1201. It has a precision of one decimal (0.1g) and maximum capacity of 1,200 g. Two modules exceeded this mass, and were weighted using a kitchen scale with a precision of 1g. Cell thickness and dimensions are measured with an SPI 15-719-8 electronic caliper. If dimensions for length and width exceeded the range of the caliper, they were measured with a tape measure. Based on the measurements, surface area and density are calculated for each cell and module.

Cell thickness and surface density. When all measurements are combined in one plot, trends can be observed. Cell thickness and surface density of solar cells and modules (1930s-2020s) are displayed in figure 2-13 (a) and (c), and the solar cell development by technology over time (1960s-2020s) in (b) and (d). A long-term trend can be observed for silicon solar cells, especially mono c-Si, because of the good data availability. The modules, and thin film, CIGS and organic cells do not have enough data points to derive any trend. In the Fraunhofer report [42], cell thickness is assumed to be constant, however, this experimental data suggests a decline over time. Cell thickness steadily reduces from the 1960s to the 2000s, and declines to 200-150 µm in the 2020s. This trend toward thinner wafers is also confirmed by [26], especially for n-type solar cells. Thinner wafers require less materials (primarily silicon), thus, less materials will be returned at end-of-life. For cells, surface density (g/cm2) is also dropping (c and d), which is mostly driven by thinner cells.

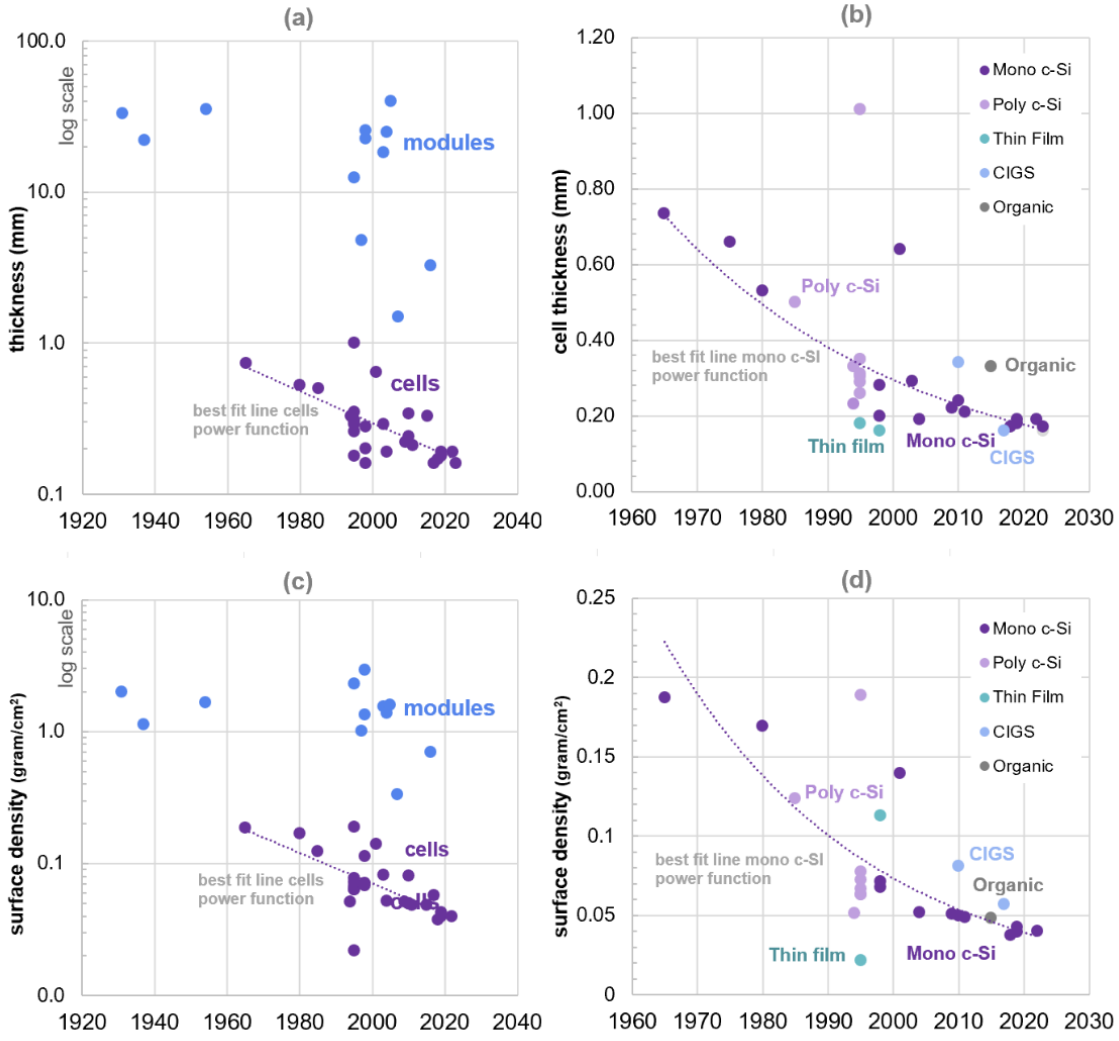

Figure 2-13: Solar cell thickness (mm) and surface density g/cm^2 from the 1930s to 2020s. a) Thickness of cells and modules. b) Cell thickness over time sorted by technology: mono c-Si, poly c-Si, CIGS, Thin Film, Organic. c) Surface density over time for cells and modules. d) Surface density of cells by technology.

Weight-to-power ratio. To calculate the total mass of solar cells, the amount of material needed is dependent on two key metrics: panel efficiency (W/m2) and cell thickness (mm). Therefore, the next step is to add the power output of each solar cell. Power output is found in datasheets available in the online archive of the Museum of Solar Energy, provided by suppliers, and in historical sources. The performance of the IRC Astro cell is found in an 1959 article from the American Radio History archives [82]. Solar cell efficiency tables

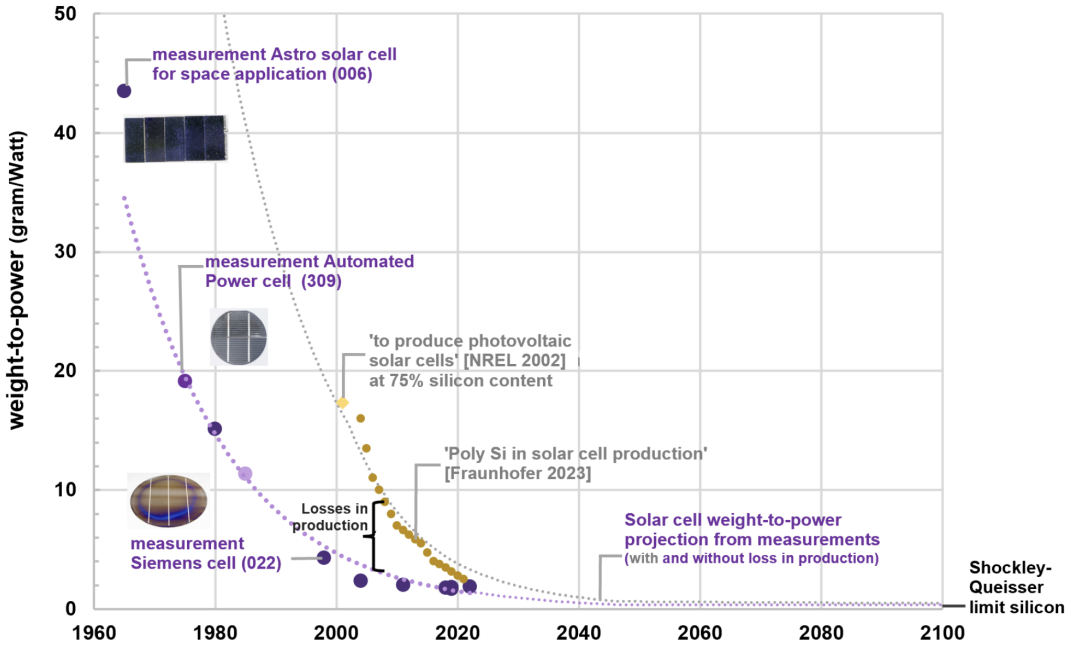

Figure 2-14: Weight-to-power ratio of mono c-Si, poly c-Si and thin film solar cells from the 1960s to 2020s, based on experimental results. An exponential fit is applied to mono c-Si, and a coefficient of determination R^2 of 0.9915 is found.

[83] were also consulted. Figure 2-14 presents the weight-to-power ratio of solar cells from the 1960s to 2020s. This is the cell weight divided by its power output. As efficiency increases and/or mass reduces, the weight-to-power ratio declines. This is an important metric because it determines how much material is required to achieve the same amount of power.

An inspiration to investigate material composition was the statement by NREL researchers in the introductory chapter, that very little historical information on solar cell composition is available [38]. Both NREL and Fraunhofer have no data before 1995 and the 1980s, respectively. This limits the understanding of the development of solar cells, relevant to raw materials required and end-of-life predictions. In general, power ratings from panels before the 1990s are indeed more challenging to obtain. The measurements of solar cells and modules in this chapter allow for a 'fitting' of how the solar cell mass has developed compared to surface area and power output. Figure 2-15 compares the experimental results with the Fraunhofer study. Reported wafer thickness is in general alignment with the

experimental data, and values are slightly lower than the measurements (fig. 2-15 e). In the reference study, cell thickness remains fairly constant whereas the experiment shows a declining cell thickness over time. A recent study confirms a faster decline in wafer thickness, and predicts 125-140 µm for the best available technology (assuming n-type mono c-Si) in 2032 [26]. This is in line with the observed trendline in cell thickness.

A larger difference is observed in the weight-to-power ratio (fig. 2-15 f), where the reference is about twice as high. This is explained by its definition: the measured values are 'cell mass (g/W)' and Fraunhofer reports 'poly c-Si consumption in solar cell production (g/Wp)'. These are two different concepts. One reason for the difference could be that most of the measured samples are either from the US or non-Chinese producers, whereas Fraunhofer reports about Chinese wafers. Cells and modules from the US historically have a higher power output, leading to a lower weight-to-power ratio. Second, double the amount of material required for Si production can be explained by the 60% of kerf, or losses, during silicon production [84]. This is a significant waste flow. Material demand and losses during the manufacturing phase of solar cells is out of scope for this thesis, but this finding presents a good opportunity for further investigation in follow-up research.

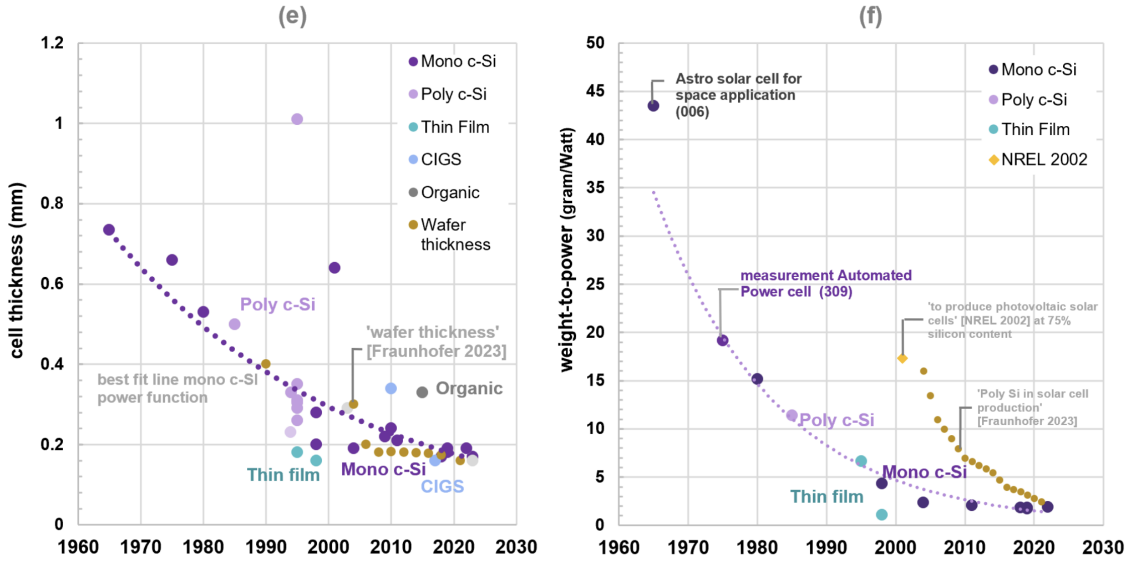

Figure 2-15: Cell thickness and weight-to-power ratio of mono c-Si, poly c-Si and thin film solar cells compared to Fraunhofer report.

Chapter 3

Predictive Model: What is the potential for material recovery from solar panels?

"All models are wrong, but some are useful"–George E. P. Box

This chapter investigates the scale and implications of the growing number of end-of-life solar panels entering the global waste treatment system. Through a dynamic Material Flow Analysis (MFA) the potential for secondary materials recovery from discarded solar panels is examined. The research question for this chapter is: *What is the potential for material recovery from decommissioned solar panels?*

As mentioned in the introduction, the 2016 study [15] by IRENA-IEA is a guidance for this model. Estimates for the cumulative PV capacity and PV panel waste volume until 2050 are given. In the IRENA report, a 30-year PV module lifetime is assumed to model regular-loss and early-loss scenarios. Key findings are that global cumulative end-of-life (EOL) PV modules could total 8 million metric ton by 2030 and up to 60-78 million metric ton by 2050. Compared to 43,000 t (regular-loss) or 250,000 t (early-loss) in 2016, this indicates a significant PV waste volume surge in 2030-2050.

Limitations of the IRENA study include the use of outdated input data and simplified model assumptions. Moreover, although this is the most comprehensive study to date, the input assumptions are over 10-30 years old. For instance, the Photon database [85] was accessed in 2015 for standard panel data sheets from 1990-2013, and standard panel data were predicted using the 2014 International Technology Roadmap for Photovoltaic (ITRPV). Newer ITRPV publications leading up to 2023 contain more accurate information on PV cell composition and global trends [86]. This is an important assumption, thus the data quality of this report is assessed in this thesis work. The authors of the IRENA report also indicate in their uncertainty analysis that the scenarios should be considered "order of magnitude estimates and directional rather than highly accurate or precise, owing to the simple assumptions and lack of statistical data". Photovoltaic technology is evolving rapidly, and timely information is required for optimizing material recovery. Therefore, this chapter provides an update to the model, addresses uncertainties in the data, and includes more recent publications and technologies.

3.1 Model setup and approach

For the global analysis, a top-down approach is taken because an aggregate of individual countries often leads to data gaps, and is a time consuming process. Figure 3-1 contains the six methodological steps of this study. Steps 1 to 3 primarily follow the methodological approach of the 2016 report by IRENA and IEA-PVPS [15]. First, to gain an understanding of this seminal work, as it provides a foundation to most state-of-the-art models for PV waste predictions. Second, to validate the prior work through replicability, and, where relevant, propose improvements. For example, contributions can be made in areas where data is outdated. In step 1, the method based on global installed PV capacity is chosen because it is generally well-reported, and PV panel mass can roughly be derived from those numbers. For PV panel characteristics, technology assumptions are made based on the most common PV panels representative for the current state, with datasheets from suppliers.

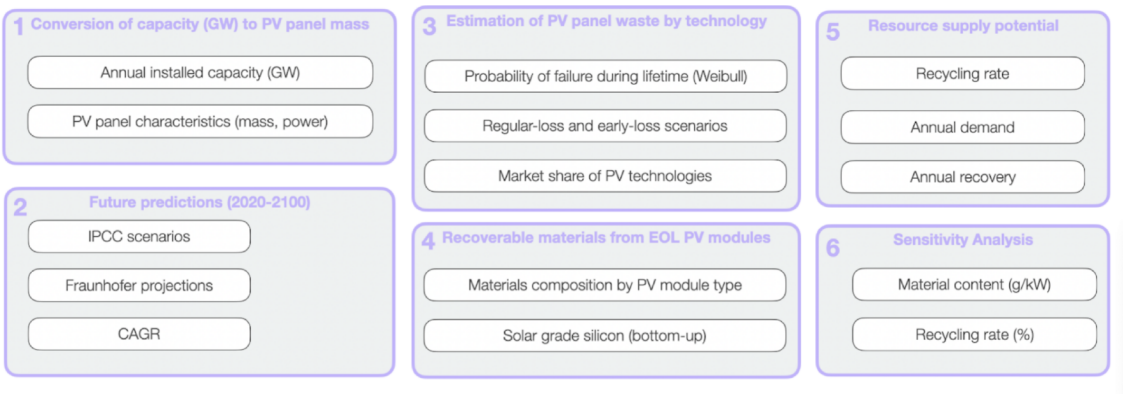

Figure 3-1: Method for calculating global PV panel waste and material recovery potentials.

For steps 4 and 5 of this analysis, the methodology presented in the recent paper by Song et al. on PV panel waste in China [87] provided inspiration because the authors take a technology-based approach and include material composition in their analysis. Compared to IRENA, this study adds more granularity on a material level, to find the recovery potential of materials and calculate resource supply potential from secondary materials, to be used in new production of PV panels. This idea is therefore adapted in this thesis. In addition, an MFA on rare earth elements in Europe [88] provided guidance on structuring the analysis.

The material recovery potential (step 4), resource supply potential (step 5), and sensitivity analysis (step 6) are examined in more detail for one material: silicon. This is motivated by a sentence in the Material Flow Analysis handbook [89]: "Each balance alone provides limited information. The ensemble of all balances yields a comprehensive understanding of the material flows. Hence, both balances of goods and substances are necessary." Thus, this study evaluates a good (solar panel) as well as a substance (silicon). The MFA handbook is consulted for calculating stocks and flows, with this equation:

$$m_{stock}(t) = \int_{t_0}^{t} \dot{m}_{input}(\tau)d\tau - \int_{t_0}^{t} \dot{m}_{output}(\tau)d\tau + m_{stock}(t_0) \tag{3.1}$$

3.1.1 Uncertainty analysis and data quality

The emphasis of this model is on statistical evaluation with probabilistic distributions. To calculate uncertainties of the output data, Monte Carlo simulations were performed with normal, log-normal, and triangular distributions. Weibull distributions were applied to estimate the probability of the lifetimes of solar panels and calculate regular-loss and early-loss scenarios as proposed by the IRENA-IEA-PVPS report [15].

Sensitivity analysis involves adjusting a single factor within a model to explore the impact on the overall results. In this study, a sensitivity analysis is made for silicon, to study the effects of two parameters: Si material content (g/W) and recycling rate (%).

Lastly, a pedigree matrix is used to evaluate the quality of some of the input data. Five data quality indicators—Reliability, Completeness, Temporal correlation, Geographical correlation and Further technological correlation—are rated from one to five. For this study, the method of Laner et al [90] is selected because it is specifically tailored to MFA.

3.2 Material Flow Analysis

3.2.1 Global installed capacity (GW)

Figure 3-2 shows global cumulative installed PV capacity, and consists of historic values and future predictions. Most historic values are reported in megawatts (MW). Given that the future installed capacity will scale rapidly, the global installed capacity is converted from MW to GW. Based on estimated PV learning curves for c-Si, a-Si, there was an approximate 10 MW installed capacity in the 1980s. Values between 1980 and 1992 were found by linear interpolation between the points, using the compound annual growth rate (CAGR). Historic values from 1992-2022 are reported by IEA-PVPS.

Future PV capacity until 2050 is estimated based on three IEA scenarios: Announced Pledges, Net Zero, and Stated Policies as provided in the World Energy Outlook dataset [91]. Future PV capacity from 2050 until 2100 is based on the IPCC medium scenario S2. This scenario projects a solar energy demand of 200 Exajoule per year for 2100 [92]. Values between 2050 and 2100 are calculated with linear interpolation. In addition, the IPCC S5 scenario aligns with the IEA Announced Pledges beyond 2050. For annual installed capacity after the 2050 IEA Net Zero scenario, a linear interpolation is made on the top uncertainty range of the interquartile range of the IPCC scenario.

For comparison, two projections are included from literature: Bloomberg and IRENA. Bloomberg is indicated with light grey dots and predicts the highest installed capacity [93]. Assumptions in the original 2016 IRENA report indicated in dark grey dots. Their expectation of installed capacity is lower than all IPCC projections and the current track.

Figure 3-3 shows the global annual installed capacity—how many gigawatts of solar PV will be installed each year. Similar to figure 3-2, the base scenario in this study is the IEA Announced Pledges until 2050 combined with the IPCC S5 (middle scenario) until 2100.

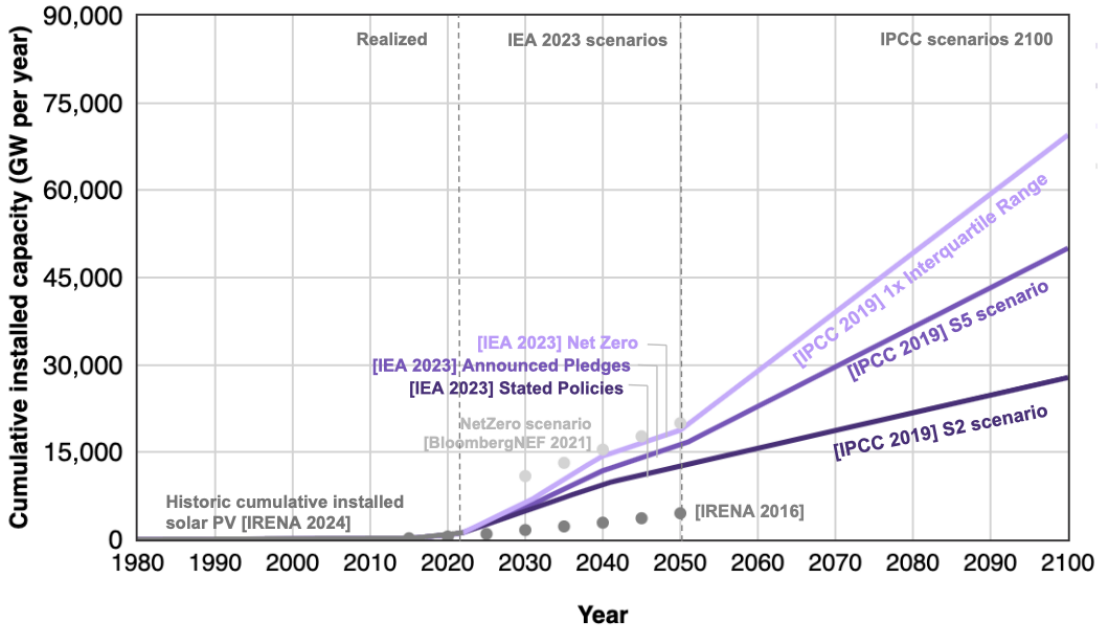

Figure 3-2: Global cumulative installed PV capacity and future projections (GW/year), compared to Bloomberg and IRENA.

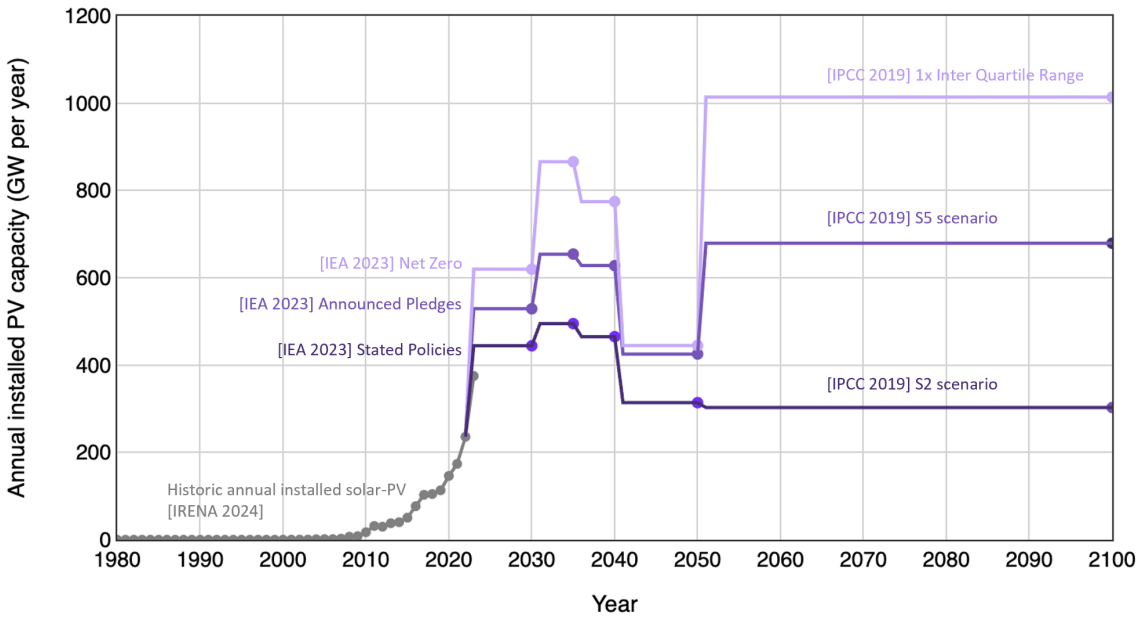

Figure 3-3: Global annual installed PV capacity and future projections (GW/year)

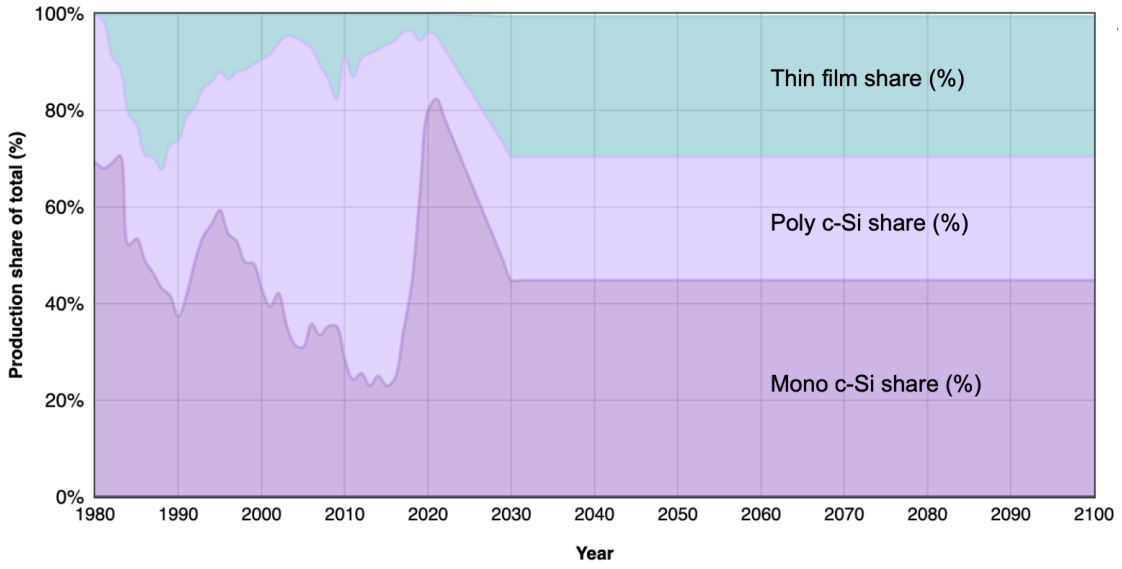

Figure 3-4: Annual PV module production, by technology (data from 1980-2030 [42])

3.2.2 Solar PV market share by technology

To obtain solar panel mass, a technology breakdown is made to divide the annual production by panel type. Data from 1980-2022 is based on historic values reported by Fraunhofer [42] and were shown in figure 2-2. Projections until 2030 are based on IRENA. Beyond 2030 the technology breakdown per panel type is considered to be constant, in line with Ovaitt et al.[38], and assumed due to the high uncertainty. Combined, figure 3-4 becomes the PV technology input for the model. Based on historical data thin film is expected to grow, especially for CdTe with an annual PV module production of 8.5 GWp in 2023 [42], but this can also decline again over time, as we have seen since the 80s.

3.2.3 PV panel weight-to-power ratio (metric ton/MW)

The next step is to obtain the material demand for each type of solar panel technology. The weight-to-power ratio consists of the panel weight divided by the rated power of each panel (figure 3-5). The measurements in the previous chapter are used to model the weight-to-power ratio until 2100, including the estimated losses during production for each year.

Average power output per panel (W)			Average mass per panel (kg)			PV panel weight-to-power ratio (t/MW)		
Mono-Si	Poly-Si	Thin Film	Mono-Si	Poly-Si	Thin Film	Mono-Si	Poly-Si	Thin Film
385	270	455	22	18.5	33.3	57.1	68.5	73.2

Table 3.1: Results PV panel weight-to-power ratio (t/MW) in 2022

The mass of each panel is obtained from the specification of one of the large manufacturers of each type: mono-Si (22 kg), poly-Si (18.5 kg) and thin-film (33 kg). Thin-film's high mass is based upon First Solar 6-series panels. For earlier years, the average panel power was obtained from Fraunhofer [42]. For the years 2022 to 2035 applies a 2.9% compounded annual growth rate, the rate observed from 2010 to 2022. After 2035 a slower 1% annual improvement is estimated up until 2100. In this base model, the panel weight is assumed to remain constant over time. The result of this step is the total estimated material demand for each panel type for each year. Table 3.1 includes results of the weight-to-power ratio for the year of 2022.

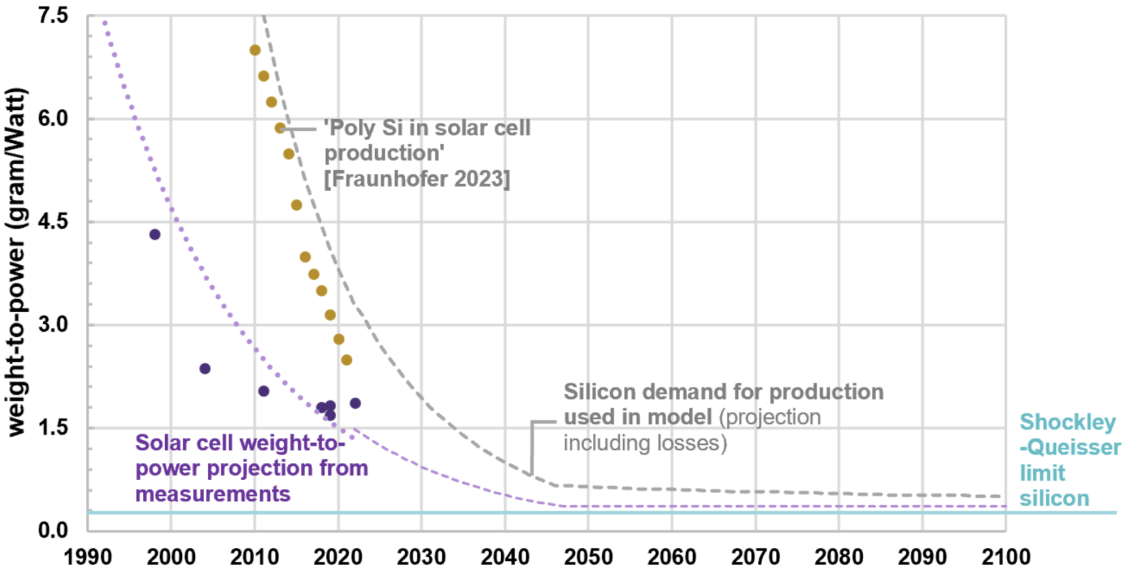

Figure 3-5: Solar PV weight-to-power ratio, estimate (kilotonnes/GW)

3.2.4 Loss scenarios with Weibull distribution

The next analysis step evaluates the probability of PV panel failure, when the installed panels reach their end-of-life. For the model it is only relevant to know when these panels become waste. Solar PV modules are reported to have an average *technical service life* of about 25 years. However, as technology advances, cell efficiency increases, and costs drop, solar modules are more frequently replaced before their technical service life. This is called *early replacement*. One study evaluates the lifecycle impacts of replacing PV modules after 15 years for efficiency gains [94]. Extreme weather events also contribute to the need for replacements [95]. Table 3.2 shows how long solar panels last according to various studies.

Type	**Technical Lifespan**	**Early replacement**
Mono c-Si	30, 50, 24 [96]	10, 15 [94], 14 [96]
Poly c-Si	30	10, 15 [94], 14 [96]
Tandem	40 (SunPower Maxeon)	

Table 3.2: Average lifespan (years) of solar power modules

3.2.5 The Weibull function

The timing of PV panel failure or intentional replacement varies per system, and some reach their technical lifespan sooner than others. Because each solar PV module will reach end-of-life at a different rate, loss scenarios are calculated with a probability distribution. The Weibull function will be used to calculate return flows.

The probability distribution function (PDF) of the Weibull function is:

$$f(x) = \begin{cases} \frac{k}{\lambda}(\frac{x}{\lambda})^{k-1} e^{-(x/\lambda)^k}, & \text{if } x \geq 0 \\ 0, & \text{if } x < 0 \end{cases} \tag{3.2}$$

where λ is the scale parameter, k the shape parameter, and x the location parameter [97]. In solar cell recycling literature, terminologies are adjusted. Here, alpha α is used for the shape factor, beta β for the scale factor and T for the average solar module lifetime.

The cumulative distribution function (CDF) of the Weibull function is:

$$f(x) = \begin{cases} 1 - e^{-(x/\lambda)^k}, & \text{if } x \geq 0 \\ 0, & \text{if } x < 0 \end{cases} \tag{3.3}$$

Weibull parameters in literature are shown in table 3.3. For example, Ovaitt et al. [38] provide a table with Weibull shape parameters, and propose a new range of values. This verifies many of the temporal data quality issues I noticed in the IRENA report.

Scenario	Lifetime (years)	α shape factor	β (average lifetime T)	Source
Regular loss	40	5.3759	30	IRENA, 2016
Early loss	40	2.4928	30	IRENA, 2016
Baseline	10-35	4.414 to 12.596	17.38 to 41.18	Ovaitt et. al., 2022

Table 3.3: Weibull distribution parameters in literature

Based on IRENA, two scenarios are applied: a 'regular-loss' and 'early-loss'. The regular-loss describes the end of the functional life, when the panel has degraded to such an extent that it is assumed to be taken out of production. The early-loss distribution describes the functional loss as well as events and technical failures that occur earlier. Both distributions are applied, because the impact of both scenarios is large on the timing of when panels return from productive use, and hence are available for collection and recycling. In addition, table 3.4 shows that lower and upper bounds were added. Figure 3-6 contains the Weibull curve. As the early-loss distribution does not add up to one, the distribution is scaled to 1 to ensure all panels reach end of life.

	Regular-Loss Scenario			**Early-Loss Scenario**		
	Baseline	**Lower bound**	**Upper bound**	**Baseline**	**Lower bound**	**Upper bound**
Shape factor (a)	5.3759	3.3	8.7484	2.4928	1.5	4.5
Average lifetime (T)	30	25	35	30	25	35

Table 3.4: Selected Weibull parameters for c-Si PV panels in Early-Loss and Regular-Loss scenarios.

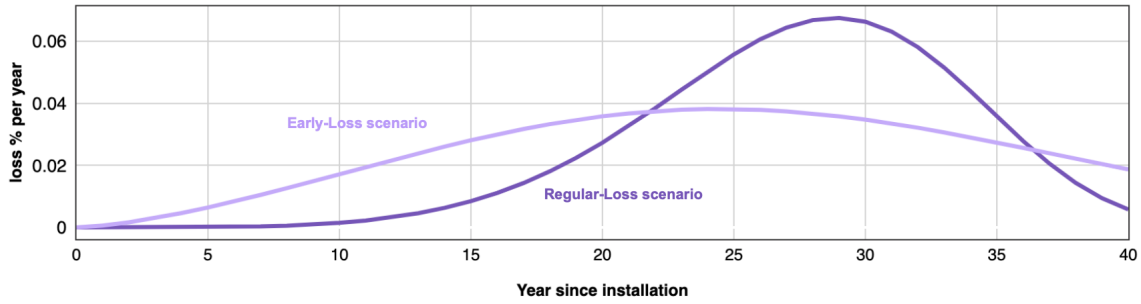

Figure 3-6: Weibull function, early-loss and regular-loss scenarios

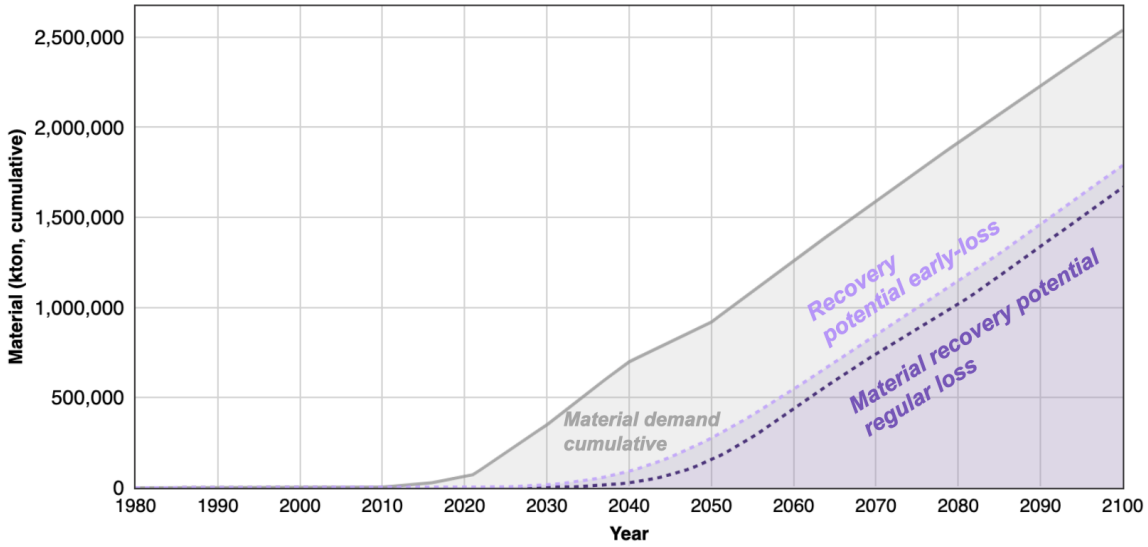

Figure 3-7: Cumulative PV panel EOL return flow (kilotonnes), early-loss and regular-loss scenarios

The Weibull is applied to each year is using a vector multiplication. Material demand for panel production is multiplied by the Weibull distribution for the subsequent 40 years, resulting in the total panel mass at end-of-life. This calculation is executed for each year from 1980 up to 2100 for the input vector, and results in an output vector that runs from 1980 up until 2140 when the last panels are becoming end-of-life. The Weibull end-of-life is explained in table 3.4 which contains the distribution and applied factors. These factors are applied in Python code to calculate the return flow at end-of-life. The results are presented in Figure 3-7.

3.2.6 Material recovery potential

Now that the end-of-life mass is found, the next step is to assess main materials in silicon panels. Material composition of the panels are based on literature [98]. The results are shown in figure 3-8. As expected, glass and aluminum make up the bulk of the mass. This 'top-down' analysis shows that peak EOL material is around 2060. However, it assumes that panel material ratios remain the same, which is not the case as we have seen in chapter 2. Therefore, in the next section a sensitivity analysis is made for silicon. This will account for the change in mass over time.

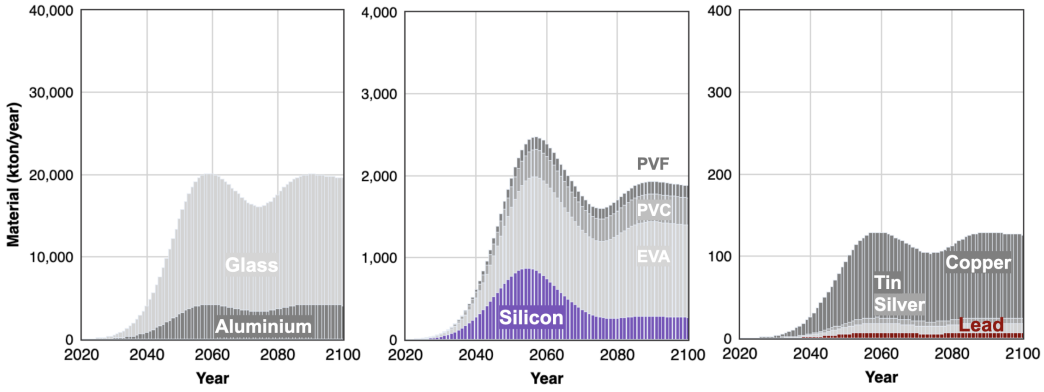

Figure 3-8: Potential for material recovery from PV modules at end-of-life (kilotonnes/year)

3.2.7 Replacement of existing installed capacity

Another improvement to the current PV waste model is to consider the additional material volume of solar panel replacement. All solar panels installed today, will retire in about 20-30 years. The IRENA model does not take this into consideration. Because the purpose of that study was to give an indication of waste volume until 2050, there was no need to include the effects of panel replacement as a driver for new material demand. Because this study looks beyond 2050 all the way to 2100, this cannot be neglected. The projected IPCC climate targets assume that solar PV capacity that has already been installed stays in production. Therefore, this EOL model should factor in panels to be re-installed after

the old ones are decommissioned. The Weibull function is applied to calculate the installed capacity for this additional demand, and the difference is significant after 2050 (figure 3-9).

Figure 3-10 contains the updated projection of waste volume for the early-loss and regular-loss scenarios. It indicates that solar PV is theoretically capable of reaching the EU's 100% circular economy target in 2050. Yet, the vast amount of material needed for replacements will exceed the available secondary material flow beyond 2050. In addition, it should be noted that this is the material recovery *potential*, not the actual recovery. Recovery rates should also be taken into account, as we will see in the sensitivity analysis for silicon.

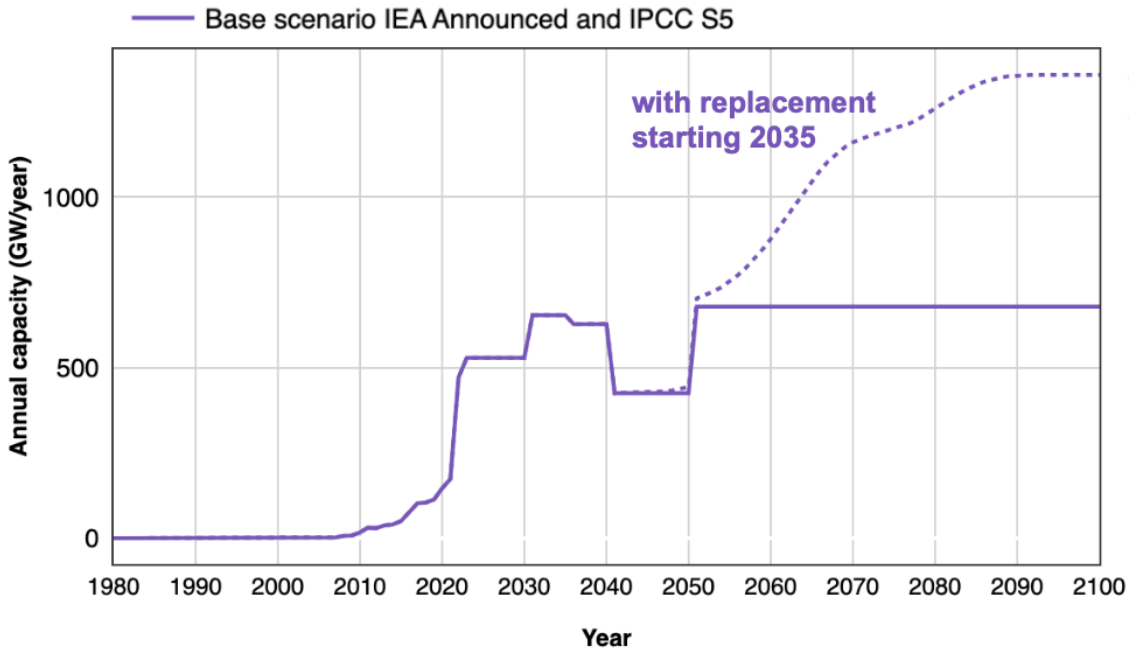

Figure 3-9: Annual installed capacity including replacements.

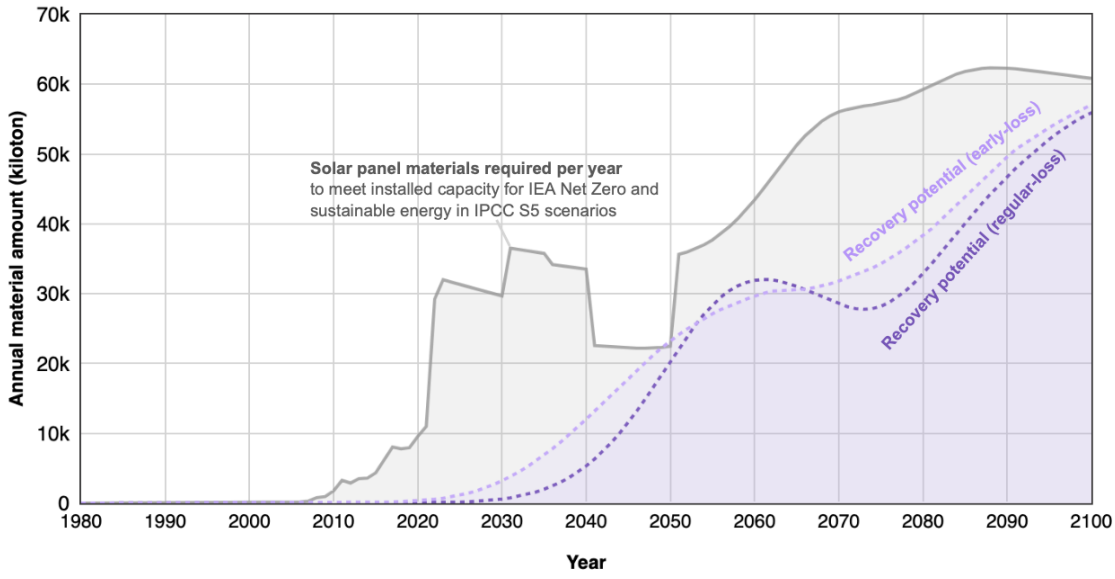

Figure 3-10: Annual installed capacity, including replacements, and EOL return flow mass for the early-loss and regular-loss scenarios.

3.3 Sensitivity analysis for silicon

In addition to the material flow analysis of solar panels, a detailed substance flow analysis is made for silicon. The objective is to add more granularity to the model by tabulating the amount of silicon in each panel by year. Then to recalculate, using the Weibull distribution for regular loss, the resulting volume at end-of-life. As we observed in chapter 2, silicon content in solar cells dropped notably in the past 15 years, and industry sources confirm this [99]. Other end-of-life modeling studies do not seem to consider this. For example, similar studies on PV waste for individual countries (e.g. Spain), assume that "the PV market will continue to be dominated by silicon PV technologies and the proportions of raw material mass that compose a PV module will remain constant in time" [100]. Referencing outdated percentages mentioned in the 2016 IRENA report: 76% glass, 10% polymer, 8% aluminum, 5% silicon, 1% copper, 0.1% silver. Which in turn is based on a conference paper from 2006 [101] and an industry report from 2007 [102]. Photovoltaic technology changes rapidly, and contemporary studies should not, if possible, base complex analysis on static data from two decades ago.

Year	2000	2004	2010	2020	2030	2040	2050	2075	2100
Si content (g/W)	16.8	16	7	2.5	1.7	1.0	0.65	0.57	0.51
Recovery rate	10%	10%	10%	10%	18.2%	33.0%	60%	60%	60%

Table 3.5: Parameters for baseline model: typical silicon content in c-Si solar cells (grams/Watt) based on data from [103] [42] [104] [99], extrapolated to 2100. Selected recovery rate as baseline modeling parameter.

Table 3.5 contains the input parameters used in the base model, for silicon content and recovery rate at end-of-life. This study applies the weight-to-power ratio from the measurements in chapter 2, as shown in figure 2-14. According to Fraunhofer, the silicon content was 16 g/W in 2004, 7 grams per Watt in 2010, dropping to 2.5 grams per Watt in 2022 [42]. This is in line with reported values by Tongwei, a major Chinese solar panel manufacturer. At present, 2.0-2.5 grams of silicon is applied for each Watt [104].

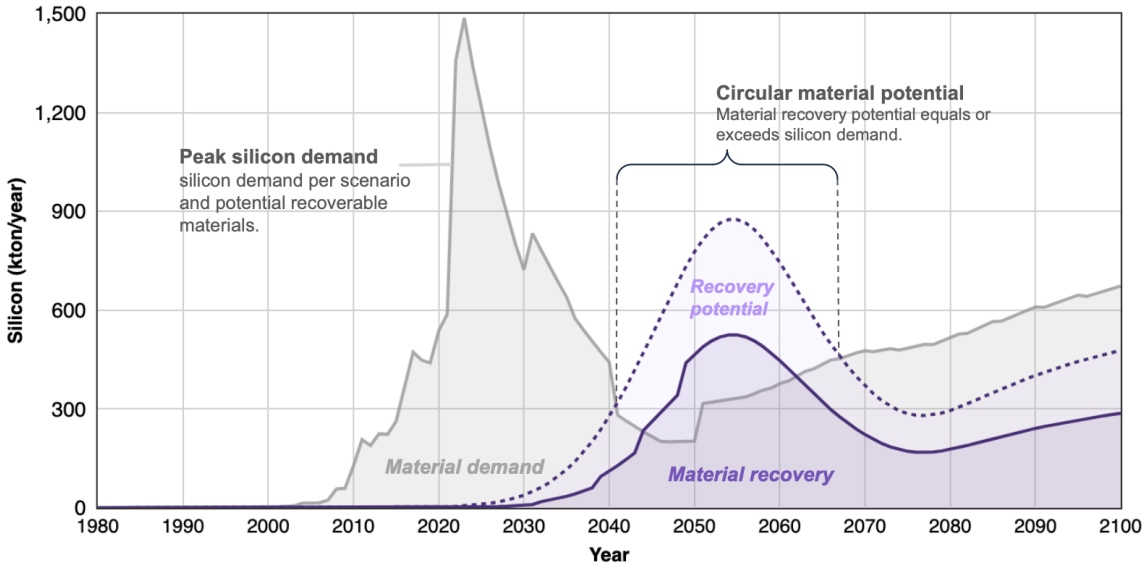

Figure 3-11: Annual silicon demand for solar PV production, recovery potential, and recovered solar-grade silicon (kilotonnes/year).

3.3.1 Silicon recovery potential

Silicon demand and end-of-life return flows are calculated using the same method as above, with the weight-to-power ratio. The contribution of this study is that the silicon concentration declines each year. The recovery rate is based on the commonly made assumption that 10% of all EOL solar panels are currently recycled, and is estimated to reach 60% in the year 2100 (Table 3.5). In the sensitivity analysis in the next section, the effects of higher and lower recovery rates will be studied. Figure 3-11 shows the resulting silicon demand and return flows. When additional material demand from PV panel replacement is not considered, the amount of returned silicon is estimated to surpass silicon demand for new panels from 2041 onward. Theoretically, silicon can be 'circular' during that time. The main factors driving this result are the dropping silicon concentration, the growing end-of-life volume, and the expected improvement in recovery rates. For actual use of recovered silicon in new solar cell production, purity levels are important. Solar-grade silicon can turn into metallurgical-grade silicon after recycling. It is plausible that this recovered product will not be used for solar cells, but 'down-cycled' for use in other industries. This is out of scope for this study, because in this model solar-grade silicon is assumed to be reused in the solar industry.

3.3.2 Sensitivity analysis

How sensitive the model is to the inputs and variables determines how large a response in outcome is to a change in one of the inputs. Seeing these model responses helps in understanding which inputs and variables impact the outcomes the most. Understanding this impact yields valuable insight where leverage exists and decisions have the largest positive effect. Six variables are chosen for the sensitivity analysis of silicon: solar PV installed capacity, the thin film share, the power per panel, the weight-to-power ratio, the average solar panel lifetime, and the recovery rate at end-of-life. Each variable is set to a 'lower' value and then an 'upper' value (table 3.6). For comparison, the results of the base case are presented in figure 3-11.

Variable	Unit	Base	Lower	Upper
Solar PV installed capacity	GW	IEA Stated Policies + IPCC S5	-44% (IEA Stated Policies + IPCC S2)	+35% (IEA Net Zero + IPCC + 1x IQR)
Thin film share	%	29% in 2040	-25% share starting 2040	+40% share starting 2040
Power per panel	%/yr	+0.5% until 2050, +0.25% after	-0.2% after 2030	+0.3%
Weight-to-power ratio Si	%/yr	0.5% from 2030	No improvements after 2030	Double improvement factor until 25% above SQ-limit
Average lifetime (T)	Years	25	15	30
Recovery rate	%	60% in 2050	40% starting from 2050	85% starting from 2050

Table 3.6: Sensitivity analysis on silicon return flows, with a base, lower and upper value for five variables.

First, the sensitivity analysis yields the result that the recovery rate is the most impactful variable on raw (primary) silicon demand until 2100. Of the 45,000 kilotons silicon needed to produce the solar panels required in the 'IEA Announced Pledges and the IPCC S5' scenario, a total of 18,000 kilotons would be obtained from recovered material; leaving a gap that requires raw (primary) silicon of 27,100 kilotons. With a recovery rate of at least 60% by 2050, the retrieved silicon can meet the demand for first-use silicon by the solar PV industry in the year 2044. Still, this is dependent on whether panels are replaced or not after reaching end-of-life. This study takes replacement into account from 2035 as it is assumed that the IEA scenarios have already considered this, but not the IPCC scenarios because IPCC reports solar energy production instead of installed capacities. In the situation where panels would *not* be replaced, i.e. are only installed once (figure 3-11), the effects on recovery are negligible until the mid-2050s and material circularity is achieved in both cases in 2047. Notwithstanding, by 2060 the demand curve is significantly higher due to replacement of panels from the 2020s and 2030s. The consequence is that after 2060, silicon demand can no longer be fulfilled with secondary supply. In the base case, the cumulative amount of primary silicon is 27,100 kilotonnes from the 1980s to 2100.

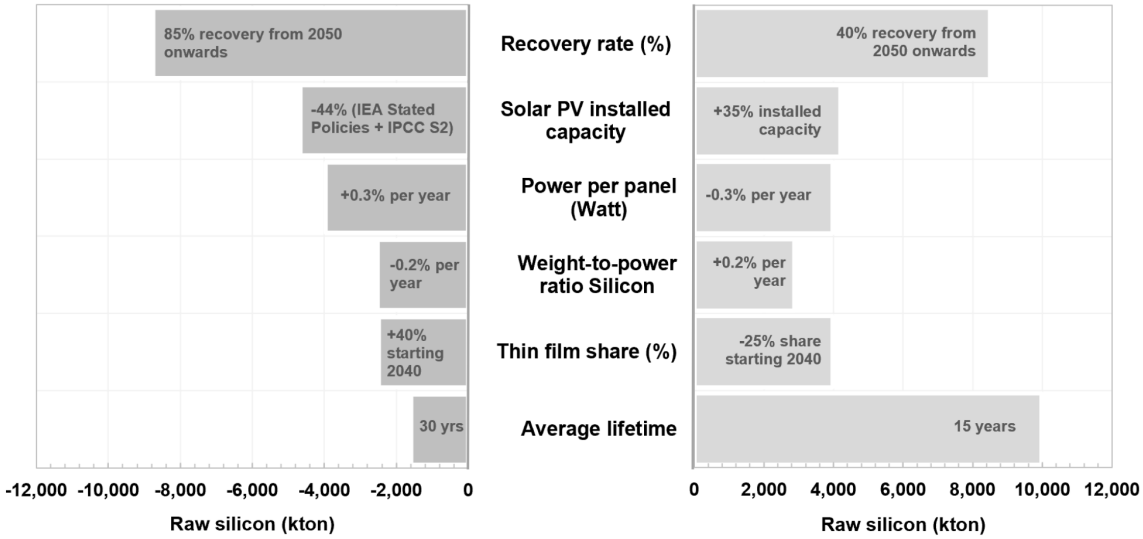

Figure 3-12: Results from the sensitivity analysis for silicon.

Results of the sensitivity analysis on the six variables are presented in figure 3-12. The horizontal axis of the chart indicates the amount of raw silicon needed for new production, compared to the base case. On the left side (lower case), all variables lead to a reduction in raw silicon demand, because more material is recovered from discarded solar panels. Results on the right side (upper scenario) indicate how much more raw silicon would be needed for each change in variable. From the six options for improvements, changes in the recovery rate have the most impact on the total amount of recoverable silicon. The baseline scenario assumes 60% silicon recovery from EOL panels in 2050. The lower scenario 40% and the upper 85%. This highlights the importance and effectiveness of circular economy targets for material recovery. Better recycling pays off with almost 9,000 kilotonnes.

The next largest impact on raw silicon requirement is installed capacity. The installed capacity in the lower case, being the IEA Stated Policies and IPCC S2 scenario, sees a reduction of 44% in solar PV installed capacity. By the end of the century, approximately 4,100 kilotonnes of silicon is saved compared to the base case. In contrast, the expected demand for solar in the IPCC Net Zero scenario leads to an additional 4,000 kilotonnes silicon consumption by 2100.

The power per panel (% per year Wp) development has a relatively large impact of 4,000 kilotons silicon. A main reason is that more power is produced per surface area—requiring less panels and hence material. In the base case, the power per panel is 385 Wp in 2023, with a growth rate of 0.5% per year until 2050. Thereafter, it grows by 0.25%. The lower case is the same until 2030, and assumes efficiency improvements of 0.2% per year after that. The upper case grows 0.3% faster than the base case. The power per panel also affects the weight-to-power, which is the next variable.

The weight-to-power has a lower impact on raw silicon demand in the sensitivity analysis, but is on the same order of magnitude as power per panel—around 3,000 kilotonnes for a 0,2% faster or slower development. The weight-to-power has two variables to influence it: power per panel and weight-per-surface area. When both improve the weight-per-panel is the product of the two, making this a high leverage variable. To illustrate, the 70% increase in panel power since 2004 multiplied by the four times lighter surface area resulted in a 7x improvement in weight-to-power ratio.

The share of thin film influences the silicon demand by a surprisingly large amount of 2,000 - 4,000 kilotons. Although thin film is only 5% of all installed capacity today, the development of the thin film markets indicate growth of this technology share in the future. In particular for CdTe, of which the annual global PV module production has grown exponentially from 2.8 GWp in 2018 to 8.4 GWp in 2021 [42]. In the base scenario, it is assumed that thin film will take up 29% of the market share by 2040. A growth of 24 percent points in the coming 21 years is feasible, and is in line with how thin film grew from nothing in the 1980s to a technology share of 30% in the 1980s and early 90s, as we have seen in the historical analysis and 3-4. The sensitivity analysis indicates that if the share of thin film becomes 40% starting from 2040, almost 4,000 kilotonnes less raw silicon will be needed by 2100.

Last but not least, lowering the average distributed panel lifetime from 30 to 15 years requires a staggering 8,300 kilotons of additional raw silicon. Still, a longer lifetime of 40 years only reduces demand by 1,200 kilotons. This is caused by a set of interacting factors. As panels reach end-of-life earlier, they become available for recovery—boosting recoverable material potentials. But it pushes up raw material demand for replacement of the panels

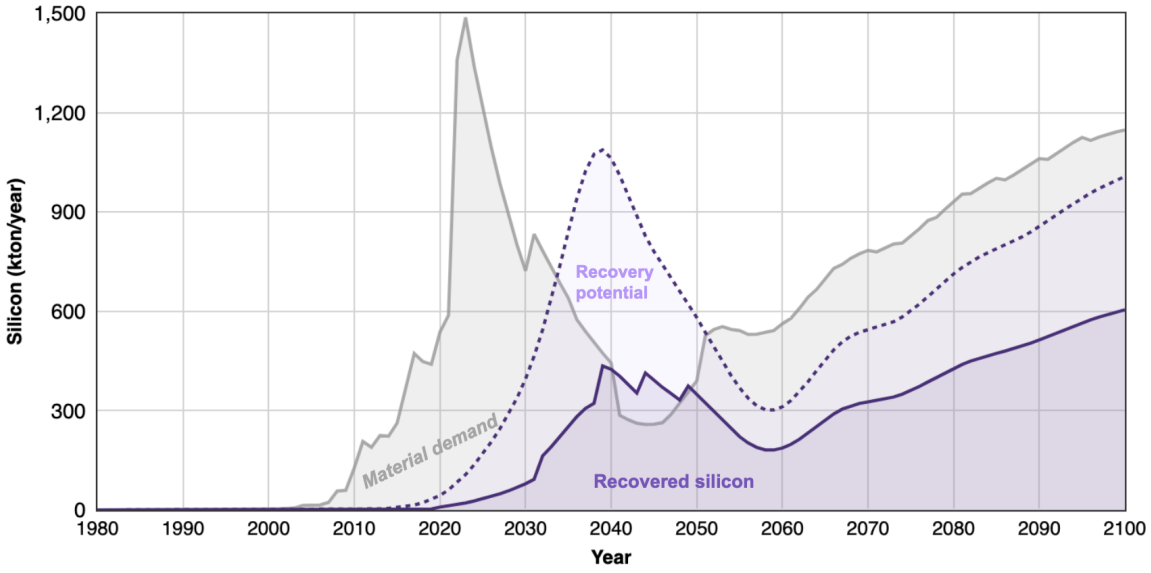

Figure 3-13: Lifetime sensitivity for raw silicon demand and secondary recovery potential reveals dynamic model behavior when panels have a 15 years average lifetime (including EOL replacements).

that were decommissioned. Yet, the replacement panels come with higher power, a lower weight-to-power ratio and presumably fewer losses during production. This is a paradox: the shorter the lifetime, the earlier material circularity is reached, but this is temporary as replacement panels and additional capacity start to outstrip the recovered materials. Looking deeper into this relationship reveals dynamic behavior (see figure 3-13): the 15 years average distributed lifetime, combined with non-smooth capacity additions leads to a lagged cycle.

Thinking deeper about this dynamic reveals a strategy to reach circularity sooner and with less expensive, toxic or environmentally harmful materials. A shorter panel lifetime would be acceptable when recovery rates are sufficiently high and costs notably lower. A trade-off emerges between expensive, scarce and harmful material use in long-lifetime panels versus simpler panels that can be recovered faster, cheaper and safer. Unless technological advancements are made, this design intervention will likely have negative consequences for the power output rating per panel during operation. Emerging from this interplay between materials and energy requires high-impact decisions to reach sustainability *and* circularity.

3.4 Exploratory scenarios for installed PV capacity

In the sensitivity analysis for silicon, installed solar PV capacity is recognized as a major variable driving the volume of EOL solar waste. Other studies have identified that IRENA's model is an underestimation for installed PV capacity, and an alternative 'high electrification' scenario is proposed [38]. Recognizing a potential growing solar PV demand from emerging end-uses, this thesis introduces two new scenarios:

1. Green Hydrogen Takes Off: Increased energy demand for electrolyzers, to decarbonize steel making, transportation and the chemicals industry.
2. Artificial Intelligence Boom: Increased energy demand from AI and data centers.

These emerging end-uses require renewable electricity to meet climate targets. Because solar energy is cheap and abundant, demand from these industries will be a driver for more installed PV capacity. In figure 3-14 the installed PV capacity in GW/year is presented. This will be unpacked in the two scenarios below.

3.4.1 Installed PV capacity scenario 1: Green Hydrogen Takes Off

The Paris Climate Agreement mandates countries to curb their carbon emissions to stay well below global warming of 1.5 degrees Celsius. This led to policies that drive industries to innovate and decarbonize their production processes. One technology receives particular attention: hydrogen. A zero-emission fuel that does not combust carbon dioxide, nitrous oxide, and other harmful particulates. There's a catch, however. Hydrogen is an energy carrier, not a fuel. Therefore, the production requires input energy and electrolyzers are used to make this conversion.

Feedstocks can be fossil-fuel based, in the form of natural gas, coal, biomass, and electricity, or renewable from solar, wind, and hydroelectric power. However, only if hydrogen is produced without fossil-fuels can it play a significant role in achieving climate goals. Decarbonizing industries require 'green hydrogen' instead of 'grey hydrogen', and the difference

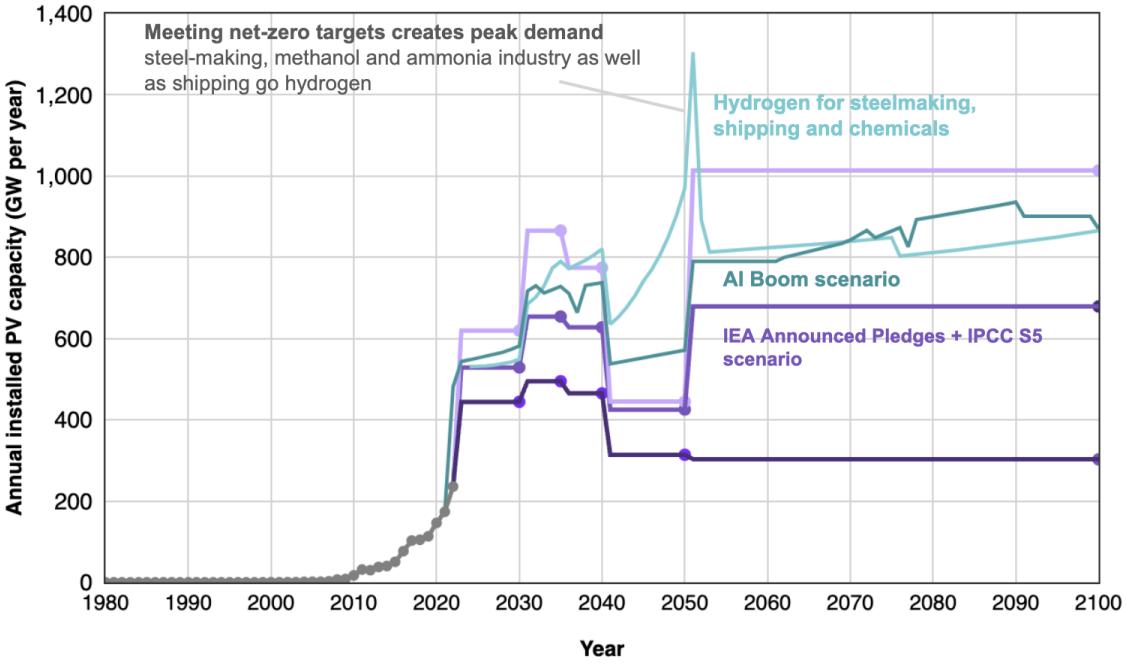

Figure 3-14: Three scenarios for annual installed capacity (GW) of solar PV: Green Hydrogen Takes Off, Artificial Intelligence Boom, and Steelmaking.

in carbon emissions between fossil and renewable hydrogen is shown in table 3.7, including conversion efficiency of the electrolyzers. In this scenario, electricity from solar PV is assumed to be a low-cost renewable feedstock for future electrolyzers. In 2021, 4% of global hydrogen production came from electrolysis, which is not a large share compared to natural gas (47%), coal (27%), and by-products from oil (22%). Because the average electricity was about 33% renewable in 2021, only 1% of hydrogen was green. In that year, pilot plants of electrolytic hydrogen had a total capacity of 0.7 GW. It is projected that this will have to grow by four orders of magnitude to 4-5 TW by 2050 to meet the 1.5 degree Celsius climate goal [105]. This scenario explores what the demand for materials for solar PV will be, if the renewable hydrogen production takes off.

Geological sources of hydrogen have recently been discovered, for example in the Bulqizë mine in Albania [106]. Yet, the technology is too immature to extract hydrogen at competitive costs, and local resistance may prevent the issuance of mining permits. Therefore, this hydrogen source is left out of scope in this scenario.

	Hydrogen current global	**Grey Hydrogen from natural gas**	**Green Hydrogen from renewables**	**Blue Hydrogen from carbon capture**
Carbon emissions (g CO2/MJ)	100	104	9.5	9 - 13
Conversion efficiency	-	70 - 85% natural gas reforming	55-65% electrolyzer efficiency	-
Feedstock	Mix of natural gas (47%), coal (27%), oil by-product (22%), and electrolysis (4%)	Natural gas/coal	Electricity from solar, wind, hydro and biomass	Natural gas/coal
Sources	[107]	[108] pathway GRCH2 from natural gas	[108] pathway WDEL1/CH2 from wind	[107]

Table 3.7: Carbon emissions from the production of green, grey and blue hydrogen.

Three primary industries that turn to hydrogen, and are considered in this scenario, include steelmaking, chemicals (methanol and ammonia), and the shipping industry. Table 3.8 contains all input values for the calculation. The resulting total installed PV capacity is visualized in figure 3-14.

Hydrogen Direct Reduction process. Steelmaking is one of the most energy-intensive industries. A promising technology to reduce emissions is the Hydrogen Direct Reduction process, reducing greenhouse gas emissions by 95% according to a developer in Sweden [109] and the Rocky Mountain Institute [110]. According to one study, the direct reduction process requires 3.48 MWh of electricity per tonne of liquid steel, predominantly used for hydrogen production with electrolysis [111]. Assuming the demand for steel will grow from 1,900 to 2,376 megatonnes [112] and 50% of all steel will be made through direct reduction, a total of 65 megatonnes renewable hydrogen would be required by 2050. In this scenario, 50% of renewable electricity comes from solar energy, this will require about 1,400 GW cumulative solar PV installed capacity by 2050. By the time we reach 2100, this leads to a total of 4,700 GW, when 80% of hydrogen is produced using electricity from solar.

	Unit	2025	2050	2075	2100
Steel industry	Steel production, Mton [112]	1,956	2,376	2,376	2,376
	Direct reduction share (%) [109]	0.2%	50%	65%	80.4%
	Hydrogen demand, Mton [107]	0.157	65	106	130
	Electricity demand, TWh[1]	4.3	1,670	2,707	3,330
	Solar PV capacity, GW	3.6	1,390	2256	2,781
Chemical industry (ammonia + methanol)	Production, Mton [113]	436	752	1,235	2,027
	Share from renewable hydrogen (%) [107]	0.2%	74%	80%	80%
	Hydrogen demand, Mton	0.4	557	988	1621
Shipping	Energy demand, Exajoule [114]	9.2	9.2	9.2	9.2
	Ammonia and methanol share (%)	0.1%	20%	70%	70%
	Hydrogen demand, Mton	0.230	130	262	389
Total	**Solar capacity, at 60% share (GW)**	**6**	**3,376**	**6,814**	**10,100**

Table 3.8: Additional solar PV capacity (GW) for green hydrogen production to decarbonize three end-uses: steel industry, chemical industry and shipping. [1]65% electrolyser efficiency, 50% solar-PV electricity share.

Chemicals industry. Another industrial sector that is expected to start using large amounts of renewable energy is the chemical industry, especially the production of ammonia and methanol. Both ammonia and methanol are feedstock chemicals and can efficiently be produced from hydrogen. In 2023, a combined 436 megatons of ammonia and methanol were produced globally, mostly from natural gas [113]. The scenario explores the impact of strong growth in the two feedstock chemicals to 752 megaton in 2050 and 2027 megaton in 2100. The hydrogen required in the production is substituted for hydrogen from renewable electricity, with 0.2% coming from renewable hydrogen and 27% in 2050. Solar PV is estimated to supply 60% of the total renewable electricity to produce the hydrogen.

Shipping industry. Last but not least, the shipping industry. In 2023, the United Nations' IMO Greenhouse Gas Strategy set out ambitions for the industry to become net zero in 2050 [115]. One technological option for fleet decarbonization is with methanol or ammonia. Both fuels can be produced from hydrogen. Large-scale production and infrastructure already exists or is under rapid development; it is expected that both fuels will play an important role. Recently Maersk, one of the largest container shipping companies in the world, announced it ordered ships for bulk transport of ammonia made from hydrogen. Regulatory issues currently prevent these types of carriers to be fueled by ammonia, but IMO is working on updating their guidelines. For vessel types that require less stringent regulations, methanol is already in use as a fuel [116].

This Green Hydrogen Takes Off scenario explores what the impact of rapid growth in the application of renewable methanol and ammonia would be for shipping on the material demand for solar panels. In this scenario, energy demand for shipping is 9.2 exajoule [114], which is assumed constant until 2100 as efficiency gains are deemed possible. For 2050, a 20% share of total energy demand is supplied by methanol and ammonia, leading to 130 megatonnes hydrogen demand. Input values for this scenario are presented in table 3.8.

The combined hydrogen requirement for shipping and the methanol and ammonia feedstock amounts to 687 megatonnes hydrogen demand, which would require 4,050 TWh of solar PV supplied electricity (60% solar share and 65% electrolyzer efficiency). At 1,300 kWh per installed Watt of solar capacity, this translates to 3,376 GW installed capacity of solar panels reaching 10,100 GW by 2100. Figure 3-15 shows all results of the Green Hydrogen Takes Off scenario.

In this scenario, around 100 kilotonnes of extra silicon per year is needed in the 2030s. This grows rapidly to a peak of 400 kilotonnes in 2050, after which most of the Net Zero transition has been completed. Then, silicon demand drops to 80 kiloton, and slowly rises thereafter as material demand for panel replacement starts, the chemical industry continues to grow, and hydrogen demand picks up toward 2100. This scenario could achieve material circularity for silicon in the late 2060s—mainly driven by the large demand in the 2040s and improving material efficiency. Still, at a 60% recovery rate this potential is not reached and primary material remains necessary.

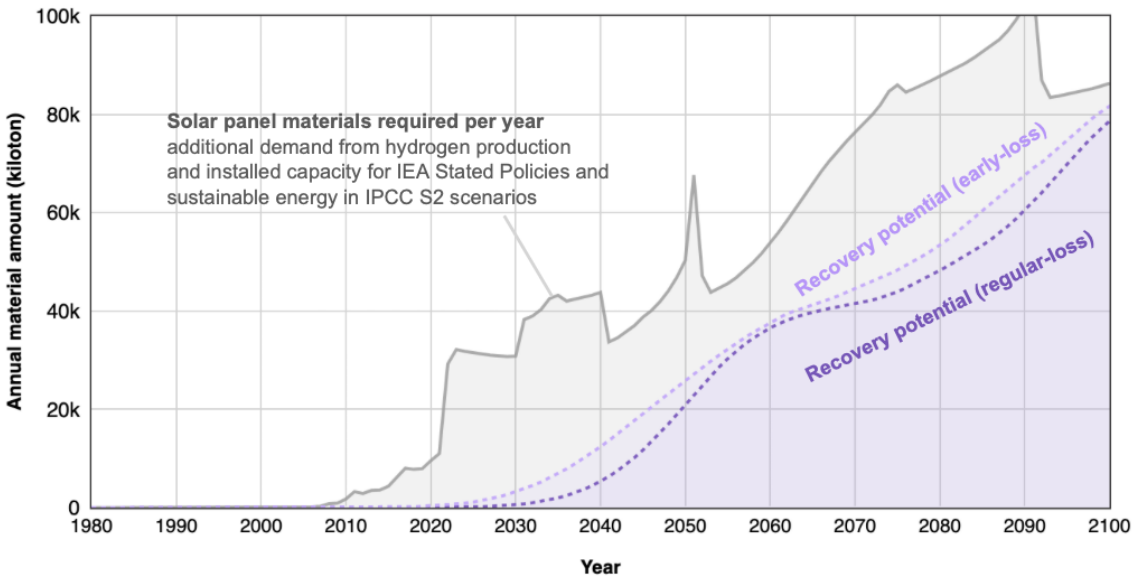

Figure 3-15: Results Hydrogen Takes Off scenario: base scenario + additional PV capacity for green hydrogen production.

3.4.2 Installed PV capacity scenario 2: Artificial Intelligence Boom

This 'AI Boom' scenario introduces an energy demand projection from an emerging end-use: data centers and artificial intelligence. Rising electricity consumption for powering data centers is unprecedented, and attributed to the adoption of large language models (LLMs) and popularity of ChatGPT. The additional electricity required results in a need for more renewable energy, beyond what is projected by the IEA and IPCC. Similar to the previous scenario, the tech industry needs to reduce carbon emissions. To decarbonize data infrastructure, technology companies turn to wind and solar energy as a main strategy due to their low costs and low greenhouse gas emissions [117].

Current data center energy use is 365 TWh, as presented in table 3.9. By 2100, this AI Boom scenario reaches a staggering electricity use of 18,200 TWh for data centers and AI. This is based on a global population of 10.4 billion people [118] multiplied by 12,500 kWh electricity demand per capita—equivalent to the current per capita electricity use in the US, Canada or Finland. To determine the data center share of electricity use, this number is multiplied by 14%, the current share of data center energy use in Denmark, a leading country in this area [119]. This is a boom scenario compared to the relatively modest 365 TWh currently in use by data centers and AI, and excludes cryptocurrency mining. Most data center providers already have purchasing power agreements for renewable electricity, which underpins the fast growth chosen in the scenario. In this scenario, the renewable share of the electricity demand is growing from an estimated 5% in 2022 to 60% in 2032, which represents the mandated amount for data centers in China – the largest growing region [120]. This renewable share is already surpassed by most large technology companies in the United States, with Google and Microsoft being carbon-neutral and Google announcing to only use carbon-neutral electricity by 2030 [121].

Year	**2015**	**2022**	**2026**
Electricity demand (TWh)	200	365	640

Table 3.9: Data center electricity demand (Source: [120] p.35, excluding crypto)

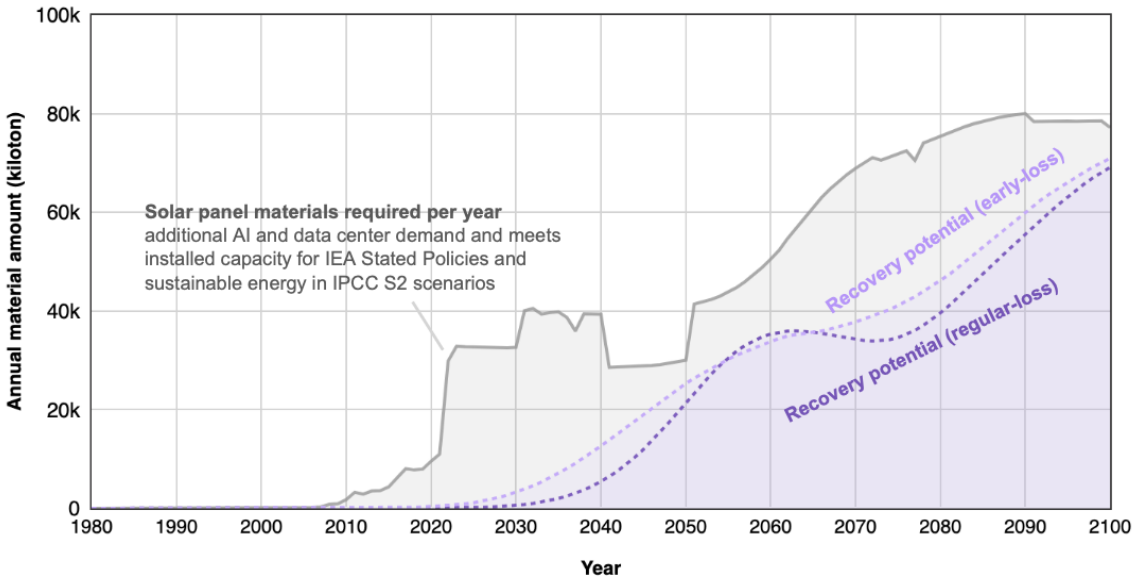

Figure 3-16: Results AI Boom Scenario: base scenario + additional PV capacity for decarbonizing AI and data centers

After 2032, the fast growth phase slows to linear growth to level out at 80% renewables in 2050, which is when net zero should be achieved for data centers. The solar share of the renewable part is set to 70% as solar PV as it is the cheapest electricity source in most countries, but intermittent, making this a futuristic scenario as electricity storage or data center load balancing would be required. Data center load balancing of the grid is expected to become the norm in the 2030s-2040s, as grids become congested, power prices start to fluctuate more, and climate targets become more stringent [117]. As shown in figure 3-14, taking a solar panel yield of 1300 kWh per Watt peak requires 400 GW of additional solar PV by 2032 and a cumulative demand of 11,300 GW by 2100—this would take 10-12 years to produce at current Chinese solar production capacity [122]. The required additional annual installed solar PV capacity amounts to 100 to 400 GW per year compared to the base scenario of IEA Announced Pledges and IPCC S5 (figure 3-16). Applying the weight-to-power calculated for silicon cells in this study, it would require an additional 5,000 to 7,000 kiloton of high-grade silicon. Compiling all findings of this chapter, three plots show results for first-use PV material demand and recovery potentials (fig. 3-17), silicon (fig. 3-18), and the additional silicon for Hydrogen and AI Boom scenarios (fig. 3-19).

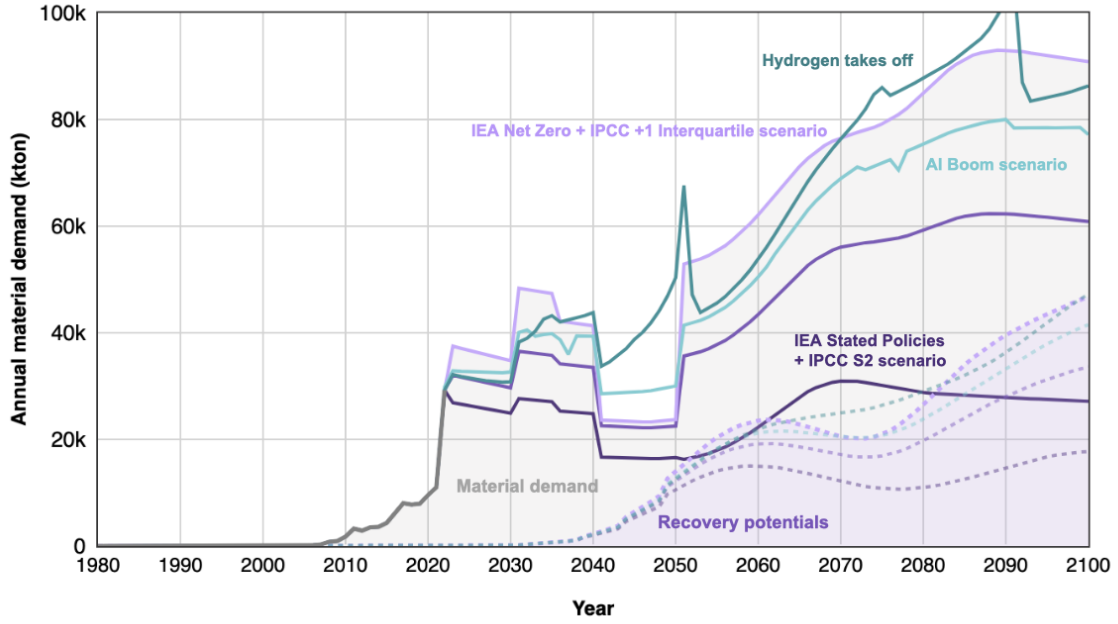

Figure 3-17: Overview of all scenarios combined (1): total material demand and recovery potential of solar photovoltaics from 1980 to 2100 (kilotonnes).

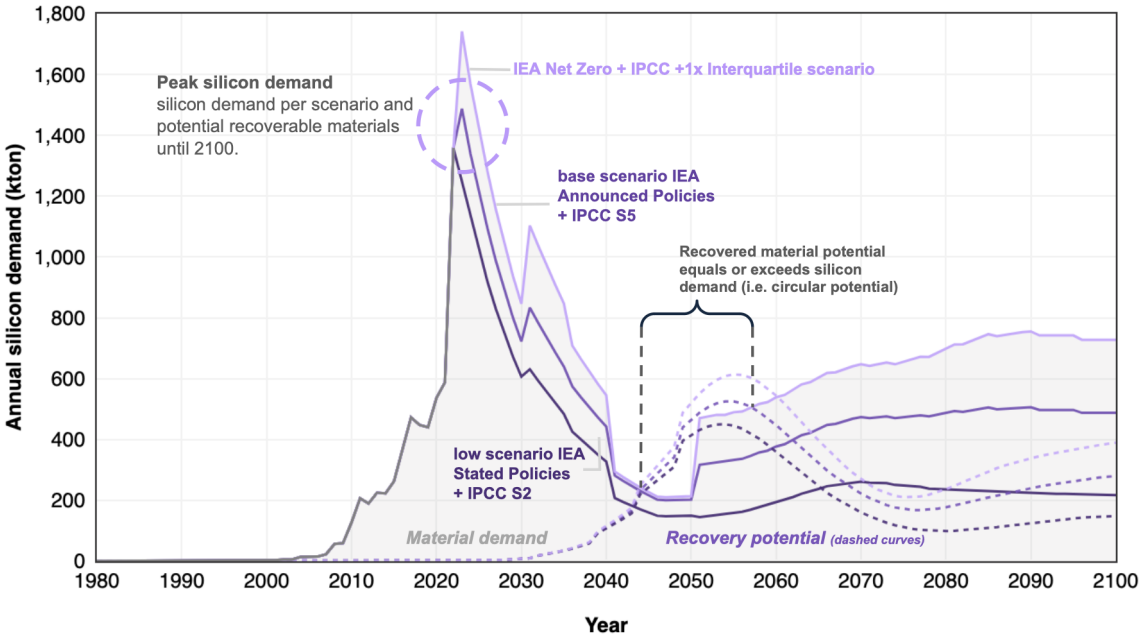

Figure 3-18: Overview of all scenarios combined (2): silicon demand for production and total material recovery potential of silicon from 1980 to 2100 (kilotonnes).

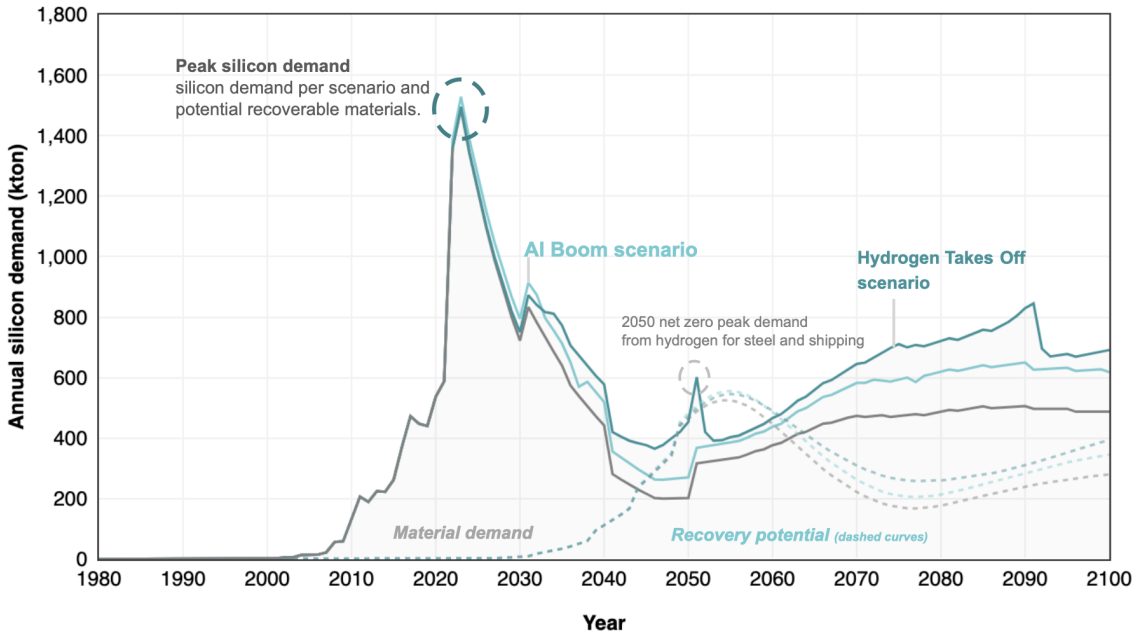

Figure 3-19: Overview of AI Boom and Hydrogen Takes Off scenarios for silicon demand.

Chapter 4

Conclusions, Recommendations and Future Work

4.1 Conclusions

This study sought to answer three key questions:

1. What is the material composition of solar cells, and how does this impact the material recovery potential at end-of-life?
2. How much waste from solar PV modules can we expect worldwide, from now to the year 2100?
3. Is recovered silicon from recycling PV modules sufficient to meet demand for future panel production, and if so, when?

4.1.1 Material composition and impacts on recovery potential

Chapter 2 answers the first question about material composition. Based on characterization and historical analysis, the following observations are made:

Silicon. Specific focus is given to silicon in solar cells, because this is a high-value material and a relatively large waste fraction due to the high volumes of installed monocrystalline and polycrystalline solar PV capacity. In addition, prior research indicates that the highest embodied carbon in c-Si panels can be attributed to silicon production, especially the purification processes [123]. Material recovery at end-of-life is therefore recommended.

Reduction of lead. X-Ray Fluorescence (XRF) and Energy Dispersive Spectroscopy (EDS) confirm the presence of lead in solar cells. This is a problematic finding, and in general not on the radar of circular economy policymakers. Lead poses environmental and health threats to those who collect and recycle the materials at end-of-life. In the 1990s, efforts were made to use lead-free solder and the material was largely phased out in c-Si modules by the 2010s. Today, lead is mostly applied in thin films, including perovskites, CdTe and CIGS [69][124]. Due to awareness about toxicity and more stringent regulations, research efforts are now focused on phasing out lead in these solar technologies as well [69].

Lower weight-to-power ratio. Historical analysis and characterization confirm the hypothesis that material composition changes over time. Power output increases while the areal density of the cells declines, indicating a higher material efficiency. This poses the question: where does this efficiency gain come from? For materials circularity, this means that over time, less material will be needed to produce solar panels. For recyclers, it means a gradual reduction of secondary material per panel over time.

Increased material complexity. The early days of solar cells were marked by fairly simple material combinations, including silver, silicon, lead, copper, tin, and aluminum. Similar to other industries, contemporary products are made of proprietary material combinations to achieve higher performance. As we progress in time, the material composition becomes more heterogeneous, especially for emerging thin film technologies. Solar cells can now include gallium, germanium, indium, cobalt, bromide, and many other elements.

Crossovers between technologies. Solar cells do not only contain more materials, cell architecture increasingly becomes a complex, sandwiched product. Third-generation solar cells are often multi-layered products, also called tandem cells. For instance, perovskites are combined with polysilicon cells to offer higher performance at competitive price points. Although cell efficiency increases, it is more challenging to deconstruct the product at end-of-life. To what extent does the race for higher cell efficiency lead to downstream problems from a material, environmental and social perspective?

High losses during silicon production. Based on the experimental part of this research, significantly more silicon seems to go into the supply chain of c-Si cells compared to the measured results of solar cell mass over time. A difference of approximately 50% was found between the measured results for weight-to-power (g/W) and literature [84], explained by cutting losses during production (kerf). Material demand and losses during the production of solar cells is out of scope for this thesis, but this finding presents a good opportunity for further investigation in follow-up research.

Possible use of rare-earth elements. Preliminary XRF-results indicate a possible presence of rare-earth elements and scarce minerals in solar cells. In industrial applications, the handheld X-Ray Fluorescence instrument is used to detect coatings. It is therefore suspected that rare-earth elements may be used in coatings to boost performance of solar photovoltaics. Examples of measured elements include praseodymium, neodymium, and ytterbium. Although the solar industry is mentioned as an end-use in MFA studies about rare earths [88], can be found in specialized scientific literature [125], such as the application of anti-reflective coatings, for dye sensitized cells [73] and perovskites [74], the presence of these elements is generally not known to the recycling industry and the broader public. For this audience, very basic circle diagrams are provided, including the one in figure 2-1, from the IRENA report. Newer studies investigate the recyclability of REEs from solar [126], but are not yet broadly known. In the ongoing race for beating solar cell efficiency records, the search space for additives in contemporary solar cells spans almost the entire periodic table. Specifically for thin films, efforts to eliminate lead seems to result in the use of scarce and rare earth elements.

4.1.2 Expected waste volume and material recovery potential

The Material Flow Analysis in chapter 3 explores the global PV waste volume and material recovery potential, including a sensitivity analysis for silicon. This section answers the remaining research questions posed in the introduction. First, the model and base scenario are described. Next, silicon is covered in more detail for the expected waste volume, silicon content, and drivers to reduce raw silicon consumption in new production. Last, the effects of two exploratory solar PV demand scenarios are covered, and this section concludes with a broader view on the role of demand for new production.

Model description and base scenario. Different scenarios describe the amount of solar PV that is installed and makes up the starting input for the model. Historical values from the 1930s to the 2020s are collected as a foundation for building up the stock-based model. For future projections, the base case is built upon the IEA Announced Pledges scenario up to 2050 and then continues with the IPCC S2 scenario until 2100. This base case amounts to a cumulative total of installed solar PV capacity of 50,040 gigawatt (GW) by 2100. Starting from this capacity, the model calculates annual stocks based on the breakdown by panel technology, cell efficiency, material composition and panel mass, the weight-to-power ratio for active cell material, end-of-life distributions, replacement distribution and finally the recovery rate. The result amounts to 3,630 metric megatonnes of material required for new solar cell production, equivalent to about 10,000 Empire State buildings. Materials mostly include glass and aluminum but also copper, silver, plastics, tin, lead and silicon.

Circular economy for silicon is feasible in 2050, but it comes with a caveat. Achieving the goal of material circularity for silicon by 2050 is challenging but achievable, however, action should be taken before the 2030s to drastically increase recovery rates and boost material efficiency. Recovery rates have to exceed 60% to become circular. Nonetheless, if solar PV grows more rapidly, as in the IEA Net Zero-IPCC high scenario, it is not materially feasible to reach material circularity, as demand outstrips the recoverable materials from old panels. In that case, only very aggressive material efficiency measures and large-scale substitution to thin film technology might achieve this United Nations goal for solar cell materials.

Volume of silicon. Zooming in on high-purity silicon, 45,000 kilotonnes of high-purity silicon is required in the IEA Announced Pledges-IPCC S5 scenario, where 18,000 kilotonnes would be obtained from recovered material from panels that reach their end-of-life. This leaves a large gap of 27,100 kilotonnes that needs to be mined, shipped and purified. By 2050, the silicon demand for solar panel production would amount to 400-700 kilotonnes per year, much less than the 6,000-7,000 kilotonnes reported by Hallam et al. [127]. This study agrees on the historic and current silicon demand per Watt, but it differs in the installed solar PV capacity by 2050. This study amounts to 16 TW cumulative installed capacity in the base case scenario (IEA Announced Pledges) and 19 TW in the high scenario (IEA Net Zero), compared to 63.4 TW in their work. Furthermore, the retrospective analysis made in this study augment the shorter available data range in the literature and arrive at a steeper material efficiency curve, i.e. the weight-to-power. Even in the high scenario in this study, the silicon demand does not reach its current peak and remains below 1,500 kilotonnes. Strengthening this finding is that a higher share of thin film panels is expected, leading to a sharp reduction in silicon as the thin film panels require an order-of-magnitude less material. To illustrate, a 40% increase in thin films from 2040 onward results in a reduction in silicon of 2,000 to 3,000 kilotonnes. From a material perspective, it can be concluded that a very high level of solar panel production can be sustained—enough to meet the high installed capacities of the 'IEA Net Zero - IPCC high' scenario, as well as the AI Boom and Hydrogen Takes Off scenarios.

Silicon content. The amount of silicon in or consumed by solar cell production is reported to be 16 grams/Watt in 2004 and 2-2.5 grams per Watt peak for 2021-2023 according to [42][127][93][104]. Despite this number being widely reported, it does not line up with the performed measurement of solar cells, which was 1 gram lower total cell mass per Watt. This surprising finding warrants follow up on both the measurements as well as validation of the 2-2.5 grams value. One hypothesis is that the difference emerges from having measured mostly non-Chinese solar cells. If true, this would indicate higher silicon use in China, however this is not likely given the modern state and competitiveness of industrial production. On the other hand, it could be a difference in definitions, or simply because information is 3 to 5 years old, while industry is moving on and under-reporting competitive information

of this kind. The conclusion from the results is that this adds uncertainty to the future silicon demand, as a 30% difference in weight-to-power translates into 13,500 kilotonnes of cumulative silicon demand up to 2100.

Drivers to reduce raw silicon use in c-Si panels. The following measures are effective in reducing silicon demand for new production: solar panel energy efficiency improvements, a lower weight-to-power ratio of the cell (grams of silicon needed to produce one Watt of electricity under standard test conditions), a higher thin film share, and a longer panel lifetime. A further increase in energy efficiency of 0.3% per year, would result in a reduction of 4,000 kilotonnes of raw silicon by 2100. Next, speeding up improvement of the material efficiency (weight-to-power) would reduce 2,200 kilotonnes of newly mined and upgraded silicon. A bigger challenge, from a material scarcity and circular perspective, is that a higher growth rate in solar PV leads to a receding 'demand-to-recovered material gap'—where recoverable materials from solar panels at their end of life never meet or exceed the increasing silicon demand for new panels. This is exemplified in the higher growth rate scenario 'IEA Net Zero and IPCC high' which requires an additional 4,000 kilotonnes of raw silicon—and surpasses the recoverable potential silicon in end-of-life panels. In conclusion, in order to reduce raw silicon demand for new production, the focus should be on boosting both the recovery rate and the material efficiency. The main reason for this is that it is a higher order goal to increase solar energy production. Improving energy efficiency and panel lifetime are already main objectives of the solar PV industry, leaving only the other main decision levers of recovery and material efficiency (which includes the option to substitute silicon to thin film technologies).

Projections for installed solar PV capacity from emerging end-uses. To study the material impact of solar power demand from emerging end-uses, two exploratory scenarios are developed: one for artificial intelligence and one for hydrogen.

Artificial Intelligence Boom scenario. The AI scenario shows an exponential growth of global energy demand for artificial intelligence and data centers, starting from 365 TWh in 2022. By 2060, this is projected to be 8,000 TWh. The energy consumption grows to 18,000 TWh in 2100, reaching 14% of the total electricity demand. This scenario requires

an additional 11,300 GW of solar PV by 2100–an enormous amount which would take 10-12 years at current Chinese solar production capacity [122]. Based on the weight-to-power ratio calculated for silicon cells in this study it would require a cumulative 4.000-8.000 kilotonnes of high-grade silicon by 2100.

Green Hydrogen Takes Off scenario. A second scenario explores the impact of the additional electricity requirements for green hydrogen production, powered by solar energy. Hydrogen is considered a promising future technology to decarbonize steel production, the chemicals industry (ammonia and methanol) and shipping. Under pressure of achieving climate goals, the combined demand for hydrogen from these three sectors reaches a massive 1,000 GW additional solar installed capacity around 2050 in this scenario, outpacing the AI boom scenario and going beyond the high scenario. The impact of this scenario presents a second peak in silicon demand around 2050 of 600 kilotonnes per year, but dropping thereafter as extra capacity additions level out to more manageable volumes, hence pushing the achievement of material circularity to later in the 2050s. But not for long as replacement demand pushes silicon demand above the availability of recovered silicon in the 2060s.

The role of demand for new production. Taking a broader view, becoming circular is unachievable when material demand is growing strongly. For instance, the high scenario 'IEA Net Zero-IPCC high' requires 5,000 tons of additional raw silicon. Even with an 85% recovery rate, as long as installed capacity continues to grow at a high pace, a gap remains and demand for silicon exceeds secondary supply. Generalizing, what can be concluded is that the growth rate of the solar panel installed capacity has to be exceeded by the material efficiency to be able to meet circularity. More specifically, the growth in installed solar PV capacity divided by the material efficiency times the recovery rate needs to be above 1 in order to meet (primary) material demand by recovered (secondary) material, i.e. achieving material circularity. Concretely, in the base scenario, the recovery potential has to exceed 60% in order to be able to meet silicon demand solely from potential recoverable material. When new solar PV installed capacity is much lower, such as in the IEA Stated Policies-IPCC S2 low scenario, circularity can be achieved earlier for silicon.

Ultimately, all scenarios indicate that the largest silicon demand wave is in the beginning

of the 2020s, followed by a declining silicon demand due to increasing energy efficiency, higher material efficiency and substitution. A second peak is possible when solar PV capacity grows strongly towards 2100 and panels are replaced at a shorter timeframe than expected—leading to replacement cycles and dynamically 'peaking' material use. This places the recent exponential growth in solar panel production capacity (mainly in China) in a long-term perspective; potentially leading to a boom-and-bust behavioral dynamic in supply and demand—which could result in oversupply, physical shortages of materials and large price swings—hampering efforts to decarbonize and manifest the large role that solar PV can play in helping stabilizing the world's climate.

4.2 Recommendations

How to improve the material recovery potential of solar photovoltaics at end-of-life? Here are a few recommendations.

Plan for recycling capacity that scales. In the coming decades, we will experience an exponential surge of waste from decommissioned solar panels. The most critical factor for the reclamation of silicon, silver, copper, and other valuable elements is to improve the recovery rate at end-of-life. Pay close attention to timing, however. The risk of incorrect forecasting is that regions anticipate certain material quantities and start building recycling capacity. In the past, recycling services went out of business because they mistimed solar panel waste volumes [22]. Therefore, start small, and base plans on timely and locally relevant data.

Create more awareness about materials toxicity. This study found various toxic elements in solar cells, including lead and cadmium. It is also known that PFAS is applied as a coating on solar photovoltaics [128]. Coatings leach into the environment first, when a panel degrades. Consider the following: how much is the lifetime or performance of a PV panel extended by the application of coatings and toxic substances? Can we do without them? Manufacturers know exactly what materials go into their product, and update safety protocols accordingly. But solar panels can end up anywhere, from downtown Boston to a rural African town, and recycling technologies vary widely among countries. Regardless of geographical location, recycling solar panels requires manual labor. Especially in developing countries, insufficient awareness about toxic substances in solar cells, combined with inadequate or lacking personal protection equipment, puts workers at risk. Lead exposure is detrimental for the health and safety of those who recycle the materials at end-of-life; the people who are the foundation of our circular economy. To mitigate these risks in the future, each new panel should at least get a simple and clear label indicating hazardous materials, even if they appear in small quantities.

Focus on correct identification. To the untrained eye, it can be challenging to distinguish thin films from crystalline silicon solar cells, because they can look similar once sandwiched in a module (e.g. solar module artifact 299 is based on Copper Indium Diselenide). Especially in recent years, when tandem products become the norm. For optimal material recovery at end-of-life, and the safety of those who perform this heroic act, special focus should be given to clear instructions on how to identify these panels to make sure they are recycled correctly.

Disclose material composition in data sheets. For proprietary reasons, high-tech industries may be reluctant in providing information on material composition, especially when it comes to coatings. A proposed way to improve the recoverability of materials at end-of-life, is with a material passport. Solar panels are among the handful of products that already have well-documented and standardized data sheets. To save time and costs for stakeholders across the entire supply chain, develop an industry-wide agreement to integrate product composition data in existing solar PV data sheets.

Optimize for high purity levels. This study evaluated the potential recovery of silicon from solar cells, to be used as a secondary material in new solar cell production. Out of scope, at least for this study, was the use of this recovered product in other industries. It is plausible, however, that the solar-grade silicon becomes metallurgical-grade silicon after its first use. Still, from an environmental and material recovery perspective [32], it is worth it to upgrade the recovered silicon to be used again in solar cells.

Apply circular design principles to solar panels. If we want solar panels to be 100% circular in 2050, we have to implement changes today. 2050 is already in 26 years—the lifetime of a solar panel. The Extended Producer Responsibility is already in effect in some regions, including the EU and Washington State, leading to a growing awareness about solar panel product design in relation to material recoverability at end-of-life. But it is not common practice yet. How do we redesign solar panels to optimize for higher material recovery and lower risks of exposure to hazardous materials? Mapping the environmental and social impacts of raw and secondary materials (e.g. embodied carbon and toxicity) helps in prioritizing future PV panel design and recycling strategies.

4.3 Future work

Improving waste parameters. For circular economy policies to be effective, waste statistics desperately need more granularity. One main area of future work is to expand on the loss function (Weibull) of the model. Alternative PV panel lifetime assumptions should be considered, and tested with the model. In addition, new scenarios could be included to account for extreme weather events due to climate change.

Applying the model to specific regions and materials. This model is made for global analysis, but has the capacity to include regional datasets. A future direction could therefore be to develop regional modeling of installed PV capacity and EOL flows. Similarly, silicon was studied in-depth, but the model also has detailed information on CdTe and other materials, allowing for a deep dive into specific elements of interest. To do this in a meaningful way, technology assumptions for thin film and c-Si can be further refined, based on more literature research and testing. For example, by following up on the observation that silicon content could be an order of magnitude higher in some Chinese panels.

More precise characterization. Having access to a collection of solar cells and modules that span almost a century is a rare occurrence and offers unique opportunities for improving data quality in mathematical models. Future work builds on the collaboration with historians, materials scientists, and the Museum of Solar Energy, and includes XRF and EDS with more extensive sample preparation, the use of filters to study specific regions of the spectrum, more advanced software, and x-ray diffraction to determine not only material composition, but also the quantities and phases.

Environmental impacts and toxicity. Beyond the scope of an MFA, I'm interested in studying environmental impacts of materials in PV panels (such as toxicity and carbon emissions), because those could pose risks across the supply chain and at end-of-life. Mass Spectrometry could test the presence of per- and polyfluoroalkyl substances (PFAS), a known chemical applied as solar panel coating. This MFA provided a better understanding of the scale of the upcoming PV waste problem, enabling us to proactively think about our sustainability and circular economy legacy at the turn of the century.

Appendix A

Measurements of Physical Properties: Solar Modules and Cells

Nº	Year	Mass (g)	Length (mm)	Width (mm)	Diameter (mm)	Thickness (mm)	Density (g/cm3)
262	1931	78.2			58.4	25.60	1.14
070	1937	40.7	58.6	30.2		12.40	1.85
014	1954	7.6	38.6	38.2		4.91	1.05
307	1990s	371.4	350.0	153.0		3.25	2.13
301	1997	960.9	330.0	176.0		35.20	0.47
299	1998	1355.0	328.0	206.0		33.00	0.61
303	2003	1139.7	491.0	204.0		22.00	0.52
300	2004	180.6	210.0	85.0		4.80	2.11
298	2005	892.3	246.0	270.0		22.50	0.60
190	2007	1021.4	306.0	217.0		18.20	0.85
306	2016	702.8	320.0	160.0		25.00	0.55
296	2018	2010.0	350.0	360.0		40.00	0.40
265	2021	3.0	32.0	28.1		1.50	2.22

Table A.1: Results of measurements and calculated density for solar PV modules from the 1930s to 2020s. PV modules provided by the Museum of Solar Energy [44].

Nº	Year	Mass (g)	Length (mm)	Width (mm)	Diameter (mm)	Thickness (mm)	Density (g/cm3)
006	1960s	1.7	45.4	20.0		0.74	2.55
158	1970s	13.3			100.0	0.53	3.20
310	1980s	12.5	100.8	100.1		0.50	2.48
009	1990s	0.6	114.0	24.0		0.18	1.22
109	1990s	9.9	125.0	125.0		0.31	2.08
117	1990s	18.9	156.0	156.0		0.35	2.22
123	1990s	6.9	114.0	95.5		0.26	2.44
124	1990s	8.7	114.3	114.0		0.29	2.30
155	1990s	3.4	96.0	49.0		0.31	2.33
295	1990s	45.4	155.0	155.0		1.01	1.87
118	1994	6.2	150.0	80.6		0.33	1.55
004	1998	8.0	177.5	39.9		0.16	7.07
011	1998	0.4	50.5	21.3		0.20	3.57
022	1998	12.0			150.0	0.28	2.43
119	2001	33.5	155.0	155.0		0.64	2.18
293	2003	1.7	103.3	20.0		0.29	2.84
284	2004	8.1	125.0	125.0		0.19	2.73
308	2008	15.9	96.7	56.6		1.12	2.59
015	2009	3.0	120.0	49.0		0.22	2.32
311	2010s	3.6	159.0	47.0		0.33	1.46
003	2010	18.2	167.0	134.5		0.34	2.38
294	2010	12.1	156.0	156.0		0.24	2.07
027	2011	11.7	155.0	155.0		0.21	2.32
102	2017	10.2	210.0	85.0		0.16	3.57
121	2018	9.1	156.0	156.0		0.17	2.20
291	2019	9.7	156.8	156.8		0.18	2.19
292	2019	11.2	161.7	161.7		0.19	2.25
290	2020s	11.0	166.0	166.0		0.19	2.10

Table A.2: Results of measurements and calculated density for solar PV cells from the 1960s to 2020s. PV cells provided by the Museum of Solar Energy [44].

Nº	**Year**	**Mass (g)**	**Surface area (mm2)**	**Thickness (mm)**	**Density (g/cm3)**
309	1970s	3.3926	1501	0.68	3.32
309	1970s	3.3929	1501	0.63	3.59
309	1970s	3.3927	1501	0.66	3.42
118	1994	0.3068	288.78	0.22	4.83
118	1994	0.3068	288.78	0.23	4.62
118	1994	0.3690	288.78	0.22	5.81
312	2023	0.4474	513.4	0.17	5.13
312	2023	0.4471	513.4	0.17	5.12
312	2023	0.4472	513.4	0.18	4.84

Table A.3: Results for solar PV cells 309, 118 and 312. For statistical significance, three measurements are taken for cell thickness and mass. The latter is measured using a scale with four digit decimal precision.

Appendix B

End-of-Life Parameters

This appendix shows various input assumptions for current and future waste predictions, based on the literature.

B.0.1 IRENA early-loss scenario assumptions

In the early-loss scenario, IRENA assumes the following [15]:

- 0.5% of PV panels (by installed PV capacity in MW) is assumed to reach end-of-life because of damage during transport and installation phases
- 0.5% of PV panels will become waste within two years due to bad installation
- 2% will become waste after ten years
- 4% will become waste after 15 years due to technical failures.

B.1 Recycling technologies and recovery ratios

For the Full Recovery End of Life Photovoltaic (FRELP) process and the Arizona State University (ASU) Heath et al. report the following recovery rates [32].

Material	Recovery rate FRELP	Recovery rate ASU	Purity
Silver	94%	74%	99%
Copper	97%	83%	99.993%
Aluminum	97%	94%	Scrap
Silicon	97%	90%	Metallurgical grade
Glass	98%	99%	98%

Table B.1: Recovery rates and purity levels of two recycling methods: FRELP and ASU, as reported by [32].

B.2 End-of-life pathways

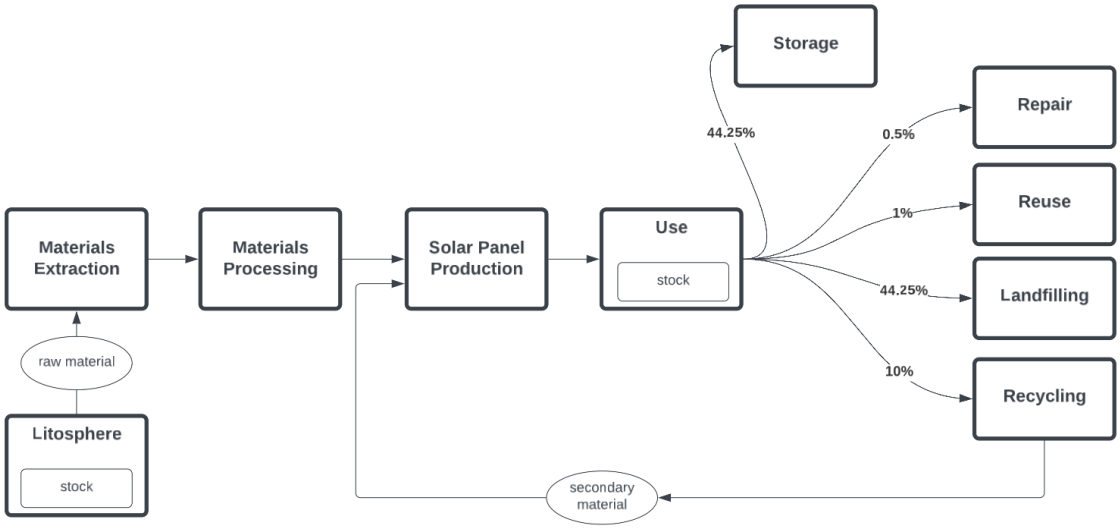

Figure B-1: End-of-life pathways for solar panels, based on Walzberg et al. [129]

B.2.1 Delays in recycling: storage

Walzberg et al. studied the social and behavioral factors of solar PV recycling in relation to techno-economic, market and policy conditions. The authors identified four types of stakeholders and modeled them as agents in a machine learning algorithm (PV owners, installers, recyclers and manufacturers). Five EOL management options are considered

(repair, reuse, recycling, landfilling and storage) [129] and shown in figure B-1.

Supplementary information Table 1 contains the following assumptions for parameter values. Unless otherwise stated, these percentages are selected according to 'best current estimate from publicly available sources': Repair: 0.5% Reuse: 1% Recycling: 10% Landfilling: 44.25% Storing: 44.25% (waste currently not recycled, repaired, or reused is assumed divided equally between landfill and storage pathways.

Purchase options: New: 99.95% Used: 0.05% [129]

B.3 Collection, recycling, and recovery rates

After solar panels reach their service life, they must be collected for recycling. Hotta et al. report that definitions may vary between countries and contexts [130]:

1. Recycling rate emphasizing the input side: cyclical use rate or ratio of recycled materials used in a certain product;

$$\text{Cyclical Use Rate} = \frac{Idr + Imr}{Ix + Imr + Idr} \tag{B.1}$$

2. Recycling rate emphasizing the resource recovery: ratio of materials recovered from end of life/waste products;

$$\text{Recovery Rate} = \frac{Idr}{Rpd + Rcd} \tag{B.2}$$

$$\text{Recommercialization Rate} = \frac{Idr}{Rcd} \tag{B.3}$$

3. Recycling rate emphasizing proper collection: ratio of collected materials for recycling purpose (collection rate);

$$\text{Collection Rate} = \frac{Rcd}{cp} \tag{B.4}$$

4. Recycling rate emphasizing alternatives to final disposal: waste diversion rate [130].

Bibliography

[1] N. Bakker, *Photovoltaics in Historical Built Environments: Interactive Design Manual*, First edition. NHL University of Applied Sciences, 2013, ISBN: 978-94-91790-03-4.

[2] M. F. Ashby, *Materials Selection in Mechanical Design*, Fourth edition. Amsterdam Heidelberg: Butterworth-Heinemann, 2011, 646 pp., ISBN: 978-1-85617-663-7.

[3] S. Prabhu N and R. Majhi, "Disposal of obsolete mobile phones: A review on replacement, disposal methods, in-use lifespan, reuse and recycling," *Waste Management & Research*, vol. 41, no. 1, pp. 18–36, Jan. 1, 2023.

[4] B. London, *Ending the Depression through Planned Obsolescence*. New York, 1932.

[5] E. Maitre-Ekern and C. Dalhammar, "Regulating Planned Obsolescence: A Review of Legal Approaches to Increase Product Durability and Reparability in Europe," *Review of European, Comparative & International Environmental Law*, vol. 25, no. 3, pp. 378–394, 2016.

[6] W. Steffen, K. Richardson, J. Rockström, *et al.*, "Planetary boundaries: Guiding human development on a changing planet," *Science*, vol. 347, no. 6223, p. 1 259 855, Feb. 13, 2015.

[7] J. D. Reina-Rozo, "Art, Energy and Technology: The Solarpunk Movement," *International Journal of Engineering, Social Justice, and Peace*, vol. 8, no. 1, pp. 47–60, 1 Mar. 5, 2021.

[8] J. Kirchherr, D. Reike, and M. Hekkert, "Conceptualizing the circular economy: An analysis of 114 definitions," *Resources, Conservation and Recycling*, vol. 127, pp. 221–232, Dec. 1, 2017.

[9] M. Geissdoerfer, P. Savaget, N. M. P. Bocken, and E. J. Hultink, "The Circular Economy – A new sustainability paradigm?" *Journal of Cleaner Production*, vol. 143, pp. 757–768, Feb. 1, 2017.

[10] B. K. Sovacool, S. H. Ali, M. Bazilian, *et al.*, "Sustainable minerals and metals for a low-carbon future," *Science*, vol. 367, no. 6473, pp. 30–33, Jan. 3, 2020.

[11] Y. Liang, R. Kleijn, and E. van der Voet, "Increase in demand for critical materials under IEA Net-Zero emission by 2050 scenario," *Applied Energy*, vol. 346, p. 121 400, Sep. 15, 2023.

[12] G. Gaustad, M. Krystofik, M. Bustamante, and K. Badami, "Circular economy strategies for mitigating critical material supply issues," *Resources, Conservation and Recycling*, Sustainable Resource Management and the Circular Economy, vol. 135, pp. 24–33, Aug. 1, 2018.

[13] Statista. "Cumulative installed solar PV capacity 2022 (in megawatts)," Statista. (2023), [Online]. Available: `https://www.statista.com/statistics/280220/global-cumulative-installed-solar-pv-capacity/` (visited on 12/14/2023).

[14] T. Curtis, H. Buchanan, G. Heath, L. Smith, and S. Shaw, *Solar Photovoltaic Module Recycling: A Survey of U.S. Policies and Initiatives*, en. Mar. 2021, NREL/TP-6A20–74 124, 1774839, MainId:6273. [Online]. Available: `https://www.osti.gov/servlets/purl/1774839/`.

[15] S. Weckend, A. Wade, and G. Heath, "End of Life Management: Solar Photovoltaic Panels," IEA-PVPS and IRENA, NREL/TP-6A20-73852, 1561525, Aug. 17, 2016, NREL/TP-6A20–73 852, 1 561 525. [Online]. Available: `https://www.osti.gov/servlets/purl/1561525/` (visited on 11/09/2023).

[16] State of Washington Department of Ecology, "Manufacturer Plan Guidance for the Photovoltaic Module Stewardship Program," July 2019 (Revised 2020). [Online]. Available: `https://apps.ecology.wa.gov/publications/summarypages/1907014.html` (visited on 12/07/2023).

[17] State of California. "Photovoltaic Modules (PV modules) - Universal Waste Management Regulations," Department of Toxic Substances Control. (2020), [Online]. Available: https://dtsc.ca.gov/photovoltaic-modules-pv-modules-universal-waste-management-regulations/ (visited on 12/07/2023).

[18] New York State. "Rulemaking - Adding Solar Panels To The Universal Waste Regulations - NYSDEC." (2024), [Online]. Available: https://dec.ny.gov/regulatory/regulations/rulemaking-adding-solar-panels-to-the-universal-waste-regulations (visited on 12/07/2023).

[19] MassDEP, *Solar Panel Recycling. A Review of Existing Markets and Practices Discussion Draft*, Aug. 2023. [Online]. Available: https://www.mass.gov/doc/discussion-draft-solar-panel-recycling-a-review-of-existing-markets-practices-august-2023/download (visited on 11/14/2023).

[20] S. Huang, "Solar Energy Technologies Office Photovoltaics End-of-Life Action Plan," DOE, DOE/EE-2571, 1863490, 8846, Mar. 1, 2022, DOE/EE–2571, 1863490, 8846. [Online]. Available: https://www.osti.gov/servlets/purl/1863490/ (visited on 04/23/2024).

[21] EU, *Directive 2012/19/EU of the European Parliament and of the Council of 4 July 2012 on waste electrical and electronic equipment (WEEE)*, Official Journal of the European Union, Jul. 4, 2012. [Online]. Available: http://data.europa.eu/eli/dir/2012/19/oj/eng (visited on 11/18/2023).

[22] C. Libby, S. Shaw, G. Heath, and K. Wambach, "Photovoltaic Recycling Processes," in *2018 IEEE 7th World Conference on Photovoltaic Energy Conversion (WCPEC) (A Joint Conference of 45th IEEE PVSC, 28th PVSEC & 34th EU PVSEC)*, Jun. 2018, pp. 2594–2599.

[23] L. Frisson, K. Lieten, T. Bruton, *et al.*, "Recent Improvements in Industrial PV Module Recycling," in *Sixteenth European Photovoltaic Solar Energy Conference*, H. Scheer, B. McNelis, W. Palz, H. Ossenbrink, and P. Helm, Eds., 1st ed. Taylor & Francis Group, Routledge, Nov. 25, 2020, pp. 2160–2163, ISBN: 978-1-315-07440-5.

[24] R. Deng, N. L. Chang, Z. Ouyang, and C. M. Chong, "A techno-economic review of silicon photovoltaic module recycling," *Renewable and Sustainable Energy Reviews*, vol. 109, pp. 532–550, Jul. 1, 2019.

[25] A. Polman, M. Knight, E. C. Garnett, B. Ehrler, and W. C. Sinke, "Photovoltaic materials: Present efficiencies and future challenges," *Science*, vol. 352, no. 6283, aad4424, Apr. 15, 2016.

[26] J. Zuboy, M. Springer, E. C. Palmiotti, *et al.*, "Getting Ahead of the Curve: Assessment of New Photovoltaic Module Reliability Risks Associated With Projected Technological Changes," *IEEE Journal of Photovoltaics*, vol. 14, no. 1, pp. 4–22, Jan. 2024.

[27] M. A. Green, "Third generation photovoltaics: Ultra-high conversion efficiency at low cost," *Progress in Photovoltaics: Research and Applications*, vol. 9, no. 2, pp. 123–135, 2001.

[28] NREL. "Best Research-Cell Efficiency Chart." (2024), [Online]. Available: `https://www.nrel.gov/pv/cell-efficiency.html` (visited on 04/29/2024).

[29] W. Shockley and H. J. Queisser, "Detailed Balance Limit of Efficiency of p-n Junction Solar Cells," *Journal of Applied Physics*, vol. 32, no. 3, pp. 510–519, Mar. 1, 1961.

[30] M. Schmid, "Revisiting the Definition of Solar Cell Generations," *Advanced Optical Materials*, vol. 11, no. 20, p. 2 300 697, 2023.

[31] IEA-PVPS. "Trends in PV Applications 2023," IEA-PVPS. (2023), [Online]. Available: `https://iea-pvps.org/trends_reports/trends-2023/` (visited on 12/15/2023).

[32] G. A. Heath, T. J. Silverman, M. Kempe, *et al.*, "Research and development priorities for silicon photovoltaic module recycling to support a circular economy," *Nature Energy*, vol. 5, no. 7, pp. 502–510, Jul. 2020.

[33] J. Peng, L. Lu, and H. Yang, "Review on life cycle assessment of energy payback and greenhouse gas emission of solar photovoltaic systems," *Renewable and Sustainable Energy Reviews*, vol. 19, pp. 255–274, Mar. 1, 2013.

[34] V. Savvilotidou, A. Antoniou, and E. Gidarakos, "Toxicity assessment and feasible recycling process for amorphous silicon and CIS waste photovoltaic panels," *Waste Management*, vol. 59, pp. 394–402, Jan. 1, 2017.

[35] S. R. Wu, I. Celik, D. Apul, and J. Chen, "A social impact quantification framework for the resource extraction industry," *The International Journal of Life Cycle Assessment*, vol. 24, no. 10, pp. 1898–1910, Oct. 1, 2019.

[36] J. L. Roelofs, "The Environmental and Social Impacts of Single Crystalline Silicon Photovoltaic Modules," Eindhoven University of Technology, 2022.

[37] H.-L. Daniela-Abigail, R. Tariq, A. E. Mekaoui, *et al.*, "Does recycling solar panels make this renewable resource sustainable? Evidence supported by environmental, economic, and social dimensions," *Sustainable Cities and Society*, vol. 77, p. 103 539, Feb. 1, 2022.

[38] S. Ovaitt, H. Mirletz, S. Seetharaman, and T. Barnes, "PV in the circular economy, a dynamic framework analyzing technology evolution and reliability impacts," *iScience*, vol. 25, no. 1, p. 103 488, Jan. 2022.

[39] I. D'Adamo, F. Ferella, M. Gastaldi, N. M. Ippolito, and P. Rosa, "Circular solar: Evaluating the profitability of a photovoltaic panel recycling plant," *Waste Management & Research*, vol. 41, no. 6, pp. 1144–1154, Jun. 1, 2023.

[40] G. Granata, P. Altimari, F. Pagnanelli, and J. De Greef, "Recycling of solar photovoltaic panels: Techno-economic assessment in waste management perspective," *Journal of Cleaner Production*, vol. 363, p. 132 384, Aug. 20, 2022.

[41] P. Dias, S. Javimczik, M. Benevit, H. Veit, and A. M. Bernardes, "Recycling WEEE: Extraction and concentration of silver from waste crystalline silicon photovoltaic modules," *Waste Management*, WEEE: Booming for Sustainable Recycling, vol. 57, pp. 220–225, Nov. 1, 2016.

[42] D. S. Philipps and W. Warmuth, "Photovoltaics Report," Fraunhofer ISE, Feb. 21, 2023. [Online]. Available: `https://www.ise.fraunhofer.de/en/publications/studies/photovoltaics-report.html` (visited on 03/02/2024).

[43] M. Jaxa-Rozen and E. Trutnevyte, "Sources of uncertainty in long-term global scenarios of solar photovoltaic technology," *Nature Climate Change*, vol. 11, no. 3, pp. 266–273, Mar. 2021.

[44] Museum of Solar Energy, *Online solar cell archive*, 2024. [Online]. Available: `https://solarmuseum.org` (visited on 03/21/2024).

[45] First Solar, *First Solar Series 6 Datasheet*, 2021. [Online]. Available: `https://www.firstsolar.com/-/media/First-Solar/Technical-Documents/Series-6-Datasheets/Series-6-Datasheet.ashx` (visited on 05/16/2024).

[46] D. M. Chapin, *Energy from the Sun*. Bell Telephone Laboratories, Incorporated, 1962.

[47] E. Becquerel, "Memoire sur les Effets Electriques Produits sous l'Influence des Rayons Solaires," *Comptes Rendus Hebdomadaires des Seances de L'Academie des Sciences*, vol. 9, pp. 561–567, 1839.

[48] M. G. Norton, "Here Comes the Sun," in *A Modern History of Materials: From Stability to Sustainability*, Cham: Springer International Publishing, 2023, pp. 127–146, ISBN: 978-3-031-23990-8.

[49] A. Einstein, "Über einen die Erzeugung und Verwandlung des Lichtes betreffenden heuristischen Gesichtspunkt," *Annalen der Physik*, vol. 322, no. 6, pp. 132–148, 1905.

[50] W. Smith, "Effect of Light on Selenium During the Passage of An Electric Current," *Nature*, vol. 7, no. 173, pp. 303–303, Feb. 1873.

[51] C. Fritts, "On a new form of selenium cell, and some electrical discoveries made by its use.," *American Journal of Science*, vol. 3, no. 156, pp. 465–472, 1883.

[52] A. Chodos, "This Month in Physics History," *APS Advancing Physics*, vol. 18, no. 4, p. 2, Apr. 2009. [Online]. Available: `http://www.aps.org/publications/apsnews/200904/physicshistory.cfm` (visited on 04/27/2024).

[53] R. S. Ohl, "Light-sensitive electric device," U.S. Patent 2402662A, Jun. 25, 1946. [Online]. Available: `https://patents.google.com/patent/US2402662A/en?oq=US2402662A` (visited on 04/25/2024).

[54] D. M. Chapin, C. S. Fuller, and G. L. Pearson, "A New Silicon p-n Junction Photocell for Converting Solar Radiation into Electrical Power," *Journal of Applied Physics*, vol. 25, no. 5, pp. 676–677, May 1, 1954.

[55] M. D. Archer, R. Hill, and J. O. Schumacher, *Clean Electricity From Photovoltaics*. World Scientific, Jun. 4, 2001, ISBN: 978-1-78326-205-2.

[56] M. A. Green, "Crystalline Silicon Photovoltaic Cells," *Advanced Materials*, vol. 13, no. 12-13, pp. 1019–1022, 2001.

[57] H. Fischer and W. Pschunder, "Low-cost solar cells based on large-area unconventional silicon," *IEEE Transactions on Electron Devices*, vol. 24, no. 4, pp. 438–442, Apr. 1977.

[58] E. M. Sachs, D. Ely, and J. Serdy, "Edge stabilized ribbon (ESR) growth of silicon for low cost photovoltaics," *Journal of Crystal Growth*, vol. 82, no. 1, pp. 117–121, Mar. 1, 1987.

[59] D. E. Carlson and C. R. Wronski, "Amorphous silicon solar cell," *Applied Physics Letters*, vol. 28, no. 11, pp. 671–673, Jun. 1976.

[60] F. Pfisterer and W. H. Bloss, "Development of Cu2S-CdS thin film solar cells and transfer to industrial production," *Solar Cells*, vol. 12, no. 1, pp. 155–161, Jun. 1, 1984.

[61] A. Kojima, K. Teshima, Y. Shirai, and T. Miyasaka, "Organometal Halide Perovskites as Visible-Light Sensitizers for Photovoltaic Cells," *Journal of the American Chemical Society*, vol. 131, no. 17, pp. 6050–6051, May 6, 2009.

[62] H. C. Weerasinghe, N. Macadam, J.-E. Kim, *et al.*, "The first demonstration of entirely roll-to-roll fabricated perovskite solar cell modules under ambient room conditions," *Nature Communications*, vol. 15, no. 1, p. 1656, Mar. 12, 2024.

[63] J. Zheng, Z. Ying, Z. Yang, *et al.*, "Polycrystalline silicon tunnelling recombination layers for high-efficiency perovskite/tunnel oxide passivating contact tandem solar cells," *Nature Energy*, vol. 8, no. 11, pp. 1250–1261, Nov. 2023.

[64] R. R. Lunt and V. Bulovic, "Transparent, near-infrared organic photovoltaic solar cells for window and energy-scavenging applications," *Applied Physics Letters*, vol. 98, no. 11, p. 113 305, Mar. 17, 2011.

[65] M. Saravanapavanantham, J. Mwaura, and V. Bulović, "Printed Organic Photovoltaic Modules on Transferable Ultra-thin Substrates as Additive Power Sources," *Small Methods*, vol. 7, no. 1, p. 2 200 940, 2023.

[66] R. Nielsen, A. Crovetto, A. Assar, O. Hansen, I. Chorkendorff, and P. C. Vesborg, "Monolithic Selenium/Silicon Tandem Solar Cells," *PRX Energy*, vol. 3, no. 1, p. 013 013, Mar. 12, 2024.

[67] L. Drake. "XRF User Guide - Terminology," XRF User Guide. (2018), [Online]. Available: `http://www.xrf.guru/Concepts/XRFTerminology/index.html` (visited on 05/03/2024).

[68] H. L. Needleman and D. Bellinger, "The health effects of low level exposure to lead," *Annu. Rev. Publ. Health.*, vol. 12, no. 1, pp. 111–140, 1991.

[69] G. Schileo and G. Grancini, "Lead or no lead? Availability, toxicity, sustainability and environmental impact of lead-free perovskite solar cells," *Journal of Materials Chemistry C*, vol. 9, no. 1, pp. 67–76, Jan. 7, 2021.

[70] C. Licht, L. T. Peiró, and G. Villalba, "Global substance flow analysis of gallium, germanium, and indium: Quantification of extraction, uses, and dissipative losses within their anthropogenic cycles," en, *Journal of Industrial Ecology*, vol. 19, no. 5, pp. 890–903, 2015.

[71] K. Hamada, D. Hirotani, M. A. Kamarudin, *et al.*, "Pb-free Sn Perovskite Solar Cells Doped with Samarium Iodide," *Chemistry Letters*, vol. 48, no. 8, pp. 836–839, Aug. 5, 2019.

[72] Y. Zhang, M. Kim, L. Wang, P. Verlinden, and B. Hallam, "Design considerations for multi-terawatt scale manufacturing of existing and future photovoltaic technologies: Challenges and opportunities related to silver, indium and bismuth consumption," *Energy & Environmental Science*, vol. 14, no. 11, pp. 5587–5610, 2021.

[73] L. P. D'Souza, R. Shwetharani, V. Amoli, C. A. N. Fernando, A. K. Sinha, and R. G. Balakrishna, "Photoexcitation of neodymium doped TiO2 for improved performance in dye-sensitized solar cells," *Materials & Design*, vol. 104, pp. 346–354, Aug. 15, 2016.

[74] K. Wang, L. Zheng, T. Zhu, *et al.*, "Efficient perovskite solar cells by hybrid perovskites incorporated with heterovalent neodymium cations," *Nano Energy*, vol. 61, pp. 352–360, Jul. 1, 2019.

[75] H. Mizuno, K. Makita, T. Sugaya, *et al.*, "Palladium nanoparticle array-mediated semiconductor bonding that enables high-efficiency multi-junction solar cells," *Japanese Journal of Applied Physics*, vol. 55, no. 2, p. 025 001, Jan. 6, 2016.

[76] C. Bracher, H. Yi, N. W. Scarratt, *et al.*, "The effect of residual palladium catalyst on the performance and stability of PCDTBT:PC70BM organic solar cells," *Organic Electronics*, vol. 27, pp. 266–273, Dec. 1, 2015.

[77] A. Zeng, W. Chen, K. D. Rasmussen, *et al.*, "Battery technology and recycling alone will not save the electric mobility transition from future cobalt shortages," *Nature Communications*, vol. 13, no. 1, p. 1341, Mar. 15, 2022.

[78] L. Lottspeich, P. Müller, and T. Kaden, "Metal contamination of silicon wafers in diamond wire sawing processes depending on the sawing parameters," *AIP Conference Proceedings*, vol. 1999, no. 1, p. 140 003, Aug. 10, 2018.

[79] S. M. Feldt, E. A. Gibson, E. Gabrielsson, L. Sun, G. Boschloo, and A. Hagfeldt, "Design of Organic Dyes and Cobalt Polypyridine Redox Mediators for High-Efficiency Dye-Sensitized Solar Cells," *Journal of the American Chemical Society*, vol. 132, no. 46, pp. 16 714–16 724, Nov. 24, 2010.

[80] X. Zeng, J. A. Mathews, and J. Li, "Urban Mining of E-Waste is Becoming More Cost-Effective Than Virgin Mining," *Environmental Science & Technology*, vol. 52, no. 8, pp. 4835–4841, Apr. 17, 2018.

[81] Y. He, H. Hosseinzadeh-Bandbafha, M. Kiehbadroudinezhad, W. Peng, M. Tabatabaei, and M. Aghbashlo, "Environmental footprint analysis of gold recycling from elec-

tronic waste: A comparative life cycle analysis," *Journal of Cleaner Production*, vol. 432, p. 139 675, Dec. 20, 2023.

[82] S. H. Winkler, "Solar Cells for Space Vehicles," *American Radio History*, 1959.

[83] M. Green, E. Dunlop, J. Hohl-Ebinger, M. Yoshita, N. Kopidakis, and X. Hao, "Solar cell efficiency tables (version 57)," *Progress in Photovoltaics: Research and Applications*, vol. 29, no. 1, pp. 3–15, 2021.

[84] D. Sarti and R. Einhaus, "Silicon feedstock for the multi-crystalline photovoltaic industry," *Solar Energy Materials and Solar Cells*, EMRS 2001 Symposium E: Crystalline Silicon for Solar Cells, vol. 72, no. 1, pp. 27–40, Apr. 1, 2002.

[85] Photon. "Photon Databases." (2023), [Online]. Available: `https://www.photon.info/en/photon-databases` (visited on 11/11/2023).

[86] VDMA. "International Technology Roadmap for Photovoltaic (ITRPV)." (2023), [Online]. Available: `https://www.vdma.org/international-technology-roadmap-photovoltaic` (visited on 11/11/2023).

[87] G. Song, Y. Lu, B. Liu, H. Duan, H. Feng, and G. Liu, "Photovoltaic panel waste assessment and embodied material flows in China, 2000–2050," *Journal of Environmental Management*, vol. 338, p. 117 675, Jul. 15, 2023.

[88] D. Guyonnet, M. Planchon, A. Rollat, *et al.*, "Material flow analysis applied to rare earth elements in Europe," *Journal of Cleaner Production*, vol. 107, pp. 215–228, Nov. 16, 2015.

[89] P. H. Brunner and H. Rechberger, *Handbook of Material Flow Analysis: For Environmental, Resource, and Waste Engineers*. CRC press, 2016, ISBN: 1-315-31344-8.

[90] D. Laner, J. Feketitsch, H. Rechberger, and J. Fellner, "A Novel Approach to Characterize Data Uncertainty in Material Flow Analysis and its Application to Plastics Flows in Austria," *Journal of Industrial Ecology*, vol. 20, no. 5, pp. 1050–1063, 2016.

[91] IEA. "World Energy Outlook 2023 Free Dataset - Data product," IEA. (2023), [Online]. Available: `https://www.iea.org/data-and-statistics/data-product/world-energy-outlook-2023-free-dataset-2` (visited on 12/15/2023).

[92] IPCC, *Global Warming of 1.5°C: IPCC Special Report on Impacts of Global Warming of 1.5°C above Pre-industrial Levels in Context of Strengthening Response to Climate Change, Sustainable Development, and Efforts to Eradicate Poverty*, 1st ed. Cambridge University Press, Jun. 9, 2022, ISBN: 978-1-00-915794-0 978-1-00-915795-7. [Online]. Available: https://www.cambridge.org/core/product/identifier/9781009157940/type/book (visited on 12/15/2023).

[93] PV Magazine. "BloombergNEF says global solar will cross 200 GW mark for first time this year, expects lower panel prices," PV Magazine International. (Feb. 1, 2022), [Online]. Available: https://www.pv-magazine.com/2022/02/01/bloombergnef-says-global-solar-will-cross-200-gw-mark-for-first-time-this-year-expects-lower-panel-prices/ (visited on 05/18/2024).

[94] J. Jean, M. Woodhouse, and V. Bulović, "Accelerating photovoltaic market entry with module replacement," en, *Joule*, vol. 3, no. 11, pp. 2824–2841, Nov. 2019.

[95] J. A. Bennett, C. N. Trevisan, J. F. DeCarolis, *et al.*, "Extending energy system modelling to include extreme weather risks and application to hurricane events in Puerto Rico," *Nature Energy*, vol. 6, no. 3, pp. 240–249, Mar. 2021.

[96] V. Tan, P. R. Dias, N. Chang, and R. Deng, "Estimating the Lifetime of Solar Photovoltaic Modules in Australia," *Sustainability*, vol. 14, no. 9, p. 5336, 9 Jan. 2022.

[97] NIST. "Weibull Distribution." (2003), [Online]. Available: https://itl.nist.gov/div898/handbook/eda/section3/eda3668.htm (visited on 05/06/2024).

[98] F. Zobel. "EoL – Development of an Industrial Recycling Process for PV Modules," Fraunhofer Institute for Solar Energy Systems ISE. (2019), [Online]. Available: https://www.ise.fraunhofer.de/en/research-projects/eol.html (visited on 12/16/2023).

[99] J. Bernreuter. "Silicon Consumption to Drop to 3.6 g/W — Bernreuter Research." (Jun. 20, 2017), [Online]. Available: https://www.bernreuter.com/newsroom/press-releases/bernreuter-research-polysilicon-consumption-to-drop-to-3-6-g-w/ (visited on 12/15/2023).

[100] J. D. Santos and M. C. Alonso-García, "Projection of the photovoltaic waste in Spain until 2050," *Journal of Cleaner Production*, vol. 196, pp. 1613–1628, Sep. 20, 2018.

[101] K. Wambach, S. Schlenker, A. Müller, *et al.*, "The second life of a 300 kw pv generator manufactured with recycled wafers from the oldest german pv power plant," presented at the 21st European Photovoltaic Solar Energy Conference and Exhibition 2006, Dresden. 2006.

[102] K. Sander, S. Schilling, J. Reinschmidt, *et al.*, "Study on the Development of a Takeback and Recovery System for Photovoltaic Modules," European Photovoltaic Industry Association: German Solar Industries Association, Berlin, 2007.

[103] V. V. Zadde, A. B. Pinov, D. S. Strebkov, *et al.*, "New Method of Solar Grade Silicon Production," presented at the 12th Workshop on Crystalline Silicon Solar Cell Materials and Processes, NREL/BK-520-32717, 2002.

[104] Tongwei. "How much polysilicon is used in solar panels - Tongwei Co., Ltd.," (Oct. 13, 2023), [Online]. Available: `https://en.tongwei.com.cn/news/36.html` (visited on 11/19/2023).

[105] IRENA. "Hydrogen." (2022), [Online]. Available: `https://www.irena.org/Energy-Transition/Technology/Hydrogen` (visited on 05/06/2024).

[106] L. Truche, F.-V. Donzé, E. Goskolli, *et al.*, "A deep reservoir for hydrogen drives intense degassing in the Bulqizë ophiolite," *Science*, vol. 383, no. 6683, pp. 618–621, Feb. 9, 2024.

[107] IEA, "Global Hydrogen Review 2023," 2023. [Online]. Available: `https://iea.blob.core.windows.net/assets/ecdfc3bb-d212-4a4c-9ff7-6ce5b1e19cef/GlobalHydrogenReview2023.pdf` (visited on 04/21/2024).

[108] M. Prussi, M. Yugo, P. L. De, M. Padella, R. Edwards, and L. Lonza. "JEC Well-to-Tank report v5," JRC Publications Repository. (Sep. 23, 2020), [Online]. Available: `https://publications.jrc.ec.europa.eu/repository/handle/JRC119036` (visited on 04/03/2024).

[109] H2 Green Steel. "H2 Green Steel has pre-sold over 1.5 million tonnes of green steel to customers." (May 10, 2022), [Online]. Available: https://www.h2greensteel.com/latestnews/h2-green-steel-has-pre-sold-over-15-million-tonnes-of-green-steel-to-customers (visited on 05/09/2024).

[110] T. Koch Blank, "The Disruptive Potential of Green Steel," Rocky Mountain Institute, 2019.

[111] V. Vogl, M. Åhman, and L. J. Nilsson, "Assessment of hydrogen direct reduction for fossil-free steelmaking," *Journal of Cleaner Production*, vol. 203, pp. 736–745, Dec. 1, 2018.

[112] USGS, *Iron and Steel Statistics and Information. Annual Publications.* 2024. [Online]. Available: https://www.usgs.gov/centers/national-minerals-information-center/iron-and-steel-statistics-and-information (visited on 03/05/2024).

[113] Statista. "Production capacity of methanol worldwide from 2018 to 2022," Statista. (2023), [Online]. Available: https://www.statista.com/statistics/1065891/global-methanol-production-capacity/ (visited on 05/12/2024).

[114] IEA. "International shipping." (2023), [Online]. Available: https://www.iea.org/energy-system/transport/international-shipping (visited on 05/17/2024).

[115] IMO. "Revised GHG reduction strategy for global shipping adopted." (Jul. 7, 2023), [Online]. Available: https://www.imo.org/en/MediaCentre/PressBriefings/Pages/Revised-GHG-reduction-strategy-for-global-shipping-adopted-.aspx (visited on 05/09/2024).

[116] P. Martin. "Maersk orders world's biggest ammonia carriers from Hyundai to ship hydrogen derivative across oceans." (Dec. 1, 2023), [Online]. Available: https://www.hydrogeninsight.com/transport/maersk-orders-worlds-biggest-ammonia-carriers-from-hyundai-to-ship-hydrogen-derivative-across-oceans/2-1-1563932 (visited on 04/04/2024).

[117] L. Lin, R. Wijayawardana, V. Rao, H. Nguyen, W. E. Gnibga, and A. A. Chien. "Exploding AI Power Use: An Opportunity to Rethink Grid Planning and Manage-

ment." (Apr. 30, 2024), [Online]. Available: http://arxiv.org/abs/2311.11645 (visited on 05/09/2024), preprint.

[118] United Nations. "Population." (2024), [Online]. Available: https://www.un.org/en/global-issues/population (visited on 05/02/2024).

[119] IEA. "Data centres & networks," IEA. (2024), [Online]. Available: https://www.iea.org/energy-system/buildings/data-centres-and-data-transmission-networks (visited on 05/09/2024).

[120] IEA, "Electricity 2024 - Analysis and forecast to 2026," 2024. [Online]. Available: https://iea.blob.core.windows.net/assets/ddd078a8-422b-44a9-a668-52355f24133b/Electricity2024-Analysisandforecastto2026.pdf (visited on 03/14/2024).

[121] C. Fraser, P. Dargusch, and G. Hill, "Meeting the net zero emissions challenge – Alphabet's carbon management actions and opportunities," *Advances in Environmental and Engineering Research*, vol. 3, no. 2, p. 13, 2022.

[122] IEA. "Solar PV manufacturing capacity by component in China, 2021-2024 – Charts – Data & Statistics." (2023), [Online]. Available: https://www.iea.org/data-and-statistics/charts/solar-pv-manufacturing-capacity-by-component-in-china-2021-2024 (visited on 04/04/2024).

[123] J. H. Wong, M. Royapoor, and C. W. Chan, "Review of life cycle analyses and embodied energy requirements of single-crystalline and multi-crystalline silicon photovoltaic systems," *Renewable and Sustainable Energy Reviews*, vol. 58, pp. 608–618, May 1, 2016.

[124] I. Celik, A. B. Phillips, Z. Song, *et al.*, "Environmental analysis of perovskites and other relevant solar cell technologies in a tandem configuration," *Energy & Environmental Science*, vol. 10, no. 9, pp. 1874–1884, 2017.

[125] H.-Q. Wang, M. Batentschuk, A. Osvet, L. Pinna, and C. J. Brabec, "Rare-Earth Ion Doped Up-Conversion Materials for Photovoltaic Applications," *Advanced Materials*, vol. 23, no. 22-23, pp. 2675–2680, 2011.

[126] V. Stratiotou Efstratiadis and N. Michailidis, "Sustainable Recovery, Recycle of Critical Metals and Rare Earth Elements from Waste Electric and Electronic Equipment (Circuits, Solar, Wind) and Their Reusability in Additive Manufacturing Applications: A Review," *Metals*, vol. 12, no. 5, p. 794, 5 May 2022.

[127] B. Hallam, M. Kim, R. Underwood, S. Drury, L. Wang, and P. Dias, "A Polysilicon Learning Curve and the Material Requirements for Broad Electrification with Photovoltaics by 2050," *Solar RRL*, vol. 6, no. 10, p. 2 200 458, 2022.

[128] J. Glüge, M. Scheringer, I. T. Cousins, *et al.*, "An overview of the uses of per- and polyfluoroalkyl substances (PFAS)," *Environmental Science: Processes & Impacts*, vol. 22, no. 12, pp. 2345–2373, 2020.

[129] J. Walzberg, A. Carpenter, and G. A. Heath, "Role of the social factors in success of solar photovoltaic reuse and recycle programmes," *Nature Energy*, vol. 6, no. 9, pp. 913–924, Sep. 2021, Publisher: Nature Publishing Group.

[130] Y. Hotta, C. Visvanathan, and M. Kojima, "Recycling rate and target setting: Challenges for standardized measurement," *Journal of Material Cycles and Waste Management*, vol. 18, no. 1, pp. 14–21, Jan. 1, 2016.